RICARDO MARQUES DA SILVA

FILOGEOGRAFIA, LIMITES ESPECÍFICOS E HISTÓRIA EVOLUTIVA DE DUAS ESPÉCIES DE ANUROS NO DOMÍNIO DA CAATINGA

João Pessoa

Paraíba – Brasil

2019

RICARDO MARQUES DA SILVA

FILOGEOGRAFIA, LIMITES ESPECÍFICOS E HISTÓRIA EVOLUTIVA DE DUAS ESPÉCIES DE ANUROS NO DOMÍNIO DA CAATINGA

Tese apresentada ao programa de Pós-Graduação em Ciências Biológicas (Zoologia) da Universidade Federal da Paraíba, como parte das exigências para a obtenção do título de Doutor em Zoologia.

Orientador:

Dr. Adrian Antonio Garda

Catalogação na publicação
Seção de Catalogação e Classificação

S586f Silva, Ricardo Marques da.
Filogeografia, limites específicos e história evolutiva de duas espécies de anuros no domínio da Caatinga / Ricardo Marques da Silva. - João Pessoa, 2019.
141 f. : il.

Orientação: Adrian Antonio Garda.
Tese (Doutorado) - UFPB/CCEN.

1. Ciências biológicas. 2. Filogeografia. 3. Caatinga. 4. Lophyohylini. I. Garda, Adrian Antonio. II. Título.

UFPB/BC CDU 57(043)

Elaborado por GRACILENE BARBOSA FIGUEIREDO - CRB-15/794

RICARDO MARQUES DA SILVA

FILOGEOGRAFIA, LIMITES ESPECÍFICOS E HISTÓRIA EVOLUTIVA DE DUAS ESPÉCIES DE ANUROS NO DOMÍNIO DA CAATINGA

Tese apresentada ao programa de Pós-Graduação em Ciências Biológicas (Zoologia) da Universidade Federal da Paraíba, como parte das exigências para a obtenção do título de Doutor em Zoologia.

Henrique Batalha-Filho Membro titular externo UFBA	Tamí Mott Membro titular externo UFAL
Pedro C. Estrela de A. Pinto Membro titular interno UFPB	Márcio Bernardino da Silva Membro titular interno UFPB

Adrian Antonio Garda
Orientador
UFPB

Ata da 122ª Apresentação e Banca de Defesa de Doutorado de Ricardo Marques da Silva

Ao(s) Vinte e nove dias do mês de maio de dois mil e dezenove, às 13:00 horas, no(a) Sala do PPGCB, da Universidade Federal da Paraíba, reuniram-se, em caráter de solenidade pública, membros da banca examinadora para avaliar a tese de doutorado de **Ricardo Marques da Silva**, candidato(a) ao grau de Doutor em Ciências Biológicas. A banca foi composta pelos seguintes professores/pesquisadores: **Dr. Adrian Antonio Garda (Orientador), Dr. Henrique Batalha Filho, Dra. Tami Mott, Dra. Sarah Mângia Barros e Dr. Márcio Bernardino da Silva.** Compareceram à solenidade, além do(a) candidato(a) e membros da banca examinadora, alunos e professores do PPGCB. Dando início à sessão, a coordenação fez a abertura dos trabalhos, apresentando o(a) discente e os membros da banca. Foi passada a palavra para o(a) orientador(a), para que assumisse a posição de presidente da sessão. A partir de então, o(a) presidente, após declarar o objeto da solenidade, concedeu a palavra a **Ricardo Marques da Silva**, para que dissertasse, oral e sucintamente, a respeito de seu trabalho intitulado **"Filogeografia, limites específicos e história evolutiva de duas espécies de anuros no domínio da Caatinga".** Passando então a discorrer sobre o aludido tema, dentro do prazo legal, o(a) candidato(a) foi a seguir arguido(a) pelos examinadores na forma regimental. Em seguida, passou a Comissão, em caráter secreto, a proceder à avaliação e julgamento do trabalho, concluindo por atribuir-lhe o conceito Aprovado. Perante a aprovação, declarou-se o(a) candidato(a) legalmente habilitado(a) a receber o grau de **Doutor em Ciências Biológicas**, área de concentração **Zoologia**. Nada mais havendo a tratar eu, **Dr. Adrian Antonio Garda**, como presidente, lavrei a presente ata que, lida e aprovada, assino juntamente com os demais membros da banca examinadora.

João Pessoa, 29/05/2019.

[redacted]

Dr. Adrian Antonio Garda (Orientador)

[redacted]

Dr. Henrique Batalha Filho

[redacted]

Dra. Tami Mott

[redacted]

Dra. Sarah Mângia Barros

[redacted]

Márcio Bernardino da Silva

Ciente do Resultado:

[redacted]

Ricardo Marques da Silva

– Gostaria que isso não tivesse acontecido na minha época — disse Frodo.
– Eu também — disse Gandalf. — Como todos os que vivem nestes tempos. Mas a decisão não é nossa. Tudo que temos de decidir é o que fazer com o tempo que nos é dado.

J.R.R. Tolkien, O Senhor dos Anéis: A Sociedade do Anel

AGRADECIMENTOS

A vida durante a pós-graduação é interessante. Ao abraçar o caminho acadêmico para cumprir nossos objetivos, muitas vezes precisamos nos desgarrar da zona de conforto e partir para outras cidades sem qualquer relação conosco até então, longe da família e amigos. Essa mudança brusca pode ser assustadora, enervante e muitas vezes nos dá sensação de estar desnorteado. Por outro lado, é a oportunidade perfeita para almejar novos rumos e crescer profissionalmente e pessoalmente. E para isso, é fundamental que tenhamos pessoas próximas que possam nos auxiliar a tornar o caminho menos pedregoso e mais agradável. Durante o doutorado, tenho certeza de que as pessoas aqui citadas, sem dúvida, tiveram esse papel.

Não posso ir além sem antes agradecer a pessoa que, talvez, seja o principal motivo de estar aqui: minha mãe, Maísa. Coube a ela a tarefa de me instigar a estudar, sempre buscar conhecimento e mostrar que a educação é essencial, seja ela de casa ou profissional. Desde muito cedo quando decidi cursar biologia, ela foi fundamental ao me instigar a correr atrás de eventos e estágios. Na pós-graduação não foi diferente e, apesar de odiar me ver longe e reclamar da saudade, sempre me incentivou. Não posso deixar de mencionar minha madrinha Marise, que não só sempre me incentivou, como sempre foi interessada em saber sobre o caminho que estava trilhando. Serei eternamente grato por tê-las.

Se hoje posso dizer que compreendo mais sobre filogeografia, devo ao meu orientador, Adrian Garda que viabilizou todo o apoio logístico, auxílio com análises e sugestões para o crescimento do trabalho. Mas acima de tudo, por aceitar encarar um aluno sem qualquer conhecimento no tema, apenas o interesse em aliar aspectos moleculares e as espécies da Caatinga. Não só isso, como também ter a preocupação em ensinar melhores formas de redação de manuscritos, puxar discussões sobre artigos, vida acadêmica e política, as quais agradeço imensamente.

Conjuntamente, preciso agradecer ao meu LAR (Laboratório de Anfíbios e Répteis/UFRN) nestes quatro anos e as pessoas que o compuseram: Felipe Camurugi, Felipe Medeiros, Flávia Mol, Emanuel Fonseca, Ricardo Rodrigues, Sarah Mângia, Diego Santana, Leandro Alves, Eliana Oliveira, Vinícius São-Pedro, Alan Filipe, Felipe Coelho e Willianilson Pessoa. Foram fundamentais durante todo ou algum momento para meu crescimento neste período, seja no lado profissional através de auxílio com análises, discussões de ideias, revisões de texto e socorro no laboratório molecular (todo dia um 7 x 1 diferente), ou pelo lado pessoal no convívio diário durante os coffe breaks e confraternizações em bares, churrascos, cinemas e afins.

Dentre as andanças neste período, sou grato por ter conhecido e hoje poder compartilhar momentos com minha namorada Vanessa. Seu companheirismo e apoio tem sido fundamentais, principalmente na reta final. Obrigado, linda!

Ao grupo de quadrinhos sem lei, onde falar besteira (e as vezes sobre quadrinhos) com vocês foi fundamental para aliviar muitos momentos! Especialmente aos lombadeiros Thiago Savela, Matheus Nahkur, Denis Ariel, Christian Decenada e André Jadson.

Aos amigos de Salvador com quem sempre posso conversar sobre a vida e também relembrar tempos passados: Cecil Fazolato, Tércio Melo, Felipe Gondim, Alessandra Andrade, Clara "Andrade", Rafael Sepúlveda, André Leite, Magno Travassos, Bruno Oliveira, Felipe Neves e Paulo Victor.

Conheci tantas pessoas fantásticas nestes quatro anos que é até injusto não citar todas. Ainda assim, preciso destacar meus professores da UFPB e também as pessoas que vieram através dela (e que, ocasionalmente, me deram um teto durante as disciplinas): Bruna E. Pontes, Juan Zurano, Lucas "Libélula", Izabel Regina, Mayara Beltrão, Maria Clara e Daniel Mesquita. Também outras que vieram através da UFRN: André Bruinjé, Thaís Araújo, Flávia Petean, Mariana Ramos, Jéssica Fernanda e Silvia Yasmin.

Sou muitíssimo grato a Coordenação de Aperfeiçoamento de Pessoal de Nível Superior (CAPES) pela bolsa fornecida, sem a qual não poderia ter concluído o doutorado. Afinal, a bolsa pagou meus aluguéis, alimentação, lazer e congressos. É para isso que ela serve.

Aos membros da banca examinadora e contribuições que trouxeram ao trabalho: Henrique Batalha, Tamí Mott, Pedro Estrela, Márcio Bernardino, Sarah Mângia e Gustavo Vieira.

Aos curadores dos museus de herpetologia e suas equipes, que forneceram tecidos, espécimes ou gravações para este trabalho: Célio Haddad (UNESP), Diego Santana (UFMS), Gustavo Vieira (UFPB), Felipe Toledo (UNICAMP), Cassio Rachid e Marcelo Napoli (UFBA), Milena Wachlevski (UFERSA), Natham Maciel (UFG) e Paulo Garcia (UFMG).

Por último, mas definitivamente não menos importante, a Alexandra Elbakyan, criadora do Sci-hub. Ferramenta fundamental para tornar o conhecimento acessível a todos.

Embarcar no trem da filogeografia foi um desafio, mas encarar este tema e ter suporte de tanta gente foi crucial para expandir meus horizontes. Obrigado!

RESUMO

Desvendar os padrões e processos de diversificação da biota Neotropical tem sido o desafio de biogeógrafos há décadas. Com a ascensão de métodos moleculares, a filogeografia é um poderoso método que alia dados genéticos e a biogeografia dos organismos. Dentre a herpetofauna, a dependência aquática e baixa capacidade dispersiva são requisitos atribuídos como justificativa para anfíbios não possuírem ampla distribuição. Neste contexto, espécies biologicamente distintas, mas com distribuição similar podem responder diferentemente aos mesmos processos histórico-demográficos e barreiras ambientais. Assim, utilizamos inferências filogeográficas para comparar a história evolutiva de *Corythomantis greeningi* e *Rhinella jimi* na Caatinga e áreas adjacentes. Reunimos amostras de tecido cobrindo toda a distribuição de ambas as espécies e utilizamos abordagem multilocus, sequenciando genes mitocondriais e nucleares (cinco para *C. greeningi* e quatro para *R. jimi*). Utilizamos reconstruções genéticas, histórico-demográficas e modelagem de nicho ecológica para ambas as espécies. Obtivemos 98 sequências para *C. greeningi* e 135 para *R. jimi*. A reconstrução Bayesiana de árvore mitocondrial recuperou estruturação somente para *C. greeningi*, associada a Cadeia de Montanhas do Espinhaço. O assinalamento populacional recuperou três populações para *C. greeningi* com compartilhamento de haplótipos entre duas delas, enquanto *R. jimi* recuperou somente uma população amplamente distribuída. Testamos as populações de *C. greeningi* através de métodos coalescentes de delimitação (BPP) e verificamos que a população associada ao Espinhaço é uma nova espécie de *Corythomantis*. A mesma análise atestou a validade taxonômica de *R. jimi*, mas reconstruções haplotípicas mostraram compartilhamento de haplótipos entre *R. jimi* e duas espécies filogeneticamente próximas: *R. marina* e *R. diptycha*. Testamos seis cenários de diversificação com computação Bayesiana aproximada para *Corythomantis* e o melhor modelo indica divergência da nova espécie no início do Plioceno, e expansão populacional e fluxo gênico entre as populações de *C. greeningi*. Inferências histórico-demográficas mostraram alterações populacionais também em *R. jimi* durante o Pleistoceno. Por fim, descrevemos uma nova espécie de *Corythomantis* restrita à Cadeia do Espinhaço. A nova espécie difere substancialmente de *C. greeningi* geneticamente, morfologicamente e acusticamente.

Palavras-chave: Filogeografia, Caatinga, Lophyohylini, Bufonidae, Diagonal de Formações Abertas

ABSTRACT

Unveil the patterns and processes of diversification of the Neotropical biota has been the challenge of biogeographers for decades. With the rise of molecular methods, phylogeography is a powerful method that combines genetic data and the biogeography of organisms. Among herpetofauna, aquatic dependence and low dispersive capacity are requirements attributed as a justification for amphibians not having a wide distribution. In this context, biologically distinct species, but with a similar distribution may respond differently to the same historical-demographic processes and environmental barriers. Thus, we used phylogeographic inferences to compare the evolutionary history of *Corythomantis greeningi* and *Rhinella jimi* in the Caatinga and adjacent areas. We collected tissue samples covering the entire distribution of both species and used a multilocus approach, sequencing mitochondrial and nuclear genes (five for *C. greeningi* and four for *R. jimi*). We use genetic, historical-demographic reconstructions and ecological niche modeling for both species. We obtained 98 sequences for *C. greeningi* and 135 *for R. jimi*. Bayesian mitochondrial gene tree reconstruction recovered structure only for *C. greeningi*, associated with the Espinhaço Mountain Range. Population assignment recovered three populations for *C. greeningi* with sharing of haplotypes between two of them, while *R. jimi* recovered only a widely distributed population. We tested the populations of *C. greeningi* using coalescent delimitation methods (BPP) and found that the population associated with Espinhaço is a new species of *Corythomantis*. The same analysis attested to the taxonomic validity of *R. jimi*, but haplotypical reconstructions showed sharing of haplotypes between *R. jimi* and two phylogenetically close species: *R. marina* and *R. diptycha*. We tested six diversification scenarios with approximate Bayesian computation for *Corythomantis* and the best model indicates divergence of the new species at the beginning of the Pliocene, and population expansion and gene flow among *C. greeningi* populations. Historical-demographic inferences also showed population changes in *R. jimi* during the Pleistocene. Finally, we describe a new species of *Corythomantis* restricted to the Espinhaço Chain. The new species substantially differs from *C. greeningi* genetically, morphologically and acoustically.

Key-words: Phylogeography, Caatinga, Lophyohylini, Bufonidae, diagonal of open formations

LISTA DE FIGURAS

Capítulo I:

Capítulo II:

Figure 1: Distribution map of samples within Caatinga and Cerrado boundaries. The blue line shows the current São Francisco River and the dashed black line shows its Paleocourse. Each circle color corresponds to a specific population and locality numbers are described in Table S1.

Figure 2: Graphical representation of the populations recovered in GENELAND. Analysis with both mtDNA and nuDNA combined (A) and only nuDNA (B) data, showing the spatial delimitation of all populations, and population one (left column), population two (mid column) and Espinhaço population (right column), respectively. Warmer colors represent higher probabilities of localities assigned to those populations. Black lines show delimitation support.

Figure 3: Haplotype network from neighbor-joining analyses for all genes of *Corythomantis*. COI (A), 16S (B), βfib (C), RPL3 (D) and Tyrosinase (E). Colors represent each recovered population, as green for population one and white for population two of *Corythomantis greeningi* whilst red represent Espinhaço population. The size of circles represent the haplotype frequency.

Figure 4: Consensus bayesian mitochondrial gene tree for all samples of *Corythomantis* across its distribution. Red bar represents specimens from the Espinhaço Mountain Range, while green and gray bars are populations 1 and 2 recovered in the population assignments, respectively. Node values of posterior probabilities (pp) are represented by circles: blue (pp = 1), yellow (0.99 > pp >0.91), and orange (0.89 > pp > 0.80). Nodes without circles have posterior probabilities below 0.79.

Figure 5: Ecologic Niche Modeling for *C. greeningi*. The recovered potential distribution in four periods are (A) current, (B) mid-Holocene (6 kya), (C) Last Glacial Maximum (21 kya) and (D) Last Inter-Glacial (120 kya). Stability area across periods (E) generated with a four models consensus. Black dots represent occurrence points. Warmer coloration indicates higher probability of occurrence based on the selected bioclimatic data.

Figure 6: Schematic representation of the six models tested using approximate Bayesian computation. a–e represents distinct diversification scenario of divergence scenarios among population 1 (P1), population 2 (P2) and *Corythomantis* sp. (C). The direction of the arrows indicates the migration direction. The best-supported model is marked by a red box.

Figure 7: Background similarity test in *Corythomantis*. Comparisons are between population one and population two (A) and between the species *C. greeningi* and *Corythomantis* sp. (B). The right column shows Schoener's D statistic values while the left column show Hellinger's based I statistic. Observed values are shown as red arrows and null distribution is shown as bar histogram.

Figure S1: Bayesian Skyline Plot generated with mitochondrial data for *C. greeningi* populations one (A) and two (B), and *Corythomantis* sp. (C). The y-axis is the effective population size, the x-axis is the time scale in years read from the present (left) to the past (right). The black line shows the median population size and the confidence intervail is in blue (95% HPD).

Figure S2: Divergence time estimated in *BEAST with different datasets. (A) 16S and nuclear data, (B) COI and nuclear data, and (C) concatenated mitochondrial data and nuclear data. (D) shows DensiTree plot showing all possible dates for this inference. X-axis show the timescale in millions of years and the blue bars are the 95% HPD.

Figure S3: Principal Components Analysis plots (PC1 X PC2 and PC1 X PC3) derived from the simulated and observed data derived from models 1, 2, and 3.

Figure S4: Principal Components Analysis plots (PC1 X PC2 and PC1 X PC3) derived from the simulated and observed data derived from models 4, 5, and 6.

Capítulo III:

Figure 1: Holotype of *Corythomantis "espinhaço"* sp. nov. (adult male, CHUFPB 28228, snout-vent length = 63.4 mm): Dorsal (A) and ventral (B) views of whole specimen; ventral views of left hand (C) and foot (D); dorsal (E) and lateral (F) views of the head.

Figure 2: Live paratopotypes of *Corythomantis "espinhaço"* sp. nov. from Palmeiras municipality, state of Bahia, Brazil: (A) adult female (CHUFPB 30496), (B) adult male (CHUFPB 30489), (C) male and female (CHUFPB 28232 and 28236) in axillary amplexus, and (D) live tadpole on a rocky stream. Photo C by Willianilson Pessoa.

Figure 3: Comparison of thigh coloration on males of *Corythomantis "espinhaço"* sp. nov. and *C. greeningi* with different SVL size. Unblotched pattern in specimens of *C. "espinhaço"* sp. nov.: (A)

59.8 mm SVL (UFV 11705 from Buritizeiro, Minas Gerais state), (B) 65.9 mm SVL (CFBH 10213 from Grão Mogol, Minas Gerais state), and (C) 63.4 mm SVL (holotype CHUFPB 28228 from Palmeiras, Bahia state). Blotched pattern in specimens of *C. greeningi*: (D) 56.7 mm SVL (UFG 9067 from Taipas, Tocantins state), (E) 72.4 mm SVL (CHUFPB 28309 from Umburanas, Bahia state), and (F) 81.1 mm SVL (CHUFPB 28283 from Buíque, Pernambuco state). Females have the same pattern.

Figure 4: Morphological differences between the heads of *Corythomantis* species. Dorsal (top) and profile (bottom) views of the head of *C. "espinhaço"* males (A; holotype CHUFPB 28228 and 28229) and females (B; CHUFPB 28235 and CFBH 30089) and *C. greeningi* males (C; CHUFPB 28284 and 28291) and females (D; CHUFPB 28277 and 28295). We highlight the *canthus rostralis* ridge (a) and nostril-snout distance (b) on both species.

Figure 5: Comparative oscillogram (top) and audiospectrogram (bottom) from the advertisement calls of the holotype CHUFPB 28228 of *Corythomantis "espinhaço"* sp. nov. (A; ASUFRN660) and *C. greeningi* (B; SUFBA263) with notes divided into group one (a) and group two (b).

Figure 6: Distribution map of *Corythomantis "espinhaço"* sp. nov. (circles, red star is the type locality) and *C. greeningi* (squares). Localities with green coloration show we used morphological data on post-metamorphic and tadpoles, or molecular data, blue coloration show we used morphological data on post-metamorphic and molecular data, white are potential localities for *C. "espinhaço"* based on literature records (see discussion), and black are literature records. Gameleira do Assuruá (1), Palmeiras (2), Contendas do Sincorá (3), Grão Mogol (4), Leme do Prado (5), Buenópolis (6), Buritizeiro (7), and Três Marias (8).

Figure 7: Habitat of *Corythomantis "espinhaço"* sp. nov. in the type locality of Palmeiras, Bahia state.

Figure 8: Profile (A), dorsal view (B), ventral view (C), and (D) external oral morphology of the tadpole of *Corythomantis "espinhaço"* sp. nov. in stage 36 in Gosner classification (CHUFPB 30501). (E) show the same tadpole of *C. "espinhaço"* sp. nov. (top) at stage 36 from the type locality (CHUFPB 30501) and *C. greeningi* (bottom) at stage 37 from Morro do Chapéu, Bahia state (CHUFPB 30500). Both tadpoles were sequenced for this study.

Figure 9: Resulting Bayesian mitochondrial gene tree placing *Corythomantis "espinhaço"* sp. nov. among other species of Lophyohylini. Numbers near tree nodes show the posterior probability. Terminals of *C. greeningi* and *Nyctimantis galeata* were collapsed for better understanding.

Figure 10: Holotype of *Corythomantis greeningi* (BMNH 1947.2.25.97) deposited in the British Museum of London. (A) Dorsal view of the head, and (B) ventral view with blotched pattern in tibia highlighted by the red arrow. Photos by Gabriela Bittencourt-Silva.

LISTA DE TABELAS

Capítulo I:

Capítulo II:

Table 2: Summary statistics information for the sequenced genes in *C. greeningi* (populations one and two) and *Corythomantis* sp. (Espinhaço population). Number of base pairs (bp), number of sequences used (N), segregating sites (S), number of haplotypes (h), haplotype diversity (Hd), standard deviation of haplotype diversity (SDHd), nucleotide diversity (pi), Tajima's D (D) and its main p value. (*) Phased sequences.

Table 3. Posterior probabilities of model comparison using approximate Bayesian computation (ABC). The best-fit model is highlight in bold. A tolerance of 0.01 and 0.1 were used in the comparisons for the rejection and Mnlogistic, respectively.

Table S1: Respective locus, its source material, primer label and sequence fragment for all five loci.

Table S2: Detailed PCR cycles for all five loci with the respective temperature and duration of each stage. (*) Touchdown.

Table S3: List of samples used for molecular data from *Corythomantis greeningi* (Cg), *Corythomantis* sp. (Csp) and *Trachycephalus typhonius* (Tt). Respective Genbank deposit number for each gene, the main locality and its acronym, respective state and coordinates.

Table S4: Additional distribution records of *Corythomantis greeningi* used in the Ecological Niche Modeling and its respective source material.

Capítulo III:

Table 1: List of specimens, respective localities, voucher numbers, and Genbank accession number for 16S and COI used in gene tree estimation. Dashes are unavailable sequences. Dashes are not sequenced molecular markers. To be submitted upon acceptance (TBS).

Table 2: Morphometric measurements (mm) of the type series of *Corythomantis "espinhaço"* sp. nov. and *C. greeningi*. Values are presented as mean ± standard deviation (range). Snout-vent length (SVL), head width (HW), comissure of the mouth to the tip of the snout (CMS), tympanum diameter (TD), eye diameter (ED), eye-nostril distance (END), eye-snout distance (ESD), nostril-snout distance (ESD), nostril-snout distance (NSD), interorbital distance (IOD), internasal distance (IND), elbow to finger III length (EFIII), hand length (HaL), tibia length (TL), foot length (FL), and thigh length (ThL).

Table 3: Parameters of the advertisement call of the holotype of *Corythomantis "espinhaço"* sp. nov. and advertisement calls of *Corythomantis greeningi* from different localities within Caatinga domain. Mean ± SD (min–max). (*) sequenced specimens.

Table 4: Measurements of tadpoles (mm) of *Corythomantis "espinhaço"* sp. nov. Values are presented as mean ± standard deviation (range). Total length (TTL), body length (BL), body width (BW), body height (BH), tail length (TAL), tail muscle height (TMH), tail muscle width (TMW), maximum tail height (MTH), upper fin height (UFH), lower fin height (LFH), internostril distance (IND), interorbital distance (IOD), eye diameter (ED), nostril diameter (ND), eye-nostril distance (EN), nostril-snout distance (NS), eye-snout distance (ES), snout-spiracle distance (SS), body end to center of spiracle (BS), and oral disc width (ODW).

SUMÁRIO

INTRODUÇÃO GERAL

A Caatinga na Diagonal de Formações Abertas da América do Sul

Durante anos, a Caatinga foi a região menos estudada quando comparada às regiões brasileiras florestadas e acreditava-se que sua biodiversidade era pobre e sem endemismos, supostamente um reflexo do seu clima árido e seco (VANZOLINI et al., 1963; RODRIGUES, 2003; LEAL et al., 2005). Nos últimos anos o cenário se inverteu e hoje é evidente como sua riqueza de espécies foi subestimada, agregando riqueza considerável para todos os grupos de vertebrados (GARDA et al., 2018). A Caatinga é o único bioma exclusivamente brasileiro, situado na porção nordeste do país e do continente sul-americano. Sua extensão original ocupava 844.463 km^2, mas processos antrópicos (*e.g.* fragmentação, pecuária, agricultura) têm reduzido seu território (IBGE, 2017; ANTONGIOVANNI; VENTICINQUE; FONSECA, 2018). A média de temperatura varia de 27 a 29 ºC em sua extensão (AB'SABER, 1998). Sua vegetação é majoritariamente aberta e xerófita, estratificada de arbusto a florestas adaptadas a baixa precipitação, alta incidência solar e ao clima semi-árido (DA SILVA; LEAL; TABARELLI, 2017; PRADO, 2003). Ela integra a diagonal de formações abertas. Uma macroregião rica em fitofisionomias, clima e biota, que cruza o continente sul-americano desde o nordeste brasileiro ao norte da Argentina e países adjacentes, composta pelo Chaco, Cerrado e Caatinga (WERNECK, 2011).

A extensão da Caatinga é composta principalmente por áreas de baixadas e planícies, com alguns afloramentos montanhosos (*e.g.* Chapada da Borborema, Chapada do Araripe, Planalto do Ibiapaba) (AB'SABER, 1949). Algumas destas cadeias montanhosas estão associadas a florestas úmidas, conhecidas como brejos de altitude, relictos de tempos passados. Durante o Pleistoceno, no período Quaternário, há documentação de oscilações climáticas, cuja consequência para os biomas neotropicais foram a expansão de biomas secos e retração de florestas em períodos secos e frios, e a expansão de florestas e retração de biomas áridos durante períodos quentes e úmidos (HAFFER, 1969; PENNINGTON; PRADO; PENDRY, 2000; WANG et al., 2004). Durante as retrações, relictos florestais permaneceram na Caatinga e são como ilhas de biodiversidade que agregam grande parte das espécies endêmicas do bioma, assim como uma parcela da biota de biomas vizinhos, além de ter papel fundamental nos processos de especiação na biota da diagonal de formações abertas (CARNAVAL, 2002; CASTRO et

al., 2019). O conhecimento acerca dos padrões e processos na Caatinga ainda são incipientes, mas inferências nestes aspectos têm aumentado nos últimos anos.

Processos de especiação e filogeografia neotropical

Estudar a história evolutiva das espécies aliada aos conhecimentos biogeográficos é fundamental para compreender o atual cenário da biodiversidade mundial. São inúmeros os tipos de especiação aplicado aos organismos, que estão relacionados a eventos vicariantes, segregação de indivíduos com e sem fluxo gênico, simpátricos ou não, sob efeitos ecológicos e outros (VENCES; WAKE, 2007). Desta maneira, é possível compreender ou propor cenários de diversificação que levaram milhões de anos para moldar um determinado grupo. A curto prazo, o processo de especiação pode resultar em novos caracteres externos à morfologia de alguns organismos (*e.g.* genética, comportamento). Em contrapartida, modificações morfológicas nem sempre se manifestam de forma acentuada devido ao conservatismo fenotípico, ou em grupos de especiação recente, como em alguns anfíbios, e nos faz recorrer a métodos moleculares (*e.g.* DNA mitocondrial) para detectar divergência entre as espécies (BICKFORD et al., 2007; MOEN; IRSCHICK; WIENS, 2013). Desta forma, um método em ascensão para este fim é a filogeografia, surgida nas últimas décadas para estudar aspectos intraespecíficos de complexos de espécies ou espécies isoladas em relação ao meio geográfico onde são encontradas (AVISE, 2000). Assim, é possível testar diversas hipóteses de variações genéticas intrapopulacionais, identificar centros de origem, avaliar dispersão e especiação dos organismos ou até questionar espécies com distribuição ampla (AVISE, 2009; HICKERSON et al., 2009).

Espécies com distribuições amplas geralmente habitam diferentes ambientes e regiões, tendo pouco peso na seleção de áreas potenciais para conservação (ANGULO; ICOCHEA, 2010; STUART et al., 2004). Precisamos recorrer à taxonomia integrativa, através de diferentes métodos na delimitação de espécies (*i.e.* moleculares, bioacústicos e morfológicos) para assegurar se um táxon está de fato ocupando uma área geograficamente extensa ou se dentro deste limite é encontrado um complexo de espécies crípticas (CAMARGO; DE SÁ; HEYER, 2006; DAYRAT, 2005; PADIAL et al., 2010). Desta forma, espécies não descritas e de distribuição restrita podem se tornar endêmicas de uma região, tornando-se vulneráveis a ações antrópicas, havendo necessidade de proteger os locais que habitam para que não sejam extintas.

Neste sentido, estudos filogenéticos e filogeográficos têm se tornado cada vez mais frequentes com plantas, invertebrados e diferentes grupos de vertebrados (BARTOLETI et al., 2018; BATALHA-FILHO et al., 2013; BITENCOURT; RAPINI, 2013; NASCIMENTO et al., 2013; SANTOS et al., 2014). Ao considerar anfíbios, estes estudos utilizam a taxonomia integrativa para resolver problemas taxonômicos e descrições de novas espécies em diversas famílias (*e.g.* Bufonidae, PRAMUK, 2006; Centrolenidae, GUAYASAMIN et al., 2009; Hylidae, FAIVOVICH et al., 2005; GARDA; CANNATELLA, 2007, FAIVOVICH et al., 2010, DUELLMAN; MARION; HEDGES, 2016; Microhylidae, DE SÁ et al., 2012, PELOSO et al., 2014; Leptodactylidae, FAIVOVICH et al., 2012, Phyllomedusidae, DUELLMAN; BARLEY; VENEGAS, 2014) ou mesmo para filogenia de anfíbios (PYRON; WIENS, 2011); a delimitação de espécies amplamente distribuídas, muitas vezes revela variações taxonômicas e a presença de espécies crípticas no mesmo táxon (CAMARGO; DE SÁ; HEYER, 2006; GEHARA et al., 2013, 2014); e estudar a história evolutiva das espécies diante de eventos histórico-geográficos (CARNAVAL, 2002; GARDA; CANNATELLA, 2007; PRADO; HADDAD; ZAMUDIO, 2012; SANTANA, 2013; MENEZES et al., 2016; THOMÉ et al., 2016; MÂNGIA et al., 2020; CAMURUGI, 2018; BRUSQUETTI et al., 2019; OLIVEIRA et al., 2018; VASCONCELLOS et al., 2019). De modo geral, trabalhos filogeográficos na diagonal de formações abertas ainda são menos frequentes se comparados a habitats florestados, mas têm aumentado nos últimos anos.

Estudos filogeográficos em ambientes florestados têm revelado estruturação genética associada a fragmentos florestais e áreas de refúgio (CARNAVAL, 2002; CARNAVAL et al., 2009), em áreas com topografia variada (GEHARA et al., 2013) e rios (MENEZES et al., 2016). Estudos de mesma natureza na diagonal de formações abertas tem encontrado diferentes padrões para anfíbios, com estruturação de linhagens e populações em função de aspectos vicariantes, eventos climáticos históricos ou associados a aspetos ecológicos (GARDA & CaANNATELLA, 2007; PRADO et al., 2012; SANTANA, 2013; OLIVEIRA et al., 2018). Por outro lado, as formações abertas da diagonal abrigam também espécies amplamente distribuídas, estruturadas em uma única população ou várias populações (THOMÉ et al., 2016; MÂNGIA et al., 2020; CAMURUGI, 2018; BRUSQUETTI et al., 2019). Em todos os casos, eventos climáticos do Pleistoceno atuaram sobre as espécies, seja a nível de especiação, seja a nível de alteração demográfica.

Anfíbios anuros e espécies modelo deste estudo

A perda da biodiversidade é um problema global, e para garantir a manutenção do patrimônio natural, comumente são necessários esforços de priorização (*e.g. Hotspots* da biodiversidade e unidades de conservação integral em países megadiversos), requerendo esforços para conservação das espécies e seus habitats (BROOKS et al., 2006; BROOKS, 2010). Um dos maiores desafios para essas priorizações é a necessidade de mapear corretamente as áreas de ocorrência do maior número possível de espécies, os ambientes que elas habitam e os processos evolutivos dos diferentes grupos (MACE; PURVIS, 2008). PYRON; WIENS (2013) reforçam que um dos principais padrões biogeográficos para megadiversidade de anfíbios na região Neotropical está relacionada a altas taxas de especiação e baixas de extinção.

São conhecidas mais de 8.000 espécies de anfíbios, das quais 7.058 correspondem a anfíbios anuros (FROST, 2019). No entanto, no cenário global as populações desse grupo biodiverso encontram-se em declínio e ameaçadas de extinção por fatores climáticos, antrópicos e patológicos (BIODIVERSITY, 2005; STUART et al., 2004; TOLEDO et al., 2006). Desta forma, medidas emergenciais e colaborativas para reverter esta lacuna são fundamentais, visto a possibilidade que novas espécies desapareçam antes mesmo de chegar ao conhecimento da comunidade científica (CRAWFORD; LIPS; BERMINGHAM, 2010). Reconhecer as linhagens independentes e destrinchar um único táxon utilizando os adventos da taxonomia integrativa auxilia a definir centros de endemismo e o preciso status de conservação desses animais (GEHAGA et al., 2014). Em suma, estudos filogeográficos têm se tornado a chave para o conhecimento pleno da origem, da evolução e dos limites de distribuição das espécies. A partir destas informações, selecionamos duas espécies de anfíbios anuros com biologia distinta e de distribuição geográfica semelhante, presentes majoritariamente na Caatinga e áreas circunvizinhas, para averiguar aspectos de sua história evolutiva.

Na família Hylidae, dentre as perereca-cabeça-de-capacete da tribo Lophyohylini, *Corythomantis greeningi* Boulenger 1896 é uma espécie monotípica e distribuída por toda a Caatinga, limitada ao sul pelo estado de Minas Gerais e a oeste, no Cerrado, ao estado do Tocantins (GODINHO; MOURA; FEIO, 2013). Habitam preferencialmente riachos em afloramentos rochosos, onde se reproduzem de forma explosiva durante a estação chuvosa, enquanto em períodos de inatividade, se alojam nas fendas das rochas ou troncos

(JARED et al., 1999). Seus girinos possuem adaptações orais para se fixarem em ambientes lóticos (JUNCÁ; CARNEIRO; RODRIGUES, 2008). A primeira inferência sobre uma possível variação na espécie foi feito por JUNCÁ et al. (2008) que investigaram espécimes de tamanhos distintos em duas localidades no estado da Bahia, mas a análise acústica entre os dois locais confirmou que em ambas se tratava de *C. greeningi*. POMBAL JR. et al., (2012) descreveram uma segunda espécie para o gênero *Corythomantis* com dados morfológicos para o município de Morro do Chapéu, no estado da Bahia. Contudo, o estudo filogenético da tribo Lophyohylini mostrou que esta espécie está incluída em outro gênero, mantendo *Corythomantis* como monotípico (BLOTTO et al., 2020). Apesar da ampla distribuição, tais características indicam que esta espécie não seja grande dispersora, devido a forte associação a um tipo de habitat. Neste cenário, espera-se que haja estruturação genética ao longo de sua distribuição.

Em contrapartida, *Rhinella jimi* (STEVAUX, 2002) é um bufonídeo de grande porte distribuído em áreas abertas da Caatinga e Mata Atlântica, desde o norte do Espírito Santo ao estado do Pará (STEVAUX, 2002; VALENCIA-ZULETA; MACIEL, 2017). Está inserido no complexo de espécies *Rhinella marina* junto com outras nove espécies (*R. diptycha*, *R. marina*, *R. poeppigii*, *R. cerradensis*, *R. veredas*, *R. icterica*, *R. achavali*, *R. rubescens*, *R. arenarum*; MACIEL et al., 2010). Sua dieta é generalista e seu modo reprodutivo é explosivo sem restrição local, aproveitando poças de água formadas por chuvas esporádicas para depositar seus ovos (STEVAUX, 2002). Não existem estudos que versem sobre a capacidade dispersiva desta espécie. Contudo, *R. jimi* apresenta características atribuídas a espécies com alta dispersão (*e.g.* dieta generalista, corpo grande e robusto, pele grossa e resistente a perda de água; BROWN; STEVENS; KAUFMAN, 1996). Ainda, seu congenero *R. marina* foi introduzido no continente australiano em 1935 visando controlar insetos praga em plantações de cana-de-açúcar (PHILLIPS et al., 2006). Seus hábitos generalistas fizeram com que se adaptasse localmente e hoje é uma espécie invasora com alto poder dispersivo naquele país (PHILLIPS et al., 2006; URBAN et al., 2008). Devido a proximidade filogenética entre as espécies, espera-se que *R. jimi* tenha a mesma capacidade dispersiva.

Desta forma, utilizamos espécies da Caatinga com ampla distribuição geográfica e modo reprodutivo similar (reprodução explosiva), que diferem no sítio reprodutivo e capacidade dispersiva, além de possuírem necessidades biológicas e ecológicas distintas. É possível que estas espécies tenham sido expostas aos mesmos eventos histórico-

geográficos na Caatinga, podendo responder de formas distintas quanto à estruturação genética a nível populacional ou a nível de espécie, além de alterações populacionais decorrente de mudanças climáticas e na paisagem. A investigação destes aspectos podem elucidar como estes eventos moldaram a história evolutiva destas espécies e contribuir para o conhecimento evolutivo dos anuros e biomas neotropicais. Esta tese está estruturada em três capítulos, sendo o primeiro capítulo intitulado "The evolutionary history of the Cururu Toad *Rhinella jimi* (Stevaux, 2002) in Northeast Brazil" onde abordamos a filogeografia de *Rhinella jimi*; o segundo capítulo intitulado "Past São Francisco River course, altitude isolation, and ecological traits as the evolutionary history plot for *Corythomantis greeningi* Boulenger 1896 (Anura, Hylidae) in dry biomes of Neotropical Region" que versa sobre a filogeografia de *Corythomantis greeningi*; e finalmente o terceiro capítulo intitulado "There and Back Again From Monotypy: A New Species of the Casque-headed *Corythomantis* Boulenger 1896 (Anura, Hylidae) from the Espinhaço Mountain Range, Brazil", com a descrição de uma nova espécie de *Corythomantis* através de taxonomia integrativa.

Referências

ANGULO, Ariadne; ICOCHEA, Javier. Cryptic species complexes, widespread species and conservation: Lessons from Amazonian frogs of the *Leptodactylus marmoratus* group (Anura: Leptodactylidae). **Systematics and Biodiversity**, *[S. l.]*, v. 8, n. 3, p. 357–370, 2010. DOI: 10.1080/14772000.2010.507264.

ANTONGIOVANNI, Marina; VENTICINQUE, Eduardo M.; FONSECA, Carlos Roberto. Fragmentation patterns of the Caatinga drylands. **Landscape Ecology**, *[S. l.]*, v. 33, n. 8, p. 1353–1367, 2018. DOI: 10.1007/s10980-018-0672-6.

AVISE, J. C. **Phylogeography: The History and Formation of SpeciesAmerican Zoologist**, 2000. DOI: 10.1668/0003-1569(2001)041[0134:BR]2.0.CO;2.

AVISE, John C. Phylogeography: Retrospect and prospect. **Journal of Biogeography**, *[S. l.]*, v. 36, n. 1, p. 3–15, 2009. DOI: 10.1111/j.1365-2699.2008.02032.x.

BARTOLETI, Luiz Filipe de Macedo; PERES, Elen Arroyo; FONTES, Fernanda von Hertwig Mascarenhas; DA SILVA, Márcio José; SOLFERINI, Vera Nisaka. Phylogeography of the widespread spider Nephila clavipes (Araneae: Araneidae) in South America indicates geologically and climatically driven lineage diversification. **Journal of Biogeography**, *[S. l.]*, v. 45, n. 6, p. 1246–1260, 2018. DOI: 10.1111/jbi.13217.

BATALHA-FILHO, Henrique; FJELDSÅ, Jon; FABRE, Pierre-Henri; MIYAKI, Cristina Yumi. Connections between the Atlantic and the Amazonian forest avifaunas represent distinct historical events. **Journal of Ornithology**, *[S. l.]*, v. 154, n. 1, p. 41–50, 2013. DOI: 10.1007/s10336-012-0866-7. Disponível em: http://link.springer.com/10.1007/s10336-012-0866-7.

BICKFORD, David; LOHMAN, David J.; SODHI, Navjot S.; NG, Peter K. L.; MEIER, Rudolf; WINKER, Kevin; INGRAM, Krista K.; DAS, Indraneil. Cryptic species as a window on diversity and conservation. **Trends in Ecology and Evolution**, *[S. l.]*, v. 22, n. 3, p. 148–155, 2007. DOI: 10.1016/j.tree.2006.11.004.

BIODIVERSITY, Animal. Climate change and amphibians P. S. Corn. **Animal Biodiversity and Conservation**, *[S. l.]*, v. 1, p. 59–67, 2005.

BITENCOURT, Cássia; RAPINI, Alessandro. Centres of Endemism in the Espinhaço Range: identifying cradles and museums of Asclepiadoideae (Apocynaceae). **Systematics and Biodiversity**, *[S. l.]*, v. 11, n. 4, p. 525–536, 2013. DOI: 10.1080/14772000.2013.865681. Disponível em: http://www.tandfonline.com/doi/abs/10.1080/14772000.2013.865681.

BLOTTO, Boris L. et al. The phylogeny of the Casque-headed Treefrogs (Hylidae: Hylinae: Lophyohylini). **Cladistics**, *[S. l.]*, p. 1–37, 2020. DOI: 10.1111/cla.12409. Disponível em: http://doi.wiley.com/10.1111/cla.12409.

BROOKS, T. M.; MITTERMEIER, R. A.; DA FONSECA, G. A. B.; GERLACH, J.; HOFFMANN, M.; LAMOREUX, J. F.; MITTERMEIER, C. G.; PILGRIM, J. D.; RODRIGUES, A. S. L. Global biodiversity conservation priorities. **Science**, *[S. l.]*, v. 313, n. 5783, p. 58–61, 2006. DOI: 10.1126/science.1127609.

BROWN, James H.; STEVENS, George C.; KAUFMAN, Dawn M. The Geographic Range: Size, Shape, Boundaries, and Internal Structure. **Annual Review of Ecology and Systematics**, *[S. l.]*, v. 27, n. 1, p. 597–623, 1996. DOI: 10.1146/annurev.ecolsys.27.1.597.

BRUSQUETTI, Francisco; NETTO, Flavia; BALDO, Diego; HADDAD, Célio F. B. The influence of Pleistocene glaciations on Chacoan fauna: Genetic structure and historical demography of an endemic frog of the South American Gran Chaco. **Biological Journal of the Linnean Society**, *[S. l.]*, v. 126, n. 3, p. 404–416, 2019. DOI: 10.1093/biolinnean/bly203.

CAMARGO, Arley; DE SÁ, Rafael O.; HEYER, W. Ronald. Phylogenetic analyses of mtDNA sequences reveal three cryptic lineages in the widespread neotropical frog *Leptodactylus fuscus* (Schneider, 1799) (Anura, Leptodactylidae). **Biological Journal of the Linnean Society**, *[S. l.]*, v. 87, n. 2, p. 325–341, 2006. DOI: 10.1111/j.1095-8312.2006.00581.x.

CARNAVAL, A. C. O. Q. Phylogeography of four frog species in forest fragments of Northeastern Brazil - A preliminary study. **Integrative and Comparative Biology**, *[S. l.]*, v. 42, n. 5, p. 913–921, 2002. DOI: 10.1093/icb/42.5.913. Disponível em: https://academic.oup.com/icb/article-lookup/doi/10.1093/icb/42.5.913.

CARNAVAL, Ana Carolina; HICKERSON, Michael J.; HADDAD, C. F. B.; RODRIGUES, Miguel T.; MORITZ, Craig. Stability predicts genetic diversity in the Brazilian Atlantic forest hotspot. **Science**, *[S. l.]*, v. 323, n. 5915, p. 785–789, 2009. DOI: 10.1126/science.1166955. Disponível em: https://www.sciencemag.org/lookup/doi/10.1126/science.1166955.

CASTRO, Deborah P.; RODRIGUES, João Fabrício M.; BORGES-LEITE, Maria Juliana; LIMA, Daniel Cassiano; BORGES-NOJOSA, Diva Maria. Anuran diversity indicates that Caatinga relictual Neotropical forests are more related to the Atlantic Forest than to the Amazon. **PeerJ**, *[S. l.]*, v. 6, p. e6208, 2019. DOI: 10.7717/peerj.6208.

CRAWFORD, Andrew J.; LIPS, Karen R.; BERMINGHAM, Eldredge. Epidemic disease decimates amphibian abundance , species diversity , and evolutionary history in the highlands of central Panama. **Proceedings of the National Academy of Sciences**, *[S. l.]*, v. 107, n. 31, p. 13777–13782, 2010. DOI: 10.1073/pnas.0914115107.

DA SILVA, José Maria Cardoso; LEAL, Inara R.; TABARELLI, Marcelo. **Caatinga: The largest Tropical Dry Forest Region on South America**. First edit ed. [s.l.] : Springer International Publishing, 2017.

DAYRAT, Benoit. Towards integrative taxonomy. **Biological Journal of the Linnean Society**, *[S. l.]*, v. 85, p. 407–415, 2005.

DE SÁ, Rafael O.; STREICHER, Jeffrey W.; SEKONYELA, Relebohile; FORLANI, Mauricio C.; LOADER, Simon P.; GREENBAUM, Eli; RICHARDS, Stephen; HADDAD, Célio F. B. Molecular phylogeny of microhylid frogs (Anura: Microhylidae) with emphasis on relationships among New World genera. **BMC evolutionary biology**, *[S. l.]*, v. 12, p. 241, 2012. DOI: 10.1186/1471-2148-12-241.

DUELLMAN, William E.; BARLEY, Anthony J.; VENEGAS, Pablo J. Cryptic species diversity in marsupial frogs (Anura: Hemiphractidae: Gastrotheca) in the Andes of northern Peru. **Zootaxa**, *[S. l.]*, v. 3768, n. 2, p. 159–177, 2014. DOI: 10.11646/zootaxa.3768.2.4.

DUELLMAN, William E.; MARION, Angela B.; HEDGES, S. Blair. Phylogenetics, classification, and biogeography of the treefrogs (Amphibia: Anura: Arboranae). **Zootaxa**, *[S. l.]*, v. 4104, n. 1, p. 1–109, 2016. DOI: 10.11646/zootaxa.4104.1.1.

FAIVOVICH, Julián et al. The phylogenetic relationships of the charismatic poster frogs, Phyllomedusinae (Anura, Hylidae). **Cladistics**, *[S. l.]*, v. 26, p. 227–261, 2010.

FAIVOVICH, Julián; FERRARO, Daiana P.; BASSO, Néstor G.; HADDAD, Célio Fernando Baptista; RODRIGUES, Miguel Trefaut; WHEELER, Ward C.; LAVILLA, Esteban O. A phylogenetic analysis of Pleurodema (Anura : Leptodactylidae : Leiuperinae) based on mitochondrial and nuclear gene sequences ,. **Cladistics**, *[S. l.]*, v. 1, p. 1–23, 2012. DOI: 10.1111/j.1096-0031.2012.00406.x.

FAIVOVICH, Julián; HADDAD, Célio F. B.; GARCIA, Paulo F. B.; FROST, Darrel R.; CAMPBELL, Jonathan A.; WHEELER, Ward C. Systematic Review Of The Frog Family Hylidae, With Special Reference To Hylinae: Phylogenetic Analysis And Taxonomic Revision. **Bulletin of the American Museum of Natural History**, *[S. l.]*, n. 294, p. 240, 2005.

GARDA, Adrian A.; CANNATELLA, David C. Phylogeny and biogeography of paradoxical frogs (Anura, Hylidae, Pseudae) inferred from 12S and 16S mitochondrial DNA. **Molecular Phylogenetics and Evolution**, *[S. l.]*, v. 44, n. 1, p. 104–114, 2007. DOI: 10.1016/j.ympev.2006.11.028.

GARDA, Adrian Antonio; LION, Marília Bruzzi; LIMA, Sérgio Maia de Queiroz; MESQUITA, Daniel Oliveira; ARAUJO, Helder Farias Pereira De; NAPOLI, Marcelo Felgueiras. Os animais vertebrados do Bioma Caatinga. **Ciência e Cultura**, *[S. l.]*, v. 70, n. 4, p. 29–34, 2018. DOI: 10.21800/2317-66602018000400010. Disponível em: http://cienciaecultura.bvs.br/scielo.php?script=sci_arttext&pid=S0009-67252018000400010&lng=pt&tlng=pt.

GEHARA, Marcelo et al. High levels of diversity uncovered in a widespread nominal taxon: Continental phylogeography of the neotropical tree frog *Dendropsophus minutus*. **PLoS ONE**, *[S. l.]*, v. 9, n. 9, p. e103958, 2014. DOI: 10.1371/journal.pone.0103958.

GEHARA, Marcelo; CANEDO, Clarissa; HADDAD, Célio F. B.; VENCES, Miguel. From widespread to microendemic: Molecular and acoustic analyses show that *Ischnocnema guentheri* (Amphibia: Brachycephalidae) is endemic to Rio de Janeiro, Brazil. **Conservation Genetics**, *[S. l.]*, v. 14, n. 5, p. 973–982, 2013. DOI: 10.1007/s10592-013-0488-5.

GODINHO, Leandro Braga; MOURA, Mario Ribeiro; FEIO, Renato Neves. New records and geographic distribution of Corythomantis greeningi Boulenger, 1896 (Amphibia: Hylidae). **Check List**, *[S. l.]*, v. 9, n. 1, p. 148–150, 2013. DOI: 10.15560/9.1.148.

GUAYASAMIN, Juan M.; CASTROVIEJO-FISHER, Santiago; TRUEB, Linda; AYARZAGÜENA, José; RADA, Marco; VILÀ, Carles. **Phylogenetic systematics of Glassfrogs (Amphibia: Centrolenidae) and their sister taxon Allophryne ruthveni**. [s.l: s.n.]. v. 2100

HAFFER, Jürgen. Speciation in Amazonian Forest Birds. **Science**, *[S. l.]*, v. 165, n. 3889, p. 131–138, 1969.

HICKERSON, M. J.; CARSTENS, B. C.; CAVENDER-BARES, J.; CRANDALL, K. A.; GRAHAM, C. H.; JOHNSON, J. B.; RISSLER, L.; VICTORIANO, P. F.; YODER, A. D. Phylogeography's past, present, and future: 10 years after Avise, 2000. **Molecular Phylogenetics and Evolution**, *[S. l.]*, v. 54, n. 1, p. 291–301, 2009. DOI: 10.1016/j.ympev.2009.09.016.

JARED, Carlos; ANTONIAZZI, Marta Maria; KATCHBURIAN, Eduardo; TOLEDO, Reynaldo Cicero; FREYMÜLLER, Edna. Some aspects of the natural history of the casque-headed tree frog Corythomantis greeningi Boulenger (Hylidae). **Annales des Sciences Naturelles - Zoologie et Biologie Animale**, *[S. l.]*, n. 3, p. 105–115, 1999. DOI: 10.1016/s0003-4339(00)86975-0.

JUNCÁ, Flora Acuña; CARNEIRO, Maria Conceição Lago; RODRIGUES, Nayara Nascimento. Is a dwarf population of Corythomantis greeningi Boulenger, 1896 (Anura, Hylidae) a new species? **Zootaxa**, *[S. l.]*, v. 1686, p. 48–56, 2008.

LEAL, Inara R.; DA SILVA, José Maria Cardoso; TABARELLI, Marcelo; LACHER, Thomas E. Changing the course of biodiversity conservation in the caatinga of northeastern Brazil. **Conservation Biology**, *[S. l.]*, v. 19, n. 3, p. 701–706, 2005. DOI: 10.1111/j.1523-1739.2005.00703.x.

MACE, Georgina M.; PURVIS, Andy. Evolutionary biology and practical conservation : bridging a widening gap. **Molecular Ecology**, *[S. l.]*, v. 17, p. 9–19, 2008. DOI: 10.1111/j.1365-294X.2007.03455.x.

MACIEL, Natan Medeiros; COLLEVATTI, Rosane Garcia; COLLI, Guarino Rinaldi; SCHWARTZ, Elisabeth Ferroni. Late Miocene diversification and phylogenetic relationships of the huge toads in the Rhinella marina (Linnaeus, 1758) species group (Anura: Bufonidae). **Molecular Phylogenetics and Evolution**, *[S. l.]*, v. 57, n. 2, p. 787–797, 2010. DOI: 10.1016/j.ympev.2010.08.025. Disponível em: http://dx.doi.org/10.1016/j.ympev.2010.08.025.

MÂNGIA, Sarah; OLIVEIRA, Eliana Faria; SANTANA, Diego José; KOROIVA, Ricardo; PAIVA, Fernando; GARDA, Adrian Antonio. Revising the taxonomy of *Proceratophrys* Miranda-Ribeiro, 1920 (Anura: Odontophrynidae) from the Brazilian semiarid Caatinga: Morphology, calls and molecules support a single widespread species. **Journal of Zoological Systematics and Evolutionary Research**, *[S. l.]*, n. May 2019, p. jzs.12365, 2020. DOI: 10.1111/jzs.12365. Disponível em: https://onlinelibrary.wiley.com/doi/abs/10.1111/jzs.12365.

MENEZES, Lucas; CANEDO, Clarissa; BATALHA-FILHO, Henrique; GARDA, Adrian Antonio; GEHARA, Marcelo; NAPOLI, Marcelo Felgueiras. Multilocus phylogeography of the treefrog *Scinax eurydice* (Anura, Hylidae) reveals a plio-pleistocene diversification in the atlantic forest. **PLoS ONE**, *[S. l.]*, v. 11, n. 6, p. 1–20, 2016. DOI: 10.1371/journal.pone.0154626.

MOEN, Daniel S.; IRSCHICK, Duncan J.; WIENS, John J. Evolutionary conservatism and convergence both lead to striking similarity in ecology, morphology and performance across continents in frogs. **Proceedings of the Royal Society B: Biological Sciences**, *[S. l.]*, v. 280, n. 1773, p. 20132156, 2013. DOI: 10.1098/rspb.2013.2156. Disponível em: https://royalsocietypublishing.org/doi/10.1098/rspb.2013.2156.

NASCIMENTO, Fabrícia F.; LAZAR, Ana; MENEZES, Albert N.; DURANS, Andressa da Matta; MOREIRA, Jânio C.; SALAZAR-BRAVO, Jorge; DANDREA, Paulo S.; BONVICINO, Cibele R. The Role of Historical Barriers in the Diversification Processes in Open Vegetation Formations during the Miocene/Pliocene Using an Ancient Rodent Lineage as a Model. **PLoS ONE**, *[S. l.]*, v. 8, n. 4, 2013. DOI: 10.1371/journal.pone.0061924.

OLIVEIRA, Eliana F.; GEHARA, Marcelo; SÃO-PEDRO, Vinícius A.; COSTA, Gabriel C.; BURBRINK, Frank T.; COLLI, Guarino R.; RODRIGUES, Miguel T.; GARDA, Adrian A. Phylogeography of Muller's termite frog suggests the vicariant role of the Central Brazilian Plateau. **Journal of Biogeography**, *[S. l.]*, v. 45, n. 11, p. 2508–2519, 2018. DOI: 10.1111/jbi.13427. Disponível em: http://doi.wiley.com/10.1111/jbi.13427.

PADIAL, José M.; MIRALLES, Aurélien; DE LA RIVA, Ignacio; VENCES, Miguel. The integrative future of taxonomy. **Frontiers in Zoology**, *[S. l.]*, v. 7, p. 16, 2010.

PELOSO, Pedro Luiz Vieira; STURARO, Marcelo José; FORLANI, Mauricio C.; GAUCHER, Phillippe; MOTTA, Ana Paula; WHEELER, Ward C. Phylogeny, Taxonomic Revision, And Character Evolution Of The Genera *Chiasmocleis* And *Syncope* (Anura, Microhylidae) In Amazonia, With Descriptions Of Three New Species. **Bulletin of the American Museum of Natural History**, *[S. l.]*, n. 386, p. 1–111, 2014.

PENNINGTON, R. Toby; PRADO, Darién E.; PENDRY, Colin A. Neotropical seasonally dry forests and Quaternary vegetation changes. **Journal of Biogeography**, *[S. l.]*, v. 27, p. 261–273, 2000. DOI: 10.1046/j.1365-2699.2000.00397.x.

PHILLIPS, Benjamin L.; BROWN, Gregory P.; WEBB, Jonathan K.; SHINE, Richard. Invasion and the evolution of speed in toads. **Nature**, *[S. l.]*, v. 439, p. 2006, 2006. DOI: 10.1038/439803a.

POMBAL JR., José Perez; MENEZES, Vanderlaine Amaral; FONTES, Angélica Figueira; NUNES, Ivan; ROCHA, Carlos Frederico Duarte Da; SLUYS, Monique Van. A second species of the casque-headed frog genus Corythomantis (Anura: Hylidae) from northeastern Brazil, the distribution of C. greeningi, and comments. **Boletim Museu Nacional Rio de Janeiro**, *[S. l.]*, v. 530, p. 1–14, 2012.

PRADO, Cynthia P. A.; HADDAD, Célio F. B.; ZAMUDIO, Kelly R. Cryptic lineages and Pleistocene population expansion in a Brazilian Cerrado frog. **Molecular Ecology**, *[S. l.]*, v. 21, n. 4, p. 921–941, 2012. DOI: 10.1111/j.1365-294X.2011.05409.x.

PRADO, Darién E. As Caatingas da Américas do Sul. **Ecologia e Conservação da Caatinga**, *[S. l.]*, p. 3–73, 2003.

PRAMUK, Jennifer B. Phylogeny of South American *Bufo* (Anura: Bufonidae) inferred from combined evidence. **Zoological Journal of the Linnean Society**, *[S. l.]*, v. 146, n. 3, p. 407–452, 2006. DOI: 10.1111/j.1096-3642.2006.00212.x.

PYRON, Alexander R.; WIENS, John J. A large-scale phylogeny of Amphibia including over 2800 species, and a revised classification of extant frogs, salamanders, and caecilians. **Molecular Phylogenetics and Evolution**, *[S. l.]*, v. 61, n. 2, p. 543–583, 2011. DOI: 10.1016/j.ympev.2011.06.012.

PYRON, R. Alexander; WIENS, John J. Large-scale phylogenetic analyses reveal the causes of high tropical Large-scale phylogenetic analyses reveal the causes of high tropical amphibian diversity Receive free email alerts when new articles cite this article - sign up in the box at the top. **Proceedings of the Royal Society B: Biological Sciences**, *[S. l.]*, v. 280, p. 20131622, 2013. DOI: 10.1098/rspb.2013.1622.

RODRIGUES, M. T. Herpetofauna da Caatinga. **Ecologia e Conservação da Caatinga**, *[S. l.]*, v. 1, p. 181–236, 2003.

SANTOS, Marcella Gonçalves; NOGUEIRA, Cristiano; GIUGLIANO, Lilian Gimenes; COLLI, Guarino Rinaldi. Landscape evolution and phylogeography of Micrablepharus atticolus (Squamata, Gymnophthalmidae), an endemic lizard of the Brazilian Cerrado. **Journal of Biogeography**, *[S. l.]*, v. 41, n. 8, p. 1506–1519, 2014. DOI: 10.1111/jbi.12291. Disponível em: http://doi.wiley.com/10.1111/jbi.12291.

STEVAUX, Maria Nazaré. A new species of *Bufo* Laurenti (Anura, Bufonidae) from northeastern Brazil. **Revista Brasileira de Zoologia**, *[S. l.]*, v. 19, n. 1, p. 235–242, 2002.

STUART, Simon N. et al. **Disappearing Jewels: the status of New World Amphibians**. [s.l: s.n.].

THOMÉ, Maria Tereza C.; SEQUEIRA, Fernando; BRUSQUETTI, Francisco; CARSTENS, Bryan; HADDAD, Célio F. B.; RODRIGUES, Miguel Trefaut; ALEXANDRINO, João. Recurrent connections between Amazon and Atlantic forests shaped diversity in Caatinga four-eyed frogs. **Journal of Biogeography**, *[S. l.]*, v. 43, n. 5, p. 1045–1056, 2016. DOI: 10.1111/jbi.12685.

TOLEDO, Luís Felipe; BRITTO, Fábio B.; ARAÚJO, Olívia G. S. A.; GIASSON, Luís M. O. G.; HADDAD, Célio F. B. H. The Occurrence Of Batrachochytrium

dendrobatidis In Brazil And The Inclusion Of 17 New Cases Of Infection. **South American Journal of Herpetology**, *[S. l.]*, v. 1, n. 3, p. 185–191, 2006.

URBAN, Mark C.; PHILLIPS, Ben L.; SKELLY, David K.; SHINE, Richard. A Toad More Traveled : The Heterogeneous Invasion Dynamics of Cane Toads in Australia. **The American Naturalist**, *[S. l.]*, v. 171, n. 3, p. E134–E148, 2008. DOI: 10.1086/527494.

VASCONCELLOS, Mariana M.; COLLI, Guarino R.; ORTIZ, Edgardo M.; RODRIGUES, Miguel Trefaut. Isolation by instability: Historical climate change shapes population structure and genomic divergence of treefrogs in the Neotropical Cerrado savanna. **Molecular Ecology**, *[S. l.]*, v. In Press., 2019. DOI: 10.1111/mec.15045.

VENCES, Miguel; WAKE, David B. Speciation, species boundaries and phylogeography of amphibians. **Amphibian Biology**, *[S. l.]*, v. 7, n. 1997, p. 2613–2660, 2007.

WANG, Xianfeng; AULER, Augusto S.; EDWARDS, R. Lawrence; CHENG, Hai; CRISTALLI, Patricia S.; SMART, Peter L.; RICHARDS, David A.; SHEN, Chuan-Chou; EDWARDS, R. Lawrence. Wet periods in northeastern Brazil over the past 210 kyr linked to distant climate anomalies. **Nature**, *[S. l.]*, v. 432, n. December, p. 2767–2769, 2004. DOI: 10.1038/nature03067.

WERNECK, Fernanda P. The diversification of eastern South American open vegetation biomes: Historical biogeography and perspectives. **Quaternary Science Reviews**, *[S. l.]*, v. 30, n. 13–14, p. 1630–1648, 2011. DOI: 10.1016/j.quascirev.2011.03.009.

Capítulo I

A história evolutiva do sapo-cururu *Rhinella jimi* (Stevaux, 2002) no nordeste brasileiro

Manuscrito a ser submetido ao periódico Biological Journal of the Linnean Society

The evolutionary history of the Cururu Toad *Rhinella jimi* (Stevaux, 2002) in Northeast Brazil

Ricardo Marques[1*] & Adrian A. Garda[1,2]

[1] Programa de Pós-Graduação em Ciências Biológicas (Zoologia), Centro de Ciências Exatas e da Natureza, Departamento de Sistemática e Ecologia, Universidade Federal da Paraíba; João Pessoa, PB 58051-900, Brazil

[2] Departamento de Botânica e Zoologia, Centro de Biociências, Universidade Federal do Rio Grande do Norte, Lagoa Nova, Natal, RN, Brazil

* Corresponding author: rcdmarquess@gmail.com

The Caatinga biome is a semi-arid region restricted to Brazil with a study neglection history towards its biota. It composes the diagonal of open formations along with other open habitat environments. Several species from these habitats were thought to be widely distributed and recent inquiries have shown they actually were independent evolutionary lineages or cryptic species complexes. *Rhinella jimi* is a widespread species from Caatinga, distributed over Northeast Brazil. Herein we used mitochondrial and nuclear molecular markers to infer on the genetic structure and demographic expansion of *R. jimi* and its status among other related species. Also, we performed ecological niche modeling projections to Pleistocene climatic fluctuations. We found *R. jimi* consists of a widespread species with a single population throughout Caatinga biome. *Rhinella jimi* is a nominal species, but share haplotypes with closed related species. Historical demography showed a population expansion during Late Pleistocene, while past projections were congruent to the projected period climate. *Rhinella jimi* show a congruent evolutionary pattern with other species from semi-arid habitats from Neotropical region.

ADDITIONAL KEYWORDS: *Rhinella* gr. *marina* – Caatinga – widespread distribution – multilocus – semi-arid biome.

Introduction

For decades, the Amazon and the Atlantic forest were the main target to investigate several aspects of species diversity while open, while dry and open formations lack in biodiversity (Vanzolini, 1963; Rodrigues, 2003; Leal et al., 2005). In the Neotropics, the diagonal of open formations of South America is an extensive region that ranges from Northeast Brazil to the north of Argentina, encompassing four biomes: Chaco, Pantanal, Cerrado, and Caatinga, where each maintain singularities for climactic aspects, fauna and flora, but are overall open habitat environments (Werneck, 2011). These arid and open habitats were considered poor in diversity and endemism due a lack of data, which has changed in recent years (Vanzolini, 1963; Colli, Bastos, & de Araujo, 2002; Silva & Santos, 2005; Nogueira et al., 2011; Werneck, 2011).

Reptiles and amphibians from these environments were once thought to be widely distributed, which was confirmed for some species (Prado, Haddad, & Zamudio, 2012; Silveira, 2017; Camurugi, 2018), whilst other studies uncovered undescribed taxa, as well as unveiled complexes of cryptic species (Werneck *et al.*, 2012; Giugliano *et al.*, 2013; Lanna *et al.*, 2018; Oliveira *et al.*, 2018). Patterns of genetic structure and demographic changes in Caatinga's biota is associated to large rivers restricting gene flow (e.g. São Francisco River; (Nascimento *et al.*, 2013; Werneck *et al.*, 2015; Lanna *et al.*, 2019), ecological contraints (Werneck *et al.*, 2012), vicariant barriers (Oliveira *et al.*, 2018), and Pleistocene climactic oscillations (Thomé *et al.*, 2016; Gehara *et al.*, 2017). Amphibians are expected to show genetic structure due to habitat philopatry and low dispersive capacities resulting from their physiological dependence on water (Reading, Loman, & Madsen, 1991; Beebee, 2005).

The *Rhinella marina* species complex encompasses eleven species of large toads: *R. achavali* (Maneyro, Arrieta & de Sá, 2004), *R. arenarum* (Hensel, 1867), *R. cerradensis* Maciel, Brandão, Campos & Sebben, 2007, *R. diptycha* (Cope, 1862), *R. horribilis* (Wiegmann, 1833), *R. icterica* (Spix, 1824), *R. jimi* (Stevaux, 2002), *R. marina* (Linnaeus, 1758), *R. poeppigii* (Tschudi, 1845), *R, rubescens* (Lutz, 1925), and *R. veredas* (Brandão, Maciel & Sebben, 2007), and are distributed from the southern United States to Uruguay (Maneyro, Arrieta, & de Sá, 2004; Pramuk, 2006; Brandão, Maciel, & Sebben, 2007; Maciel *et al.*, 2010). Past research on this group in South

America have dealt with species diversification and phylogenies (*e.g*. structured populations) (Maciel *et al.*, 2010; Vallinoto *et al.*, 2010, 2017). They are generally considered widely distributed and highly dispersive due their large and sturdy bodies and broader tolerances to biotic and abiotic variations (Brown, Stevens, & Kaufman, 1996). Nevertheless, *R. marina* showed genetic structure associated to Panama's isthmus and biogeographic, molecular and morphological inquiries later associated the northern lineage as *R. horribilis* (Slade & Moritz, 1998; Mulcahy, Morrill, & Mendelson, 2006; Acevedo, Lampo, & Cipriani, 2016). Vallinoto et al. (2017) also showed that R. marina was genetically structured by the Amazon river and the divergence between populations dated from late Miocene to early Pliocene.

Additionally, hybridization is largely reported between Bufonid species (Azevedo *et al.*, 2003; Sequeira *et al.*, 2011; Vallinoto *et al.*, 2017; Arntzen *et al.*, 2018) and is a key feature in species' evolutionary process and speciation (Blair, 1974). In *Rhinella marina* species complex, hybridization was observed between *R. diptycha* and *R. icterica* (Azevedo *et al.*, 2003), and *R. marina* and *R. diptycha* (Sequeira *et al.*, 2011; Vallinoto *et al.*, 2017). The process of natural introgression between species can hamper precise phylogenetic inferences (Harrison & Larson 2014), as in Maciel et al. (2010) that recovered a polytomy of *R. jimi*, *R. marina* and other sister species.

The largest species of the *Rhinella marina* complex are *R. marina* inhabiting the amazonian region, *R. diptycha* inhabiting the Cerrado and most of Caatinga biome, and *R. jimi*, which is distributed in a narrow coastal region of Caatinga and Atlantic forest from Pará state to northern Espírito Santo state (Stevaux, 2002; Maciel *et al*., 2010; Valencia-Zuleta & Maciel, 2017). *Rhinella jimi* was described to Maracás municipality in Bahia state, is an explosive breeder, using water ponds during the rainy season and sporadic rains (Stevaux, 2002). In contrast to most species of anurans studied in phylogeographic and phylogenetic approaches recently (e.g. Gehara et al., 2013, 2014; Menezes et al., 2016), *R. jimi* is a large toad with sturdy body, which is expected to make its dispersal successful.

Our aim is to investigate the evolutionary history of *R. jimi* to answer: (1) is *R. jimi* structured into populations according to the São Francisco river, which also acted as a soft barrier to geneflow?; and (2) Climatic fluctuations during Pleistocene have shaped the genetic diversity or demography of *R. jimi*? To do so, we use a molecular

phylogenetic study where we aim: (a) test if landscape features have promoted genetic structure in the species; (b) verify through molecular data if *R. jimi* show signs of hybridization with closely related species; (c) investigate paleoclimatic events with phylogeography approach; (d) delimit the distribution of *R. jimi* and test the validation of the species among the *Rhinella marina* species group.

Material and methods

We gathered tissue samples available at the Herpetological collection of the Universidade Federal da Paraíba and from the Laboratory of amphibians and reptiles from Universidade Federal do Rio Grande do Norte. Additional samples were donated from several museums and fieldtrips conducted under SISBIO permit #52316. Total samples comprised 135 tissues from 40 localities within the geographic distribution of *Rhinella jimi* (Figure 1).

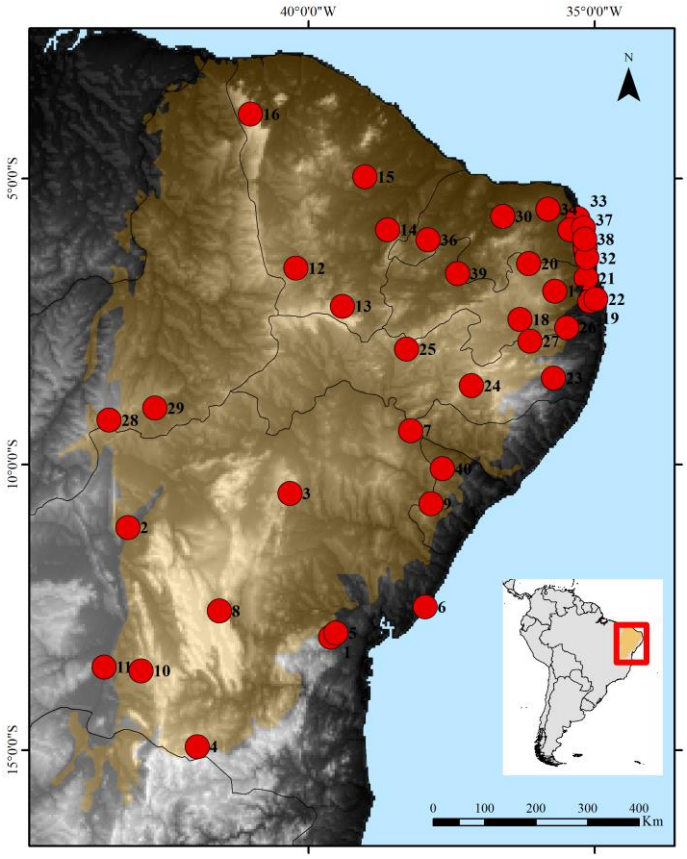

Figure 1: Map with samples of *Rhinella jimi* used within the Caatinga (orange) boundary and nearby areas. Red dots represent localities we obtained tissue samples. Locality numbers are specified in Table S3.

Through a protocol of saline extraction adapted from Brufold et al. (1992) we isolated the whole DNA from liver or muscle tissues and amplified samples through Polymerase Chain Reaction (PCR) for different gene fragments. For mitochondrial loci (mtDNA) we used 16S ribosomal RNA (16S) and Cytochrome B (CytB), while for nuclear loci (nuDNA) we selected the introns Ribosomal Protein L 3 (RPL3) and Ribosomal Protein L 9 (RPL9). We sequenced individuals for nuDNA based on exclusive haplotypes from mtDNA data, with a total of 28 and 38 samples for RPL3 and RPL9. For samples detail, amplification mixes, primer sequences, and PCR cycles check the supplementary files.

Sequence editing

We used Geneious 8.1.9 to check and manually edit all sequences. Later, sequences were aligned with MUSCLE algorithm in MEGA X 10.0.4 (Kumar *et al.*, 2018) and submitted alignments with gaps to the default options and parameter values of Gblocks (Talavera & Castresana, 2007) to obtain more consistent sequences. We sequenced both forward and reverse strands for nuDNA and ambiguities were treated with default settings in Phase algorithm (Stephens, Smith, & Donnelly, 2001) in DnaSP 5.1 (Librado & Rozas, 2009), considering pair probabilities above 80%. We used the PHI test in SPLITSTREE4 (Huson & Bryant, 2006) to test for recombination on both nuclear loci.

Population assignment

We assigned individuals to populations based on Hardy-Weinberg equilibrium assumptions using Geneland 4.0.6 (Guillot *et al.*, 2005) in R 3.4.4 (R Core Team, 2019), using with all mtDNA and nuDNA data and samples geographic coordinates. To evaluate different scenarios we ran Geneland twice, firstly using only nuDNA data secondly with mtDNA and nuDNA data combined. In both analyses we conducted 20 runs from one to six populations (k) of 5×10^6 MCMC chain sampled every 5×10^3 generations and a burn in of 2×10^2. We also tested for populations of *R. jimi* in BAPS 6.0. BAPS uses Bayesian inference to detect genetic structure, treating allele frequencies from molecular markers and diverging groups as random values (Corander

& Marttinen, 2006). To obtain our mixture results, we used only nuDNA dataset and performed clustering with linked loci in a range of one to six populations (k).

Gene tree, haplotype reconstruction and summary statistics

We used the populations detected in Geneland to estimate Gene trees, haplotype networks and summary statistics. For gene trees, we established the most suitable evolutionary model for all loci with Bayesian Information Criteria (BIC) in jModelTest 2.1.7 (Posada, 2008). We reconstructed gene trees with BEAST 1.8.4 (Drummond *et al.*, 2012) setting 4 x 10^8 generations sampled at every 4 x 10^4 steps, using the following substitution models selected in jModelTest: K80 for 16S, K80+G for CytB, TrNef+I for RPL3 and F81 for RPL9. To assure all MCMC runs had adequate estimate sample sizes (ESS>200) we checked log files in Tracer 1.6 (Rambaut & Drummond, 2007). Consensus trees were generated in TreeAnnotator 1.8.4 (Drummond *et al*., 2012) excluding 20% of trees as burn in and the final tree viewed in FigTree 1.4.2. When necessary, we used *Rhinella crucifer* as outgroup.

We reconstructed haplotype networks with PopArt 1.7 (Leigh & Bryant, 2015) using median joining network (Bandelt, Forster, & Rohl, 1994). To verify if *R. jimi* has signs of hybridization with closely related species, we downloaded sequences of *R. diptycha* and *R. marina* from Genbank for all loci and added to our dataset to generate haplotype reconstruction. We calculated summary statistics for all loci in samples of *R. jimi*, providing: segregating sites (S), number of haplotypes (h), haplotype diversity (Hd), standard deviation of haplotype diversity (SDHd), nucleotide diversity (pi), Tajima's D (D) and its P value for all loci in DnaSP 5.1 (Librado & Rozas, 2009).

Species delimitation

To test the support for the validity of *Rhinella jimi*, we conducted a species delimitation analysis with molecular data using the closest species from *Rhinella marina* group (*Rhinella diptycha* and *Rhinella marina*). Hybridization is common among these toads (Vallinoto et al. 2017), so we only used sequences of the four loci from the same individual. We used both mitochondrial and nuclear data in Bayesian Phylogenetics and Phylogeography (BPP) 3.3 (Flouri *et al.*, 2018) and performed three runs of four possible scenarios. Each run contained 2 x 10^5 generation samples and 4 x

10^4 burn-in. The four possible scenarios included the following parameter sets: 1) large ancestral populations with deep divergences, $\Theta \sim G(1, 10)$ and $\tau 0 \sim G(1, 10)$; 2) large populations with recent divergences $\Theta \sim G(1, 10)$ and $\tau 0 \sim G(2, 2000)$; 3) small ancestral population and deep divergences $\Theta \sim G(2, 2000)$ and $\tau 0 \sim G(1, 10)$; and 4) small ancestral population and recent divergences $\Theta \sim G(2, 2000)$ and $\tau 0 \sim G(2, 2000)$.

Historical demography

To reconstruct the demographic history of *R. jimi*, we ran a Bayesian skyline plot analysis (Drummond *et al.*, 2005) for the concatenated mitochondrial genes 16S and CytB. We used HKY+I substitution model estimated in jModelTest 2.1.7 (Posada, 2008) for concatenated genes and conducted a run of 4×10^8 generations, sampled every 4×10^4 steps. We calibrated the molecular strict clock to normal prior for *clock.rate* parameter, following the mitochondrial mutation rate estimated for bufonids by Macey et al. (1998) of 7×10^{-9} mutation/site/years (standard deviation 1.5×10^{-10}). To check the convergence of runs and values of effective sample size (>200) we used Tracer 1.6 (Rambaut & Drummond, 2007), as well as the graphs of population dynamics through time.

Ecologic niche modeling

We gathered information from our tissue samples, complemented with records from literature, SpeciesLink and personal unpublished data to compile geographic distribution records for *R. jimi*. Our distribution records totaled 105 points distanced at least 8 km from each other. To obtain the distribution model of *R. jimi* based on climatic variables, we produced ecological niche modeling for current period and projected its results to mid-Holocene (6,000 years ago), last glacial maximum (LGM; 21,000 ya) and last inter-glacial (LIG; 130,000 ya). We downloaded 19 climatic variables available on Worldclim at version 1.4 (Hijmans et al., 2005, available at www.worldclim.org) in a resolution of 2.5 arc-minutes (grids of 5 x 5 kilometers) for current, mid-Holocene and LGM periods, while for LIG we used a resolution of 30 arc-seconds (grids of 1 x 1 kilometers), which was rescaled to match previous periods.

In R 3.4.4 (R Core Team, 2019) we loaded all 19 climatic variables restricted to the northern portion of South America and distribution records for *R. jimi*. We tested

colinearity of variables with Pearson's correlation coefficient (0.85) and maintained only those relevant to the species' biology. Our final climatic variables set consisted of nine variables: bio1 (annual mean temperature), bio2 (mean diurnal range), bio3 (isothermality), bio7 (temperature annual range), bio12 (annual precipitation), bio14 (precipitation of driest month), bio15 (precipitation seasonality), bio18 (precipitation of warmest quarter) and bio19 (precipitation of coldest quarter). Then we ran 20 replicates in Maxent for each model using 25% of random test points with bootstrap method. Final models consisted of those with acceptable values (>0.9) of area under curve (AUC). Finally, we produced an overlap map combining rasters from all periods to verify possible areas of stability over the last 120 kya.

Results

Genetic data and population assignment

Our dataset covered a wide range of the distribution of *Rhinella jimi*, with localities throughout the Caatinga biome and its surrounds. We produced a total of 1862 base pairs (bp) for the genes 16S (517 bp), CytB (330 bp), RPL3 (497 bp) and RPL9 (518 bp) of *R. jimi*. This dataset comprised 128 specimens sequenced for mtDNA loci with a subset of 44 specimens sequenced for nuclear loci. All genes presented few segregating sites (11−13), number of haplotypes, moderate to high haplotype diversity, and low nucleotide diversity (Table 1). Values of Tajima's D neutrality test suggests recent population expansion to 16S (Table 1). We found no evidence for recombination in nuclear loci (RPL3, p = 0.567; RPL9 p = 0.9284).

Table 1: Summary statistics of all loci for the whole *Rhinella jimi* dataset. We provide for each locus the base pairs (bp), number of sequences (N), segregating sites (S), number of haplotypes (h), haplotype diversity (Hd), standard deviation of haplotype diversity (SDHd), nucleotide diversity (pi), Tajima's D (D) and its p value. (*) Phased sequences.

Locus	bp	N	S	h	Hd	SDHd	pi	D	p value
16S	517	54	13	13	0.662	0.071	0.0021	-18.337	P<0.05
CytB	330	128	13	16	0.772	0.033	0.0055	-0.9856	P>0.1
RPL3*	497	56	11	18	0.842	0.039	0.0046	-0.1283	P>0.1
RPL9*	518	76	12	8	0.658	0.033	0.0025	-12.992	P>0.1

Our three runs to test for population structure in *R. jimi* showed congruent results. In Geneland, our attempt to recover populations with mitochondrial and nuclear genes combined resulted in more iterations from the MCMC chain in the cluster of one population (k = 1) with a density of 0.45 (Figure S2). The second Geneland run using only nuclear genes obtained the same result, with a density of 0.6. BAPS provided no evidence of admixture, also generating one population (k = 1)(Figure S3). Therefore, *R. jimi* comprises a single and widespread population throughout the Caatinga biome and nearby areas.

Gene tree, haplotype reconstruction and species delimitation

The resulting Bayesian concatenated mitochondrial gene tree of *R. jimi* (Figure S1) did not uncover genetic structure across the species distribution, and posterior probability for most nodes were low, corroborating results from population assignment methods. The haplotype network showed a star-shaped network for 16S and CytB mitochondrial loci. All genes showed one or two more frequent haplotypes, with H1 from Cytb distributed in all localities. Overall, these results indicate low levels of genetic diversity for most genes and recovered no clear geographic pattern across the species' distribution (Table 1).

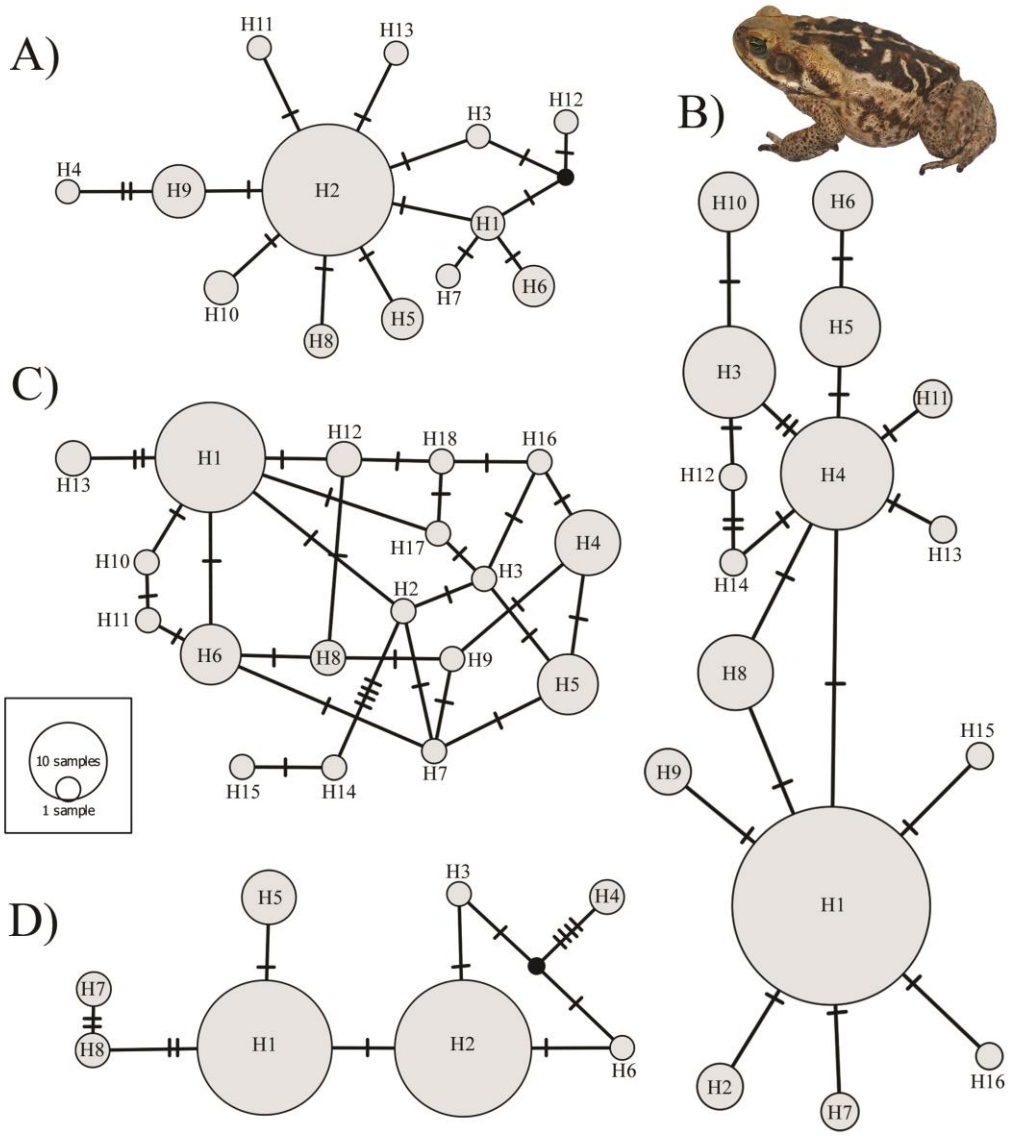

Figure 2: Haplotype network reconstruction for four sequenced loci of *Rhinella jimi*. Mitochondrial genes 16S (A), CytB (B) and phased nuclear genes RPL3 (C) and RPL9 (D).

The haplotype reconstruction with sequences of *R. jimi*, *R. diptycha* and *R. marina* showed species share haplotypes in all loci. Most haplotypes are shared between *R. jimi* and *R. marina* (Figure 3). Genetic divergence between the three species was low, ranging from 0.2% to 1.6% in mitochondrial loci and from 0.6% to 2.2% in nuclear loci (Table 2). We tested the validity of these species through 12 runs in BPP with four different parameter sets. Our results consistently supported the validity of all three species (posterior probability of 1).

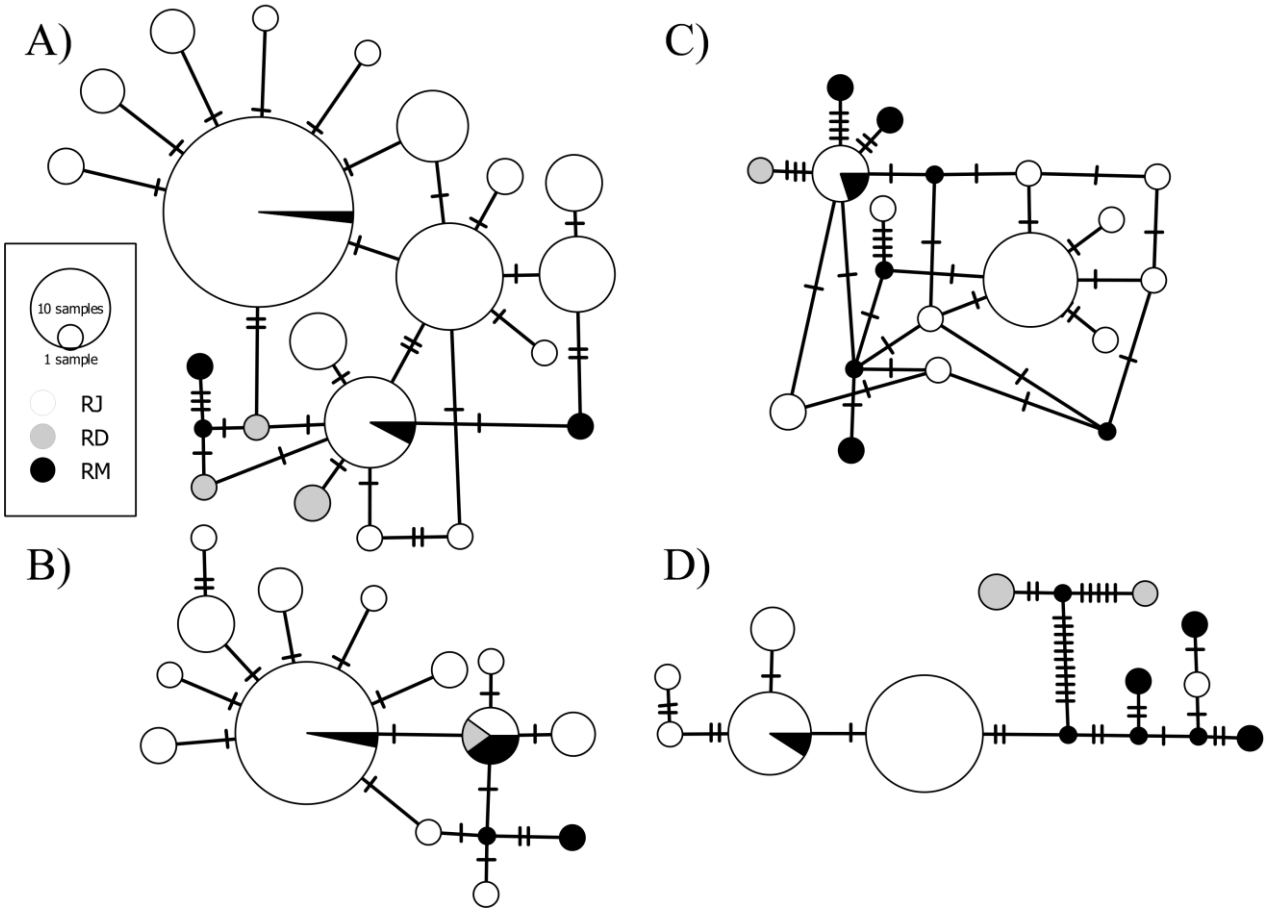

Figure 3: Haplotype network of three largerst toads of *Rhinella marina* species complex: *R. jimi* (RJ), *R. diptycha* (RD) and *R. marina* (RM) for CytB (A), 16S (B), RPL3 (C) and RPL9 (D).

Table 2: Pairwise genetic divergence of uncorrected p-distance between *R. jimi*, *R. marina* and *R. diptycha* for 16S, CytB, RPL3, and RPL9.

	16S		CytB		RPL3		RPL9	
	1	2	1	2	1	2	1	2
1. *R. jimi*								
2. *R. marina*	0.4%		1.3%		0.9%		0.6%	
3. *R. diptycha*	0.3%	0.2%	1.6%	1.2%	1.1%	1.0%	2.0%	2.2%

Historical demography

The Bayesian skyline plot result for the concatenated mitochondrial data set showed stability of effective population size of *R. jimi*, followed by demographic expansion around 95 kya during Late Pleistocene (Figure 4). Demographic expansion corroborates negative Tajima's D value observed in Table 1 for 16S mitochondrial gene.

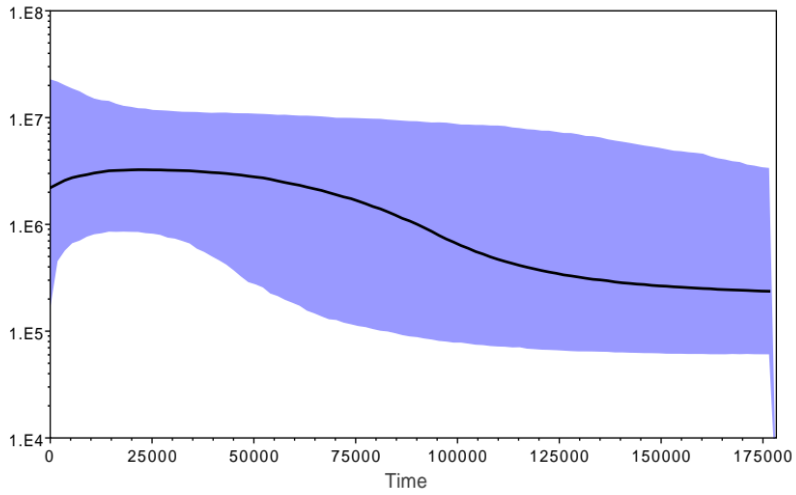

Figure 4: Bayesian skyline plot reconstruction for mtDNA data of *Rhinella jimi* showing estimate population size through time. Solid black line shows median estimate and blue bands are the 95 % highest posterior density limits. The x-axis shows time from present to past, while y-axis shows the effective population size.

Ecological niche modeling

We generated four Ecological Niche Models for *R. jimi*. Current modeling showed a potential distribution compatible with species known distribution (AUC = 0.96), restricted to northeastern Brazil in the Caatinga and Atlantic Forest biomes (Figure 5A). It shows more suitable areas to the east, near the coast of Brazil. The projection for mid-Holocene shows a similar pattern, but with wider coastal distributions (Figure 5B). In the Last Glacial Maximum, the potential distribution was contracted and mostly restricted to inner portions of the continent (Figure 5C), while the Last Inter-Glacial projection shows a wider past potential distribution of the species in northeastern Brazil and reaching small portions of Southeast and North Brazil (Figure

5D). The sum of all models shows a major stability area over most of Northeastern Brazil, but also small blotches in Northern Brazil and South America (Figure 5E).

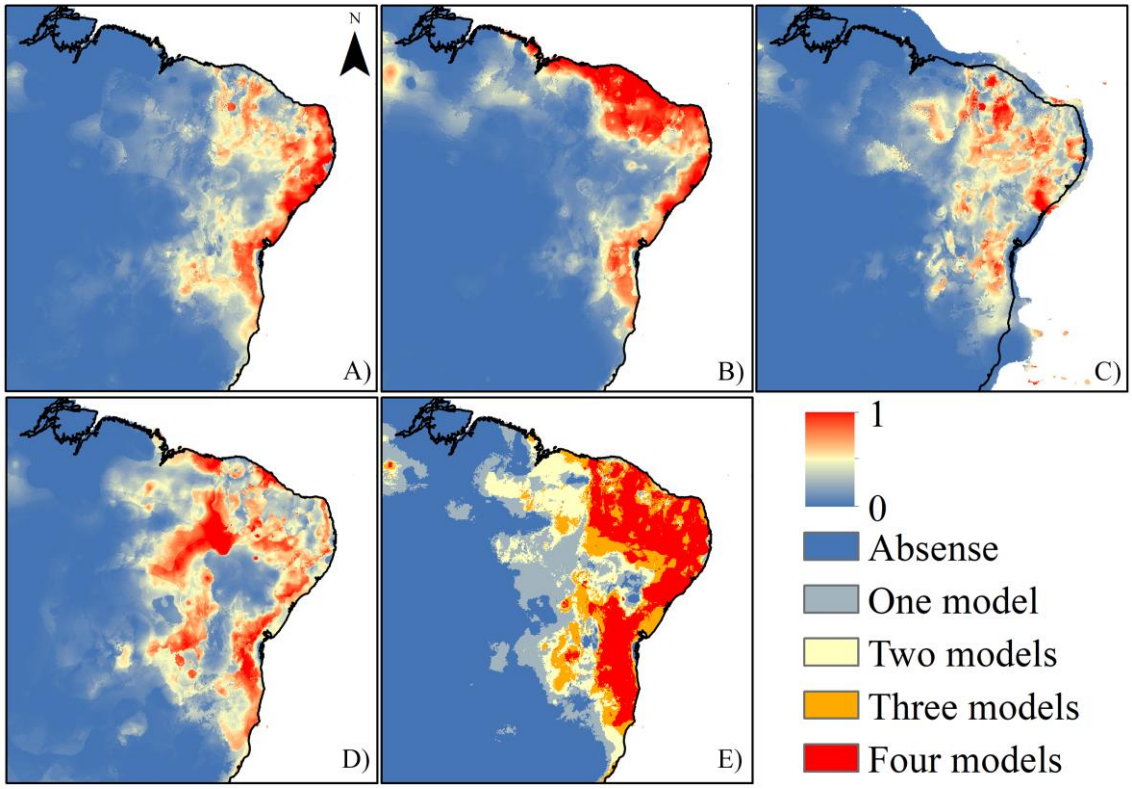

Figure 5: Projections of the potential distribution for *R. jimi* from Ecological Niche Modeling for different periods: (A) current period, (B) mid-Holocene (6 kya), (C) Last Glacial Maximum (21 kya) and (D) Last Inter-Glacial (120 kya). Warmer coloration indicates higher probability of occurrence based on bioclimatic data. Figure (E) shows stability areas with the sum of all models, detailed in the legend from none to four models.

Discussion

Our results show that *R. jimi* in northeastern Brazil comprises a single population of a widely distributed species, supported by several results. Furthermore, the most frequent CytB haplotype is distributed in all 40 sampled localities (H1, Figure 2). In addition, the lack of genetic structure associated to any geomorphologic, ecological, or climatic barrier suggests that the species is not restricted by any elements in the landscape, therefore rejecting our first hypothesis. The São Francisco river is the most wide and extensive river in Caatinga and was a vicariant barrier for many species (Nascimento *et al.*, 2013; Werneck *et al.*, 2015; Oliveira *et al.*, 2015). Genetic diversity

was also associated to river basin in some aquatic frog species (*Pseudis* spp.; Garda & Cannatella, 2007; Santana, 2013). Contrastingly, most widespread anuran species in Caatinga are not structured by rivers as vicariant barriers (Thomé *et al.*, 2016; Oliveira *et al.*, 2018), while rivers act as barriers for gene flow for Caatinga lizards (*e.g.* *Ameivula ocellifera* in Oliveira et al., 2015; *Tropidurus semitaeniatus* species complex in Werneck et al., 2015). The presence of genetic structure in anurans is also associated to mountain ranges, either as vicatiant barriers or isolation by altitude (Thomé et al., 2016; Oliveira et al., 2018; Marques et al. Chapter 2). Thomé *et al*. (2016) and Marques et al. (chapter 2) observed genetic structure associated to isolated populations on the Espinhaço Range for *Pleudorema alium* and *Corythomantis* sp., respectively, while Oliveira et al. (2018) showed the Brazilian Central Plateau was a barrier for gene flow for *Dermatonotus muelleri*. Despite we sequenced samples of *R. jimi* from lowlands and altitude regions, it does not show any genetic structure associated to altitude.

Among the widely distributed amphibian species detected in the Neotropics, most of them present large body sizes or higher tolerances to water loss (Prado et al., 2012; Mângia, 2017; Camurugi, 2018) suggesting high dispersion capabilities. The cane toad *R. jimi* is a diet generalist, has sturdy and big body with thick skin and as other toad species from semi-arid habitats, higher tolerance to water loss (Jørgensen, 1997; Moreira & Barreto, 2009). These features are mostly related to highly dispersible taxa (Brown *et al.*, 1996). Studies of its sister species in Australia, where it was introduced, showed that *R. marina* can disperse from 10 to 60 km/year according to environmental conditions (Phillips *et al.*, 2006; Urban *et al.*, 2008), what may also apply for *R. jimi*, given its phylogenetic and ecological similarity to *R. marina*. This set of features may be the critical factor allowing unrestricted gene flow across *Rhinella jimi* wide population and geographic distribution.

Rhinella jimi was formally described only recently by Stevaux (2002) based on morphological differences compared to the closely-related *R. diptycha*. The proposed distribution for *R. jimi* was a narrow coastline from northern Espírito Santo State upward to the state of Maranhão, while *R. diptycha* would be distributed throughout Cerrado and the majority of Caatinga biome. The biogeography study of the *R. marina* species complex maintained that proposition for the distribution of both species (Maciel

et al., 2010). Nevertheless, our results indicate that *R. jimi* has a much broader distribution. Specimens from most of our 40 localities were collected by us and match the morphological description of *R. jimi*. Our dataset shows that *R. jimi* is found across the Caatinga biome and neighboring areas in Cerrado Savannas and Atlantic rainforest, reaching 15º of latitude South and 42º of longitude West with a parapatric zone with *R. diptycha* yet to be established.

Ten species compose the *Rhinella marina* species complex, all distributed throughout South America (Maciel *et al*., 2010). *Rhinella jimi*, *R. diptycha* and *R. marina* are closely related and are the largest toads of the group. Although our species delimitation analysis endorses these clades as valid species, some haplotypes are shared between them in all four loci. Hybridization has been reported for several amphibian species, and is especially common among Bufonids (Haddad, Pombal Jr., & Batistic, 1994; Lamb, Sullivan, & Malmos, 2006; Littlejohn & Watson, 2008; Vallinoto *et al.*, 2017; Arntzen *et al.*, 2018; Brusquetti *et al.*, 2019), and may account for shared haplotypes in our results. Vallinoto *et al*. (2017) reported shared haplotypes between two populations of *R. marina* and between sympatric specimens of *R. marina* and *R. diptycha* in a contact zone between Amazon and Cerrado biomes. They suggest that intrinsic barriers for hybridization are still permeable, a possible scenario also for *R. jimi*. Maciel *et al*. (2010) used four loci and showed an unresolved polytomy of *R. marina* and *R. jimi* in a species gene tree, which suggests an unresolved status between these species. Despite divergence among these species date back to the late Miocene ~7 m.y.a. (Maciel *et al.*, 2010) and each occur predominantly in the biomes of the Amazon (*R. marina*), Cerrado (*R. diptycha*), and Caatinga (*R. jimi*), contact zones between these biomes may have promoted continuous introgression. Both gene flow and introgression are evolutionary processes known to affect speciation and hamper phylogenetic estimates (Avise, 2000; Leaché *et al.*, 2014).

Several climatic fluctuations occurred during Pleistocene over 200 kya, altering its biota and habitats (Pennington, Prado, & Pendry, 2000). During these climatic fluctuations, South America suffered several wet interleaved with dry periods (Auler *et al.*, 2004; Wang *et al.*, 2004), promoting the expansion of forests and retraction of dry habitats during wet periods and the retraction of forests and expansion of dry habitats

during dry periods (Pennington *et al.*, 2000; Werneck, 2011). Such historical events are supported by shared species between Amazon and Atlantic forest and high species richness in relictual forests within Caatinga biome, also called “brejos de altitude” (Costa, 2003; Santos *et al.*, 2007; Batalha-Filho *et al.*, 2013; Gehara *et al.*, 2017). Castro et al. (2019) shows that the evaluation of anuran diversity from these relictual forests resemble more the Atlantic forest than the Amazon. Hence, these ongoing processes shaped the genetic diversity for several Neotropical species (Carnaval & Moritz, 2008; Carnaval *et al.*, 2009; Batalha-Filho *et al.*, 2013; Lanna *et al.*, 2018; Dal Vechio *et al.*, 2018).

The population expansion of *R. jimi* recovered in skyline plot started at ~95 kya (Figure 3), right after the end of dry LIG period. (Gehara *et al.*, 2017) evaluated the coexpansion for several phyllogenetic and ecologically distinct species, including *R. jimi*, and observed a synchronous population expansion during Pleistocene from ~400 to 180 kya, although our expansion date does not precisely match with theirs, we used two loci that may alter results (Hedges & Kumar, 2003). Nevertheless, our second hypothesis suggests that paleoclimatic variations shaped the distribution of *R. jimi*. However, the oscillation events of expansion and retraction of dry habitats did not shaped any genetic structure, but had demographic implications for the species increasing its population size in Caatinga biome.

Compile information on the evolutionary history of local South American biota is crucial to understand the puzzle of amphibian diversification in the Neotropics (Rull, 2011). We present several evidences showing that *R. jimi* is another amphibian species is widely distributed without genetic structure. We showed R. jimi consists of a single valid species with intrinsic aspects associated to its widely distribution, together with past climatic oscillation, but retain past traces from other large toads of South America. Future prospects on the *Rhinella marina* species complex should aim for broader inferences on the diversification processes of its species and understand if contact zone associated processes (e.g. hybridization) affect other related species.

Acknowledgements

We thank to herpetological collections curators and their staff for providing tissue samples. RM thanks Coordenação de Aperfeiçoamento de Pessoal de Nível Superior (CAPES) for his PhD Scholarship (Process number 1489596).

References

Acevedo AA, Lampo M & Cipriani R. **2016**. The cane or marine toad, *Rhinella marina* (Anura, Bufonidae): two genetically and morphologically distinct species. *Zootaxa* **4103**: 574.

Arntzen JW, McAtear J, Butôt R & Martínez-Solano I. **2018**. A common toad hybrid zone that runs from the Atlantic to the Mediterranean. *Amphibia-Reptilia* **39**: 41–50.

Auler AS, Wang X, Edwards RL, Cheng H, Cristalli PS, Smart PL & Richards DA. **2004**. Palaeoenvironments in semi-arid northeastern Brazil inferred from high precision mass spectrometric speleothem and travertine ages and the dynamics of South American rainforests. *Speleogenesis and Evolution of Karst Aquifers* **2**: 1–4.

Avise JC. **2000**. Phylogeography: The History and Formation of Species. *American Zoologist* **41**: 447.

Azevedo MFC de, Foresti F, Ramos PRR & Jim J. **2003**. Comparative cytogenetic studies of Bufo ictericus, B. paracnemis (Amphibia, Anura) and an intermediate form in sympatry. *Genetics and Molecular Biology* **26**: 289–294.

Bandelt HJ, Forster P & Rohl A. **1994**. Median-Joining Networks for Inferring Intraspecic Phylogenies. *Molecular Biology* **16**: 37–48.

Batalha-Filho H, Fjeldså J, Fabre PH & Miyaki CY. **2013**. Connections between the Atlantic and the Amazonian forest avifaunas represent distinct historical events. *Journal of Ornithology* **154**: 41–50.

Beebee TJC. **2005**. Conservation genetics of amphibians. *Heredity* **95**: 423–427.

Blair WF. **1974**. Character displacement in frogs. *Integrative and Comparative Biology* **14**: 1119–1125.

Brandão RA, Maciel NM & Sebben A. **2007**. A New Species of *Chaunus* from Central Brazil (Anura; Bufonidae). *Journal of Herpetology* **41**: 309–316.

Brown JH, Stevens GC & Kaufman DM. **1996**. The Geographic Range: Size, Shape, Boundaries, and Internal Structure. *Annual Review of Ecology and Systematics* **27**: 597–623.

Brusquetti F, Netto F, Baldo D & Haddad CFBB. **2019**. The influence of Pleistocene glaciations on Chacoan fauna: Genetic structure and historical demography of an endemic frog of the South American Gran Chaco. *Biological Journal of the Linnean Society* **126**: 404–416.

Carnaval AC, Hickerson MJ, Haddad CFB, Rodrigues MT & Moritz C. **2009**. Stability predicts genetic diversity in the Brazilian Atlantic forest hotspot. *Science* **323**: 785–789.

Carnaval AC & Moritz C. **2008**. Historical climate modelling predicts patterns of current biodiversity in the Brazilian Atlantic forest. *Journal of Biogeography* **35**: 1187–1201.

Castro DP, Rodrigues JFM, Borges-Leite MJ, Lima DC & Borges-Nojosa DM. **2019**. Anuran diversity indicates that Caatinga relictual Neotropical forests are more related to the Atlantic Forest than to the Amazon. *PeerJ* **6**: e6208.

Colli GR, Bastos RP & de Araujo AFB. **2002**. The character and dynamics of the Cerrado herpetofauna. In: Oliveira PS, Marquis RJ, eds. *The Cerrados of Brazil: Ecology and Natural History of a Neotropical Savanna*. New York: Columbia University Press, 223–241.

Corander J & Marttinen P. **2006**. Bayesian identification of admixture events using multilocus molecular markers. *Molecular Ecology* **15**: 2833–2843.

Costa LP. **2003**. The historical bridge between the Amazon and the Atlantic Forest of Brazil: a study of molecular phylogeography with small mammals. *Journal of Biogeography* **30**: 71–86.

Dal Vechio F, Prates I, Grazziotin FG, Zaher H & Rodrigues MT. **2018**. Phylogeography and historical demography of the arboreal pit viper *Bothrops bilineatus* (Serpentes, Crotalinae) reveal multiple connections between Amazonian and Atlantic rain forests. *Journal of Biogeography* **45**: 2415–2426.

Drummond AJ, Rambaut A, Shapiro B & Pybus OG. **2005**. Bayesian Coalescent Inference of Past Population Dynamics from Molecular Sequences. *Molecular Biology and Evolution* **22**: 1185–1192.

Drummond AJ, Suchard MA, Xie D & Rambaut A. **2012**. Bayesian phylogenetics with BEAUti and the BEAST 1.7. *Molecular Biology and Evolution* **29**: 1969–1973.

Flouri T, Jiao X, Rannala B & Yang Z. **2018**. Species Tree Inference with BPP Using Genomic Sequences and the Multispecies Coalescent. *Molecular Biology and Evolution* **35**: 2585–2593.

Garda AA & Cannatella DC. **2007**. Phylogeny and biogeography of paradoxical frogs (Anura, Hylidae, Pseudae) inferred from 12S and 16S mitochondrial DNA. *Molecular Phylogenetics and Evolution* **44**: 104–114.

Gehara M, Canedo C, Haddad CFB & Vences M. **2013**. From widespread to microendemic: Molecular and acoustic analyses show that *Ischnocnema guentheri* (Amphibia: Brachycephalidae) is endemic to Rio de Janeiro, Brazil. *Conservation Genetics* **14**: 973–982.

Gehara M, Crawford AJ, Orrico VGD, Rodríguez A, Lötters S, Fouquet A, Barrientos LS, Brusquetti F, De La Riva I, Ernst R, Urrutia GG, Glaw F, Guayasamin JM, Hölting M, Jansen M, Kok PJR, Kwet A, Lingnau R, Lyra M, Moravec J, Pombal JP, Rojas-Runjaic FJM, Schulze A, Señaris JC, Solé M, Rodrigues MT, Twomey E, Haddad CFB, Vences M & Köhler J. **2014**. High levels of diversity uncovered in a widespread nominal taxon: Continental phylogeography of the neotropical tree frog *Dendropsophus minutus*. *PLoS ONE* **9**: e103958.

Gehara M, Garda AA, Werneck FP, Oliveira EF, da Fonseca EM, Camurugi F, Magalhães F de M, Lanna FM, Sites JW, Marques R, Silveira-Filho R, São Pedro VA, Colli GR, Costa GC & Burbrink FT. **2017**. Estimating synchronous demographic changes across populations using hABC and its application for a herpetological community from northeastern Brazil. *Molecular Ecology* **26**: 4756–4771.

Giugliano LG, de Campos Nogueira C, Valdujo PH, Collevatti RG & Colli GR. **2013**. Cryptic diversity in South American Teiinae (Squamata, Teiidae) lizards. *Zoologica Scripta* **42**: 473–487.

Guillot G, Estoup A, Mortier F & Cosson JF. **2005**. A spatial statistical model for landscape genetics. *Genetics* **170**: 1261–1280.

Haddad CFB, Pombal Jr. JP & Batistic RF. **1994**. Natural hybridization between diploid and tetraploid species of leaf-frogs, genus *Phyllomedusa*(Amphibia). *Journal of Herpetology* **28**: 425–430.

Hedges SB & Kumar S. **2003**. Genomic clocks and evolutionary timescales. *Trends in Genetics* **19**: 200–206.

Hijmans RJ, Cameron SE, Parra JL, Jones PG & Jarvis A. **2005**. Very high resolution interpolated climate surfaces for global land areas. *International Journal of Climatology* **25**: 1965–1978.

Huson DH & Bryant D. **2006**. Application of Phylogenetic Networks in Evolutionary Studies. *Molecular Biology and Evolution* **23**: 254–267.

Jørgensen CB. **1997**. 200 years of amphibian water economy: from Robert Towns to the present. *Biological Reviews* **72**: 153–237.

Kumar S, Stecher G, Li M, Knyaz C & Tamura K. **2018**. MEGA X: Molecular evolutionary genetics analysis across computing platforms. *Molecular Biology and Evolution* **35**: 1547–1549.

Lamb T, Sullivan BK & Malmos K. **2006**. Mitochondrial Gene Markers for the Hybridizing Toads *Bufo microscaphus* and *Bufo woodhousii* in Arizona. *Copeia* **2000**: 234–237.

Lanna FM, Werneck FP, Gehara M, Fonseca EM, Colli GR, Sites JW, Rodrigues MT & Garda AA. **2018**. The evolutionary history of *Lygodactylus lizards* in the South American open diagonal. *Molecular Phylogenetics and Evolution* **127**: 638–645.

Lanna FM, Gehara M, Werneck FP, Fonseca EM, Colli GR, Sites Jr. JW, Rodrigues MT & Garda AA. **2019**. Dwarf geckos and giant rivers: the role of the São Francisco River in the evolution of Lygodactylus klugei (Squamata: Gekkonidae) in the semi-arid Caatinga of north-eastern Brazil. *Biological Journal of the Linnean Society*: 1–11.

Leaché AD, Harris RB, Rannala B & Yang Z. **2014**. The influence of gene flow on species tree estimation: A simulation study. *Systematic Biology* **63**: 17–30.

Leal IR, Da Silva JMC, Tabarelli M & Lacher TE. **2005**. Changing the course of biodiversity conservation in the caatinga of northeastern Brazil. *Conservation Biology* **19**: 701–706.

Leigh JW & Bryant D. **2015**. POPART: Full-feature software for haplotype network construction. *Methods in Ecology and Evolution* **6**: 1110–1116.

Librado P & Rozas J. **2009**. DnaSP v5: A software for comprehensive analysis of DNA polymorphism data. *Bioinformatics* **25**: 1451–1452.

Littlejohn MJ & Watson GF. **2008**. Hybrid Zones and Homogamy in Australian Frogs. *Ecology* **16**: 85–112.

Macey JR, Schulte JA, Larson A, Fang Z, Wang Y, Tuniyev BS & Papenfuss TJ. **1998**. Phylogenetic Relationships of Toads in theBufo bufoSpecies Group from the Eastern Escarpment of the Tibetan Plateau: A Case of Vicariance and Dispersal. *Molecular Phylogenetics and Evolution* **9**: 80–87.

Maciel NM, Collevatti RG, Colli GR & Schwartz EF. **2010**. Late Miocene diversification and phylogenetic relationships of the huge toads in the Rhinella marina

(Linnaeus, 1758) species group (Anura: Bufonidae). *Molecular Phylogenetics and Evolution* **57**: 787–797.

Maneyro R, Arrieta D & de Sá RO. **2004**. A New Toad (Anura: Bufonidae) from Uruguay. *Journal of Herpetology* **38**: 161–165.

Menezes L, Canedo C, Batalha-Filho H, Garda AA, Gehara M & Napoli MF. **2016**. Multilocus phylogeography of the treefrog *Scinax eurydice* (Anura, Hylidae) reveals a plio-pleistocene diversification in the atlantic forest. *PLoS ONE* **11**: 1–20.

Moreira G & Barreto L. **2009**. Alimentação e variação sazonal na freqüência de capturas de anuros em duas localidades do Brasil central. *Revista Brasileira de Zoologia* **13**: 313–320.

Mulcahy DG, Morrill BH & Mendelson JR. **2006**. Historical biogeography of lowland species of toads (*Bufo*) across the trans-Mexican neovolcanic belt and the isthmus of Tehuantepec. *Journal of Biogeography* **33**: 1889–1904.

Nascimento FF, Lazar A, Menezes AN, Durans A da M, Moreira JC, Salazar-Bravo J, DAndrea PS & Bonvicino CR. **2013**. The Role of Historical Barriers in the Diversification Processes in Open Vegetation Formations during the Miocene/Pliocene Using an Ancient Rodent Lineage as a Model. *PLoS ONE* **8**.

Nogueira C, Ribeiro S, Costa GC & Colli GR. **2011**. Vicariance and endemism in a Neotropical savanna hotspot: Distribution patterns of Cerrado squamate reptiles. *Journal of Biogeography* **38**: 1907–1922.

Oliveira EF, Gehara M, São-Pedro VA, Chen X, Myers EA, Burbrink FT, Mesquita DO, Garda AA, Colli GR, Rodrigues MT, Arias FJ, Zaher H, Santos RMLL & Costa GC. **2015**. Speciation with gene flow in whiptail lizards from a Neotropical xeric biome. *Molecular Ecology* **24**: 5957–5975.

Oliveira EF, Gehara M, São-Pedro VA, Costa GC, Burbrink FT, Colli GR, Rodrigues MT & Garda AA. **2018**. Phylogeography of Muller's termite frog suggests the vicariant role of the Central Brazilian Plateau. *Journal of Biogeography* **45**: 2508–2519.

Pennington RT, Prado DE & Pendry CA. **2000**. Neotropical seasonally dry forests and Quaternary vegetation changes. *Journal of Biogeography* **27**: 261–273.

Phillips BL, Brown GP, Webb JK & Shine R. **2006**. Invasion and the evolution of speed in toads. *Nature* **439**: 2006.

Posada D. **2008**. jModelTest: Phylogenetic model averaging. *Molecular Biology and Evolution* **25**: 1253–1256.

Prado CPA, Haddad CFB & Zamudio KR. **2012**. Cryptic lineages and Pleistocene population expansion in a Brazilian Cerrado frog. *Molecular Ecology* **21**: 921–941.

Pramuk JB. **2006**. Phylogeny of South American *Bufo* (Anura: Bufonidae) inferred from combined evidence. *Zoological Journal of the Linnean Society* **146**: 407–452.

Reading CJ, Loman J & Madsen T. **1991**. Breeding pond fidelity in the common toad, *Bufo bufo*. *Journal of Zoology* **225**: 201–211.

Rodrigues MT. **2003**. Herpetofauna da Caatinga. *Ecologia e Conservação da Caatinga* **1**: 181–236.

Rull V. **2011**. Neotropical biodiversity: Timing and potential drivers. *Trends in Ecology and Evolution* **26**: 508–513.

Santos AMM, Cavalcanti DR, Da Silva JMC & Tabarelli M. **2007**. Biogeographical relationships among tropical forests in north-eastern Brazil. *Journal of Biogeography* **34**: 437–446.

Sequeira F, Sodré D, Ferrand N, Bernardi JAR, Sampaio I, Schneider H & Vallinoto M. **2011**. Hybridization and massive mtDNA unidirectional introgression between the closely related Neotropical toads Rhinella marina and R. schneideri inferred from mtDNA and nuclear markers. *BMC Evolutionary Biology* **11**: 264.

Silva JMC da & Santos MP. **2005**. A importância relativa dos processos biogeográficos na formação da avifauna do Cerrado e de outros biomas brasileiros. In: Scariot A, Souza-Silva JC, Felfili JM, eds. *Cerrado: ecologia, biodiversidade e conservação*. Brasília, Brasil: Ministério do Meio Ambiente, 220–233.

Slade RW & Moritz C. **1998**. Phylogeography of *Bufo marinus* from its natural and introduced ranges.

Stephens M, Smith NJ & Donnelly P. **2001**. A new statistical method for haplotype reconstruction from population data. *American journal of human genetics* **68**: 978–89.

Stevaux MN. **2002**. A new species of *Bufo* Laurenti (Anura, Bufonidae) from northeastern Brazil. *Revista Brasileira de Zoologia* **19**: 235–242.

Talavera G & Castresana J. **2007**. Improvement of phylogenies after removing divergent and ambiguously aligned blocks from protein sequence alignments. *Systematic Biology* **56**: 564–577.

Thomé MTC, Sequeira F, Brusquetti F, Carstens B, Haddad CFB, Rodrigues MT & Alexandrino J. **2016**. Recurrent connections between Amazon and Atlantic forests shaped diversity in Caatinga four-eyed frogs. *Journal of Biogeography* **43**: 1045–1056.

Urban MC, Phillips BL, Skelly DK & Shine R. **2008**. A Toad More Traveled : The Heterogeneous Invasion Dynamics of Cane Toads in Australia. *The American Naturalist* **171**: E134–E148.

Vallinoto M, Sequeira F, Sodré D, Bernardi JAR, Sampaio I & Schneider H. **2010**. Phylogeny and biogeography of the *Rhinella marina* species complex (Amphibia, Bufonidae) revisited: Implications for Neotropical diversification hypotheses. *Zoologica Scripta* **39**: 128–140.

Vallinoto M, Cunha DB, Bessa-Silva A, Sodré D & Sequeira F. **2017**. Deep divergence and hybridization among sympatric Neotropical toads. *Zoological Journal of the Linnean Society* **180**: 647–660.

Wang X, Auler AS, Edwards RL, Cheng H, Cristalli PS, Smart PL, Richards DA, Shen CC & Edwards RL. **2004**. Wet periods in northeastern Brazil over the past 210 kyr linked to distant climate anomalies. *Nature* **432**: 2767–2769.

Werneck FP. **2011**. The diversification of eastern South American open vegetation biomes: Historical biogeography and perspectives. *Quaternary Science Reviews* **30**: 1630–1648.

Werneck FP, Gamble T, Colli GR, Rodrigues MT & Sites JW. **2012**. Deep diversification and long-term persistence in the south american 'dry diagonal': Integrating continent-wide phylogeography and distribution modeling of geckos. *Evolution* **66**: 3014–3034.

Werneck FP, Leite RN, Geurgas SR & Rodrigues MT. **2015**. Biogeographic history and cryptic diversity of saxicolous Tropiduridae lizards endemic to the semiarid Caatinga. *BMC Evolutionary Biology* **15**: 1–24.

#

Biological Journal of the Linnean Society

The evolutionary history of the Cururu Toad *Rhinella jimi* (Stevaux, 2002) in Northeast Brazil

Ricardo Marques & Adrian A. Garda

Supporting Information (appendix S1)

Laboratory protocols

We extracted DNA from tissue samples from liver and muscle using an adapted protocol from Brufold et al. (1992). To generate Polymerase Chain Reaction (PCR) mixes, we standardized a mix with 7.5 µl of Taq Polymerase Master Mix Red Ampliqon, 0.36 µl for primers (forward and reverse) and (BSA), 2-3 µl of extracted DNA and complemented with Miliq, totaling a mix of 15 µl. We used a specific cycle for each locus as described in Table S1. The respective primer for each loci and the source material are described in Table S1. We followed standard PCR techniques to amplify portions of DNA and PCR cycles for all loci are described in Table S2. Purification and sequencing of DNA were performed in Macrogen Inc.

Table S1: List of primers used in this study, their respective locus and its source material.

Locus	Reference	Primer	Sequence 5' → 3'
16S	Palumbi et al. 1991	16SA-L	CGCCTGTTTATCAAAAACAT
		16SB-H	CCGGTCTGAACTCAGATCACGT
CytB	Lamb et al. 2000	CytBFor	TTTCTAGCAATACAYTACACAGCYGATACAT
		CytBRev	AATCGTGTTAGGGTTGCATTGTCAACTGAAAA
RPL3	Pinho et al. 2010	RPL3-5F	TGTACAGGTCAAGTGTTATC
		RPL3-6RA	ATGCCAGTTAAAAATCAGACC
RPL9	Pinho et al. 2010	RPL96intF	TGTACAGGTCAAGTGTTATC
		RPL96intR	ATGCCAGTTAAAAATCAGACC

Table S2: Detailed PCR cycles with the respective temperature and duration of each stage. (*) Touchdown.

Cycle stage	16S	CytB	RPL3	RPL9
Initial denaturation	94º C, 3 min	94º C, 3 min	92º C, 5 min	92º C, 5 min
Number of cycles	10* + 35	30	40	40
Denaturation	94º C, 50 s	94º C, 1 min	92º C, 30s	92º C, 30s
Annealing	60º C* + 50º C 1 min	54º C, 1 min	55º C, 30 s	54º C, 30 s
Extension	72º C, 1 min	72º C, 1 min	72º C, 1:30 min	72º C, 1:30 min
Final extension	72º C, 5 min	72º C, 5 min	72º C, 5 min	72º C, 5 min

Table S3: List of samples used for molecular data from *Rhinella jimi*, with voucher number, respective haplotype for each gene, municipality and biome. (*) Phased sequences.

Voucher	Haplotype				Municipality (map number)	Acronym	State	Biome
	16S	CytB	RPL3*	RPL9*				
UFBA 14100		H2			Amargosa (1)	AMA	BA	Atlantic forest
UFBA 14101		H3	H1/H2	H1/H1	Amargosa (1)	AMA	BA	Atlantic forest
UFBA 14102	H1	H3	H1/H3	H1/H2	Amargosa (1)	AMA	BA	Atlantic forest
UFBA 14103		H4			Amargosa (1)	AMA	BA	Atlantic forest
UFBA 14104	H2	H1	H4/H4	H2/H2	Amargosa (1)	AMA	BA	Atlantic forest
CHUFPB 7148		H3			Barra (2)	BAR	BA	Cerrado
CHUFPB 7149		H3			Barra (2)	BAR	BA	Cerrado
CHUFPB 7150		H3			Barra (2)	BAR	BA	Cerrado
CHUFPB 7172		H4			Campo Formoso (3)	CAF	BA	Caatinga
AAGARDA 10549		H9			Condeúba (4)	CDB	BA	Caatinga
AAGARDA 10593		H9			Condeúba (4)	CDB	BA	Caatinga
AAGARDA 10594		H9			Condeúba (4)	CDB	BA	Caatinga
AAGARDA 10595		H3			Condeúba (4)	CDB	BA	Caatinga
AAGARDA 9607	H6	H10	H8/H12	H5/H5	Elísio Medrado (5)	ELM	BA	Atlantic forest
AAGARDA 10431		H11			Elísio Medrado (5)	ELM	BA	Atlantic forest
AAGARDA 10432		H4			Elísio Medrado (5)	ELM	BA	Atlantic forest
UFBA 567	H2	H4			Mata de São João (6)	MSJ	BA	Atlantic forest
MSJRhijim1		H14	H1/H6	H1/H1	Mata de São João (6)	MSJ	BA	Atlantic forest
MSJRhijim2		H4		H1/H1	Mata de São João (6)	MSJ	BA	Atlantic forest
AAGARDA 4384	H9	H1			Paulo Afonso (7)	PAA	BA	Caatinga
AAGARDA 6592		H10			Palmeiras (8)	PAL	BA	Caatinga
AAGARDA 6593	H2	H10	H1/H1	H1/H5	Palmeiras (8)	PAL	BA	Caatinga
AAGARDA 6606	H6	H10		H5/H5	Palmeiras (8)	PAL	BA	Caatinga
AAGARDA 6786	H2	H11		H1/H1	Palmeiras (8)	PAL	BA	Caatinga
AAGARDA 6787	H10	H4			Palmeiras (8)	PAL	BA	Caatinga
AAGARDA 6788	H10	H4			Palmeiras (8)	PAL	BA	Caatinga
AAGARDA 7248	H11	H2		H1/H1	Palmeiras (8)	PAL	BA	Caatinga
AAGARDA 9076	H6	H10		H2/H2	Paripiranga (9)	PAR	BA	Caatinga
UFMGT 1461		H3			Riacho Santana (10)	RIS	BA	Caatinga
UFMGT 1473		H3			Riacho Santana (10)	RIS	BA	Caatinga

UFBA 7680		H4			Serra do Ramalho (11)	SER	BA	Cerrado
FSCHUFPB 6527		H1			Aiuaba (12)	AIU	CE	Caatinga
FSCHUFPB 6614		H1			Aiuaba (12)	AIU	CE	Caatinga
FSCHUFPB 6641		H1			Aiuaba (12)	AIU	CE	Caatinga
AAGARDA 2698	H2	H1			Crato (13)	CRA	CE	Caatinga
AAGARDA 2701	H2	H1		H4/H4	Crato (13)	CRA	CE	Caatinga
AAGARDA 2702		H1		H1/H1	Crato (13)	CRA	CE	Caatinga
AAGARDA 2703		H1			Crato (13)	CRA	CE	Caatinga
AAGARDA 10249		H4			Jaguaribe (14)	JAG	CE	Caatinga
AAGARDA 10250		H1			Jaguaribe (14)	JAG	CE	Caatinga
AAGARDA 10292		H1			Jaguaribe (14)	JAG	CE	Caatinga
AAGARDA 10408	H2	H5	H1/H1	H2/H2	Jaguaribe (14)	JAG	CE	Caatinga
AAGARDA 10409		H3			Jaguaribe (14)	JAG	CE	Caatinga
AAGARDA 11650	H2				Quixadá (15)	QUI	CE	Caatinga
AAGARDA 11673		H1			Quixadá (15)	QUI	CE	Caatinga
AAGARDA 11749		H1			Quixadá (15)	QUI	CE	Caatinga
AAGARDA 11750	H2				Quixadá (15)	QUI	CE	Caatinga
AAGARDA 11751	H2	H5	H1/H1	H2/H2	Quixadá (15)	QUI	CE	Caatinga
AAGARDA 11752		H1			Quixadá (15)	QUI	CE	Caatinga
AAGARDA 11819	H2	H1			Quixadá (15)	QUI	CE	Caatinga
AAGARDA 11840		H1			Quixadá (15)	QUI	CE	Caatinga
AAGARDA 10647		H5			Ubajara (16)	UBA	CE	Caatinga
AAGARDA 10648		H1			Ubajara (16)	UBA	CE	Caatinga
AAGARDA 10670	H13	H6		H1/H1	Ubajara (16)	UBA	CE	Caatinga
AAGARDA 10671		H6			Ubajara (16)	UBA	CE	Caatinga
AAGARDA 10798	H2	H5	H1/H1	H2/H2	Ubajara (16)	UBA	CE	Caatinga
AAGARDA 10804		H1			Ubajara (16)	UBA	CE	Caatinga
AAGARDA 10841	H2		H17/H18		Ubajara (16)	UBA	CE	Caatinga
AAGARDA 3836		H1			Areia (17)	ARE	PB	Caatinga
AAGARDA 3837		H6	H5/H5		Areia (17)	ARE	PB	Caatinga
AAGARDA 3838	H3	H1			Areia (17)	ARE	PB	Caatinga
AAGARDA 3839	H2	H6	H4/H4	H2/H2	Areia (17)	ARE	PB	Caatinga
AAGARDA 3840		H1			Areia (17)	ARE	PB	Caatinga
AAGARDA 3948	H2	H4	H4/H5	H1/H2	Areia (17)	ARE	PB	Caatinga
AAGARDA 3949	H2	H4	H1/H6	H1/H2	Areia (17)	ARE	PB	Caatinga
AAGARDA 3950		H1			Areia (17)	ARE	PB	Caatinga

ASP 86		H5			Cabaceiras (18)	CAB	PB	Caatinga
ASP 111		H1			Cabaceiras (18)	CAB	PB	Caatinga
L 256		H1			Cabaceiras (18)	CAB	PB	Caatinga
L 257		H8			Cabaceiras (18)	CAB	PB	Caatinga
L 361		H1			Cruz do Espírito Santo (19)	CES	PB	Atlantic forest
L 377		H1			Cruz do Espírito Santo (19)	CES	PB	Atlantic forest
AAGARDA 8997		H1	H10/H11		Cuité (20)	CUI	PB	Caatinga
FSCHUFPB 603		H1			Mamanguape (21)	MAM	PB	Atlantic forest
FSCHUFPB 4323		H1			Santa Rita (22)	SAR	PB	Atlantic forest
FSCHUFPB 4325		H1			Santa Rita (22)	SAR	PB	Atlantic forest
FSCHUFPB 4327		H1			Santa Rita (22)	SAR	PB	Atlantic forest
FSCHUFPB 4471		H15			Santa Rita (22)	SAR	PB	Atlantic forest
FRD 1154		H2			Bonito (23)	BON	PE	Atlantic forest
AAGARDA 7439		H4			Buíque (24)	BUI	PE	Caatinga
AAGARDA 8048		H4		H2/H3	Buíque (24)	BUI	PE	Caatinga
AAGARDA 8049	H5				Buíque (24)	BUI	PE	Caatinga
AAGARDA 8695		H4			Buíque (24)	BUI	PE	Caatinga
FRD 1077		H1			Serra Talhada (25)	SET	PE	Caatinga
FRD 1081		H1			Serra Talhada (25)	SET	PE	Caatinga
FSCHUFPB 10033		H1			São Vicente Ferrer (26)	SVF	PE	Caatinga
AAGARDA 9009	H9	H1			Taquaritinga do Norte (27)	TDN	PE	Caatinga
AAGARDA 9955	H5	H8			PARNA Serra das Confusões (28)	SDC	PI	Caatinga
AAGARDA 9956	H12	H3	H1/H12	H1/H2	PARNA Serra das Confusões (28)	SDC	PI	Caatinga
AAGARDA 11215	H9	H1			PARNA Serra das Confusões (28)	SDC	PI	Caatinga
AAGARDA 11340	H5	H8	H5/H5	H2/H2	PARNA Serra das Confusões (28)	SDC	PI	Caatinga
AAGARDA 11341			H4/H5	H1/H1	PARNA Serra das Confusões (28)	SDC	PI	Caatinga
AAGARDA 11446	H2	H8	H14/H15	H1/H1	PARNA Serra das Confusões (28)	SDC	PI	Caatinga
AAGARDA 11462	H9	H1			PARNA Serra das Confusões (28)	SDC	PI	Caatinga
AAGARDA 4705	H2	H8	H4/H16		São Raimundo Nonato (29)	SRN	PI	Caatinga

AAGARDA 4708	H2	H8		H1/H2	São Raimundo Nonato (29)	SRN	PI	Caatinga
AAGARDA 4755		H3			São Raimundo Nonato (29)	SRN	PI	Caatinga
AAGARDA 5018		H16			São Raimundo Nonato (29)	SRN	PI	Caatinga
AAGARDA 5241		H1			São Raimundo Nonato (29)	SRN	PI	Caatinga
AAGARDA 10436		H5			Angicos (30)	ANG	RN	Caatinga
AAGARDA 2838	H4	H7	H6/H7	H2/H2	Arês (31)	ARS	RN	Atlantic forest
AAGARDA 2839		H1			Arês (31)	ARS	RN	Atlantic forest
AAGARDA 2840	H2	H4	H8/H9	H1/H1	Arês (31)	ARS	RN	Atlantic forest
AAGARDA 2842	H2	H1			Arês (31)	ARS	RN	Atlantic forest
AAGARDA 2843		H1			Arês (31)	ARS	RN	Atlantic forest
AAGARDA 2905		H7			Canguaretama (32)	CAN	RN	Caatinga
AAGARDA 5080	H7	H12	H1/H1	H2/H2	Extremoz (33)	EXT	RN	Atlantic forest
AAGARDA 5081		H5			Extremoz (33)	EXT	RN	Atlantic forest
AAGARDA 6099		H1	H1/H6		João Câmara (34)	JOC	RN	Caatinga
AAGARDA 6465	H2	H5		H1/H2	João Câmara (34)	JOC	RN	Caatinga
AAGARDA 1311		H1			Macaíba (35)	MAC	RN	Caatinga
AAGARDA 3228	H8	H4	H1/H6	H1/H2	Macaíba (35)	MAC	RN	Caatinga
AAGARDA 3229	H2	H1			Macaíba (35)	MAC	RN	Caatinga
AAGARDA 3230	H2	H1			Macaíba (35)	MAC	RN	Caatinga
AAGARDA 3231		H1			Macaíba (35)	MAC	RN	Caatinga
AAGARDA 3232	H8	H4		H1/H2	Macaíba (35)	MAC	RN	Caatinga
AAGARDA 5068		H1			Martins (36)	MAR	RN	Caatinga
AAGARDA 9378	H1	H3		H2/H6	Martins (36)	MAR	RN	Caatinga
AAGARDA 1577		H1			Natal (37)	NAT	RN	Atlantic forest
AAGARDA 1578		H1			Natal (37)	NAT	RN	Atlantic forest
AAGARDA 1579		H1			Natal (37)	NAT	RN	Atlantic forest
AAGARDA 6210		H1			Nísia Floresta (38)	NIF	RN	Atlantic forest
AAGARDA 6211		H4		H1/H2	Nísia Floresta (38)	NIF	RN	Atlantic forest
AAGARDA 8782	H2	H6	H13/H13	H2/H2	Nísia Floresta (38)	NIF	RN	Atlantic forest
FSCHUFPB 5330		H1			Serra Negra do Norte (39)	SNN	RN	Caatinga
FSCHUFPB 5372		H1			Serra Negra do Norte (39)	SNN	RN	Caatinga
FSCHUFPB 5402				H7/H7	Serra Negra do Norte (39)	SNN	RN	Caatinga
FSCHUFPB 5404	H2	H8	H1/H6	H8/H8	Serra Negra do Norte (39)	SNN	RN	Caatinga
FSCHUFPB 5429	H2				Serra Negra do Norte (39)	SNN	RN	Caatinga
FSCHUFPB 5431		H1			Serra Negra do Norte (39)	SNN	RN	Caatinga

FSCHUFPB 5521	H9	H1			Serra Negra do Norte (39)	SNN	RN	Caatinga
FSCHUFPB 5523	H2	H8			Serra Negra do Norte (39)	SNN	RN	Caatinga
FSCHUFPB 5524	H2	H5	H1/H1		Serra Negra do Norte (39)	SNN	RN	Caatinga
FSCHUFPB 5575	H2	H1			Serra Negra do Norte (39)	SNN	RN	Caatinga
FSCHUFPB 41	H2	H13		H1H2	Monte Alegre (40)	MAL	SE	Caatinga

Table S4: Genbank access number for *R. crucifer*, *R. diptycha*, and *R. marina* used in analysis for all loci.

Species	**Source**	**16S**	**CytB**	**RPL3**	**RPL9**
R. crucifer	Vallinoto et al. 2010	DQ415570	DQ415596		
R. diptycha	Vallinoto et al. 2010, Sequeira et al. 2011	DQ415572	DQ415598		
R. diptycha	Vallinoto et al. 2010, Sequeira et al. 2011		JN594573	JN594597	JN594550
R. diptycha	Vallinoto et al. 2010, Sequeira et al. 2011		JN594572		JN594549
R. diptycha	Vallinoto et al. 2010, Sequeira et al. 2011		JN594574		JN594549
R. marina	Vallinoto et al. 2010, Sequeira et al. 2011	GU178791	GU178802	KY231297	JN594526
R. marina	Vallinoto et al. 2010, Sequeira et al. 2011	GU178792	GU178803	KY231300	KY231339
R. marina	Vallinoto et al. 2010, Sequeira et al. 2011	GU178793	GU178804	KY231306	JN594542
R. marina	Vallinoto et al. 2010, Sequeira et al. 2011	GU178794	GU178805	KY231303	JN594533

Table S5: Additional distribution records of *Rhinella jimi* used for Ecological Niche Modeling and its respective source material.

Latitude	**Longitude**	**Municipality**	**State**	**Biome**	**Source**
-9.7525	-36.6611	Arapiraca	AL	Caatinga	Almeida et al. 2016
-9.5381	-36.1328	Atalaia	AL	Atlantic forest	Almeida et al. 2016
-9.6438	-36.2131	Boca da Mata	AL	Atlantic forest	Almeida et al. 2016
-9.78194	-36.3508	Campo Alegre	AL	Atlantic forest	Almeida et al. 2016
-10.1250	-36.1762	Coruripe	AL	Atlantic forest	Almeida et al. 2016
-8.9516	-35.8934	Ibateguara	AL	Atlantic forest	Almeida et al. 2016
-9.6499	-35.7089	Maceió	AL	Atlantic forest	Almeida et al. 2016
-9.2241	-37.3614	Maravilha	AL	Caatinga	Almeida et al. 2016
-9.0973	-35.5877	Matriz de Camaragibe	AL	Atlantic forest	Almeida et al. 2016
-9.3095	-35.9420	Murici	AL	Atlantic forest	Almeida et al. 2016
-9.4229	-37.8300	Olho D’água do Casado	AL	Caatinga	Almeida et al. 2016
-10.2890	-36.5839	Penedo	AL	Atlantic forest	Almeida et al. 2016
-10.3844	-36.4148	Piaçabuçu	AL	Atlantic forest	Almeida et al. 2016
-9.6233	-37.7567	Piranhas	AL	Caatinga	Almeida et al. 2016

-9.4783	-35.8398	Rio Largo	AL	Atlantic forest	Almeida et al. 2016
-9.5581	-37.3835	São José da Tapera	AL	Caatinga	Almeida et al. 2016
-9.3188	-35.5610	São Luís do Quitunde	AL	Atlantic forest	Almeida et al. 2016
-9.9712	-37.0036	Traipu	AL	Caatinga	Almeida et al. 2016
-14.7008	-39.5961	Almadinha	BA	Atlantic forest	Dias et al. 2014b
-13.255	-43.4181	Bom Jesus da Lapa	BA	Cerrado	SpeciesLink
-14.0694	-42.475	Caetité	BA	Caatinga	SpeciesLink
-15.3833	-39.5500	Camacan	BA	Atlantic forest	Dias et al. 2014a
-12.7656	-38.1742	Camaçari	BA	Atlantic forest	Pers. Obs.
-12.8551	-38.2535	Camaçari	BA	Atlantic forest	Pers. Obs.
-11.8535	-37.5715	Conde	BA	Atlantic forest	SpeciesLink
-13.3426	-44.6357	Correntina	BA	Cerrado	SpeciesLink
-12.3382	-37.8510	Entre Rios	BA	Atlantic forest	Pers. Obs.
-12.1148	-37.7057	Esplanada	BA	Atlantic forest	Pers. Obs.
-13.7441	-39.4849	Gandú	BA	Atlantic forest	SpeciesLink
-13.4106	-41.2847	Ibicoara	BA	Caatinga	SpeciesLink
-14.75548	-39.091638	Ilhéus	BA	Atlantic forest	Dias et al. 2014b
-11.82261	-42.617921	Ipupiara	BA	Caatinga	SpeciesLink
-14.2836	-39.8428	Itagibá	BA	Atlantic forest	Stevaux 2002
-14.8497	-42.4333	Jacaraci	BA	Caatinga	SpeciesLink
-11.6984	-37.5054	Jandaíra	BA	Atlantic forest	Pers. Obs.
-13.9447	-40.1093	Jequié	BA	Atlantic forest	Lantyer-Silva et al. 2013[1]
-9.4168	-40.5035	Juazeiro	BA	Caatinga	Maciel et al. 2007
-13.4411	-40.4308	Maracás	BA	Atlantic forest	Stevaux 2002
-12.4501	-38.2346	Mata de São João	BA	Atlantic forest	Pers. Obs.
-13.0088	-41.3712	Mucugê	BA	Caatinga	SpeciesLink
-14.2672	-43.1619	Palmas de Monte Alto	BA	Caatinga	SpeciesLink
-10.7417	-40.3608	Pindobaçu	BA	Caatinga	SpeciesLink
-13.5789	-41.8114	Rio de Contas	BA	Caatinga	SpeciesLink
-12.94752	-38.413246	Salvador	BA	Atlantic forest	Pers. Obs.
-12.4350	-38.9508	São Gonçalo dos Campos	BA	Atlantic forest	SpeciesLink
-14.5731	-42.9403	Sebastião Laranjeiras	BA	Cerrado	SpeciesLink
-14.8847	-40.8163	Vitória da coquista	BA	Atlantic forest	SpeciesLink
-6.7167	-38.8667	Barro	CE	Caatinga	SpeciesLink
-3.5545	-38.8235	Pecém	CE	Caatinga	SpeciesLink
-2.7591	-42.8231	Barreirinhas	MA	Cerrado	SpeciesLink
-3.3995	-44.3518	Itapecuru Mirim	MA	Cerrado	SpeciesLink

-8.28333	-35.9761	Caruaru	PE	Caatinga	SpeciesLink
-3.84028	-32.4108	Fernando de Noronha	PE	Caatinga	SpeciesLink
-7.74778	-34.8256	Itamaracá	PE	Atlantic forest	SpeciesLink
-8.0883	-39.5843	Parnamirim	PE	Caatinga	Guedes et al. 2018
-8.36056	-36.5656	Sanharó	PE	Caatinga	SpeciesLink
-2.9008	-41.7965	Parnaíba	PI	Cerrado	SpeciesLink
-5.5777	-36.9146	Açu	RN	Caatinga	SpeciesLink
-6.2684	-35.2175	Goianinha	RN	Atlantic forest	Voucher AAGARDA2594
-5.0969	-36.4589	Macau	RN	Caatinga	Voucher AAGARDA3743
-5.1951	-37.3300	Mossoró	RN	Caatinga	Maciel et al. 2007
-5.5218	-36.3897	Pedro Avelino	RN	Caatinga	Voucher AAGARDA1911
-6.1904	-35.0909	Tibau do Sul	RN	Atlantic forest	SpeciesLink
-10.2111	-36.8403	Propriá	SE	Atlantic forest	SpeciesLink
-11.0355	-48.6387	Brejinho de Nazaré	TO	Cerrado	SpeciesLink

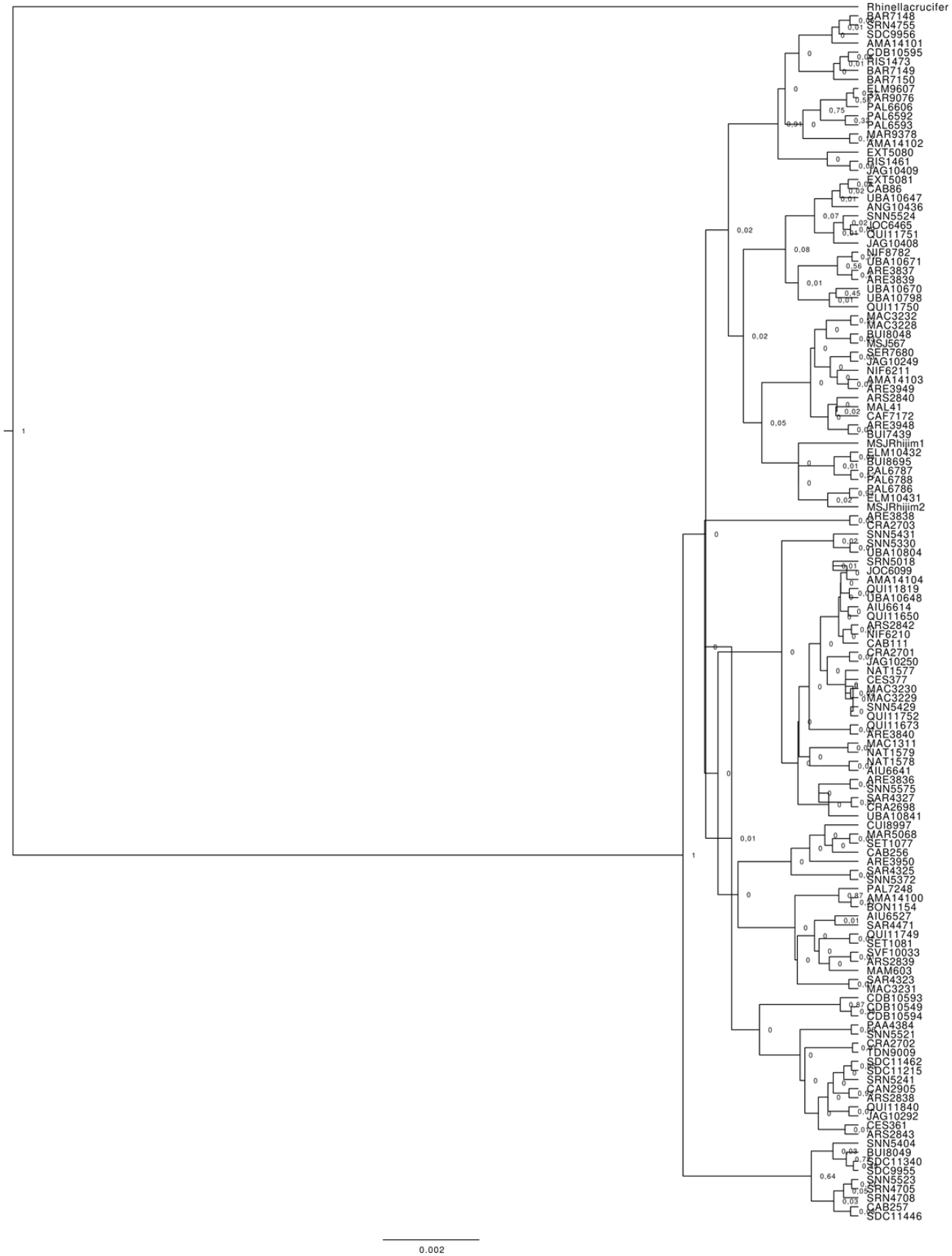

Figure S1: Resulting Bayesian mitochondrial gene tree for samples of *R. jimi.* Node values are the posterior probabilities of each branch.

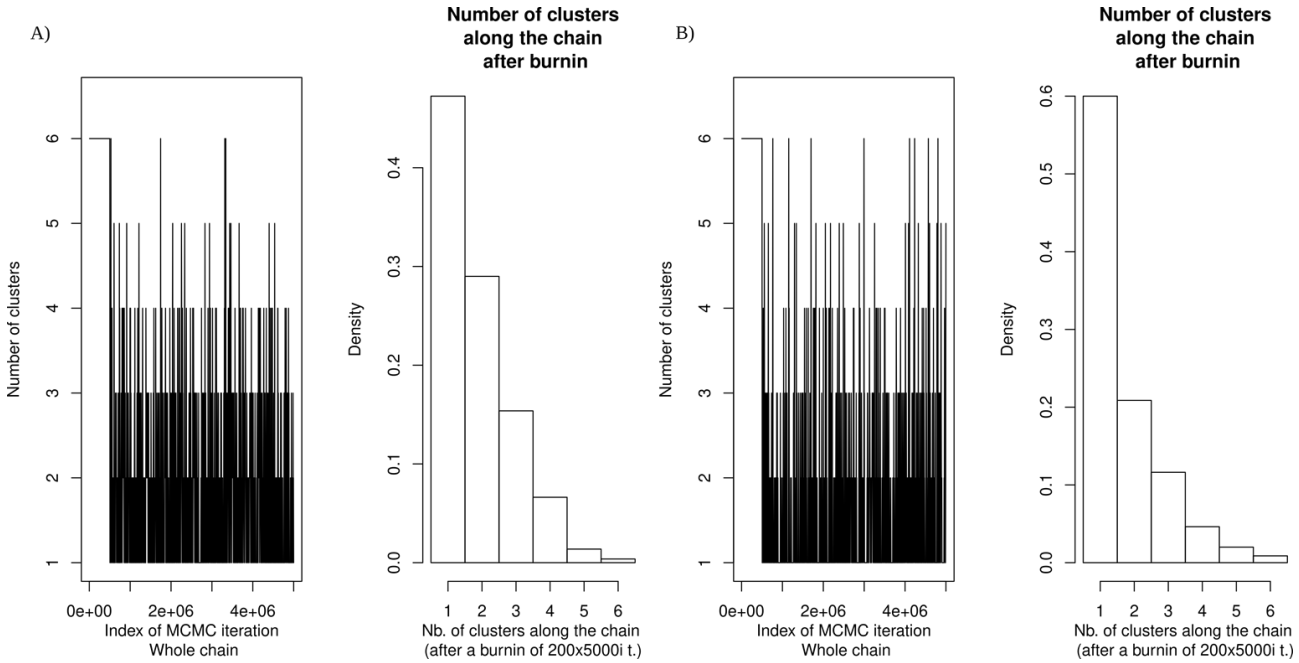

Figure S2: Number of suggested clusters for *R. jimi* inferred with (A) mtDNA and nuDNA and (B) nuDNA only in Geneland.

References

Lantyer Silva, A. S. F., Siqueira Júnior, S. & Zina, J. 2013. Checklist of amphibians in a transitional area between the Caatinga and the Atlantic Forest, central-southern Bahia, Brazil. *Check List* **9**, 725–732.

Almeida, J.P.F.A., Nascimento, F.A.C., Torquato, S., Lisboa, B.S., Tiburcio, I.C.S., Palmeira, C.N.S., Lima, M.G. & Mott, T. 2016. Amphibians of Alagoas State, northeastern Brazil. Herpetology Notes, 9:123-140.

Dias, I. R., Medeiros, T. T., Nova, M. F. V. & Solé, M. 2014a. Amphibians of Serra Bonita , southern Bahia: a new hotpoint within Brazil's Atlantic Forest hotspot. *Zookeys* **130**, 105–130

Dias, I. R., Mira-mendes, C. V. De & Solé, M. 2014b. Rapid inventory of herpetofauna at the APA (Environmental Protection Area) of the Lagoa Encantada. Herpetology Notes, **7:** 627–637

Guedes, T. B., Sazima, I. & Marques, O. A. V. 2018. Does swallowing a toad require any specialisation? Feeding behaviour of the dipsadid snake *Philodryas nattereri* on the bufonid toad *Rhinella jimi*. *Herpetology Notes* **11**, 825–828

Maciel, N.M., Brandão, R.A., Campos, L.A., Sebben, A. 2007. A large new species of *Rhinella* (Anura: Bufonidae) from Cerrado of Brazil. Zootaxa 1627, 23–39.

Palumbi S.R., Martin A., Romano S., McMillan W.O., Stice L. & Grabowski G. 1991. The Simple Fool's Guide to PCR, Version 2.0. Privately published document compiled by S. Palumbi, Dept. Zoology. Honululu: Univ. Hawaii.

Pinho, C., Rocha, S., Carvalho, B.M., Lopes, S., Mourão, S., Vallinoto, M., Brunes, T.O., Haddad, C.F.B., Gonçalves, H., Sequeira, F. & Ferrand, N. 2010 New primers for the amplification and sequencing of nuclear loci in a taxonomically wide set of reptiles and amphibians. Conservation Genetic Resources, 2, 181–185

Stevaux, M.N. 2002. A new species of *Bufo* Laurenti (Anura, Bufonidae) from northeastern Brazil. Revista Brasileira de Zoologia 19(1): 235-242.

Vallinoto, M., Sequeira, F., Sodré, D., Bernardi, J. A. R., Sampaio, I. & Schneider, H. 2010. Phylogeny and biogeography of the *Rhinella marina* species complex (Amphibia, Bufonidae) revisited: implications for Neotropical diversification hypotheses. Zoologica Scripta, 39, 128–140.

Capítulo II

Antigo curso do Rio São Francisco, isolamento por altitude e aspectos ecológicos no enredo da história evolutiva de *Corythomantis greeningi* Boulenger 1896 (Anura, Hylidae) nos biomas secos da região Neotropical

Manuscrito a ser submetido ao periódico Molecular Phylogenetics and Evolution

Past São Francisco River course, altitude isolation, and ecological traits as the evolutionary history plot for *Corythomantis greeningi* Boulenger 1896 (Anura, Hylidae) in dry biomes of Neotropical Region

Ricardo Marques[1*], Emanuel M. da Fonseca[2], Leandro A. da Silva[1], Diego J. Santana[4], Amanda S. F. Lantyer-Silva[3], Célio F. B. Haddad[3] & Adrian A. Garda[1,5]

[1]Programa de Pós-Graduação em Ciências Biológicas (Zoologia), Centro de Ciências Exatas e da Natureza, Departamento de Sistemática e Ecologia, Universidade Federal da Paraíba; João Pessoa, PB 58051-900, Brazil

[2]Department of Evolution, Ecology, and Organismal Biology, The Ohio State University, 318 W. 12th Avenue, Columbus, OH, USA.

[3]Universidade Estadual Paulista (UNESP), Departamento de Zoologia e Centro de Aquicultura (CAUNESP), Instituto de Biociências, Rio Claro, São Paulo, Brasil

[4]Instituto de Biociências, Laboratório de Zoologia, Universidade Federal de Mato Grosso do Sul, Cidade universitária, CEP 79002-970, Campo Grande, Mato Grosso do Sul, Brazil

[5]Departamento de Botânica e Zoologia, Centro de Biociências, Universidade Federal do Rio Grande do Norte, Lagoa Nova, Natal, RN, Brazil

* Corresponding author: rcdmarquess@gmail.com

Abstract

In this study we evaluate how historical events and landscape features affected the diversification of the treefrog *Corythomantis greeningi* within the Caatinga and Cerrado biomes. We postulate that (1) the genetic structure of *C. greeningi* is associated with river basins and/or prominent landscape features across its distribution; (2) Past climatic fluctuations during the Pleistocene affected the species' demographic history, and; (3) genetic diversity between populations of *C. greeningi* is structured accordingly to ecological traits and past geological events. We used a total of five loci from mtDNA and nuDNA and sequenced 99 specimens from 35 localities. We inferred genetic structure and lineage boundaries with population assignment and species delimitation methods. Then, we estimated intraspecific diversity, divergence times, demographic history and ecological niche modeling. We recovered two non-overlapping,

geographically structured lineages corresponding to *C. greeningi* and an undescribed species that most likely diverged in the Pliocene. *Corythomantis greeningi* has two populations within its geographical distribution, and the change in the course of the São Francisco River and climatic oscillations during Pleistocene affected its geographic distribution. We show that altitude, habitats, and past climatic and geological events likely acted in conjunction and lead to the diversification between lineages and species, with *C. greeningi* inhabiting lowlands across Caatinga and Cerrado, while the new species is restricted to the Espinhaço Range.

KEYWORDS: Lophiohylini, Caatinga, Cerrado, multilocus, Casque-head treefrog.

1 Introduction

Global biodiversity is the result of different speciation processes that sometimes act simultaneously in the same region, making it hard to identify which phenomena are responsible for current biodiversity patterns, especially in megadiverse regions such as the Neotropics (Vences and Wake, 2007). Some studies have unraveled diversification mechanisms of the Neotropical biota using species distributions, molecular data, or past landscape and climatic features, as well as different combinations of these datasets (Avise, 2009; Marshall et al., 2018). These works show that large rivers and mountain ranges have acted as vicariant barriers, dividing once continuous populations of terrestrial vertebrates, reducing gene flow and ultimately leading to speciation (Geurgas and Rodrigues, 2010; Lanna et al., 2020; Oliveira et al., 2018; Patton et al., 1994; Werneck et al., 2015).

Species can also be segregated along altitudinal gradients or be restricted to isolated mountains tops due to physiological constraints that hamper dispersion to higher or lower altitudes, hence restricting gene flow (Funk et al., 2015; Gehara et al., 2013; Graham et al., 2004; Lynch and Duellman, 1997; Osborne et al., 2013). In addition, recent Quaternary climatic oscillations, mostly during Pleistocene, have been shown to influence the expansion and retraction of forests and open and dry habitats. Cycles of isolation and reconnection between the Amazon and Atlantic Forest shaped biodiversity on both forested and semi-arid biomes (Amaral et al., 2013; Batalha-Filho et al., 2013; Carnaval et al., 2009; Haffer, 1959; Pennington et al., 2000; Thomé et al., 2016; Wang et al., 2004).

Within the semi-arid biomes of the dry diagonal of open formations, studies have shown that species evolutionary histories are related to species's ecological traits or landscape features of the biome (Caetano et al., 2008; Fonseca et al., 2018; Werneck et al., 2012), past climatic oscillations (Lanna et al., 2018; Magalhães et al., 2014; Thomé et al., 2016), mountain ranges (Barres et al., 2019; Oliveira et al., 2018; Prado et al., 2012; Thomé et al., 2016), and the past and current São Francisco River courses acting as a vicariant or permeable barrier (Lanna et al., 2020; Magalhães et al., 2014; Nascimento et al., 2013; Oliveira et al., 2015; Recoder et al., 2014; Werneck et al., 2015). Besides landscape features, ecological traits have had a crucial role in shaping patterns of speciation and genetic diversity. For example, *Tropidurus semitaeniatus* — a saxicolous lizard highly dependent on rocky outcrops and widely distributed within the semiarid Caatinga biome — is structured by past and present courses of the São Francisco River (Werneck et al., 2015). Another saxicolous lizard, *Phyllopezus pollicaris,* was shown to be distributed throughout the dry diagonal of open formations with lineages matching the Chaco, Cerrado, and Caatinga biomes, suggesting these regions were not subject to a single diversification history (Werneck et al., 2012). Such examples show that not only vicariant barriers, but ecological traits also have a major effect on species diversification.

Most amphibians are thought to be philopatric and not widely distributed because of their strong dependence on water, low vagility, and small body sizes (Beebee, 2005; Reading et al., 1991). Thus, they are good model organisms for phylogeographic studies that test the effects of past landscape and climatic features on whole biotas, while often unveiling cryptic species or species complexes in otherwise widespread species, as revealed in recent studies (Gehara et al., 2014, 2013; Menezes et al., 2016; Oliveira et al., 2018). Widely distributed Neotropical frog species have been investigated in this manner, reveling either many lineages with candidate species attributed to a single taxon (Gehara et al., 2014; Menezes et al., 2016; Sabbag et al., 2018) but sometimes also single species with panmictic populations across large geographic distributions (Mângia et al., 2020; Prado et al., 2012).

Corythomantis is a monotypic genus housing only *Corythomantis greeningi* Boulenger, 1896, a Casque-headed frog adapted to arid regions, mainly distributed over the Caatinga biome and neighboring areas within Cerrado biome along several river Basins, lowland regions and mountain ranges (Blotto et al., 2020; Boulenger, 1896; Colli et al., 2002; Godinho et al., 2013). It inhabits rocky river streams, where its larvae

dwell, and is an explosive breeder and that hides in rock crevices and tree trunks when not active to retain water (phragmotic behavior, see Jared et al., 1999). These philopatric habits suggest limited dispersal ability, allowing the establishment and maintenance of genetic structure among populations and possibly the existence of undescribed, cryptic species. Moreover, its adaptations to the Caatinga biome (Navas et al., 2002) suggest that populations likely responded to recent climatic fluctuations that influenced the distribution and extension of the Caatinga during the Pleistocene.

We evaluated patterns of genetic diversity across the distribution of *C. greeningi* in a multilocus phylogeographic study to test the following hypotheses: (1) The genetic structure of *C. greeningi* is associated to river basins and/or other prominent landscape features across its distribution (e.g. major rivers, mountain ranges); (2) Past climatic fluctuations during Pleistocene affected the species' demographic history, and; (3) Divergence between populations of *C. greeningi* is structured according to ecological traits and past geological events, resulting in interspecific variation.

2 Materials and methods

2.1 Taxon sampling

We obtained tissues of 99 specimens from 35 localities covering most of the geographic distribution of *Corythomantis greeningi* through Museum loans and fieldwork to key locations to complement sampling (Figure 1, Table S1). We extracted DNA from liver and muscle tissues using a saline protocol adapted from Brufold et al. (1992) and amplified five loci through Polymerase Chain Reaction (PCR). We sequenced all samples for two mitochondrial DNA (mtDNA) fragments (Cytochrome Oxidase I and 16S ribosomal DNA), and latter selected 54 samples, based on exclusive haplotypes and geographic distribution, to sequence three nuclear DNA (nuDNA) loci: Beta-fibrinogen (βfib), Ribosomal Protein L 3 (RPL3) and Tyrosinase (Tyr). For amplification conditions, primers sequences and PCR cycles, see supporting information.

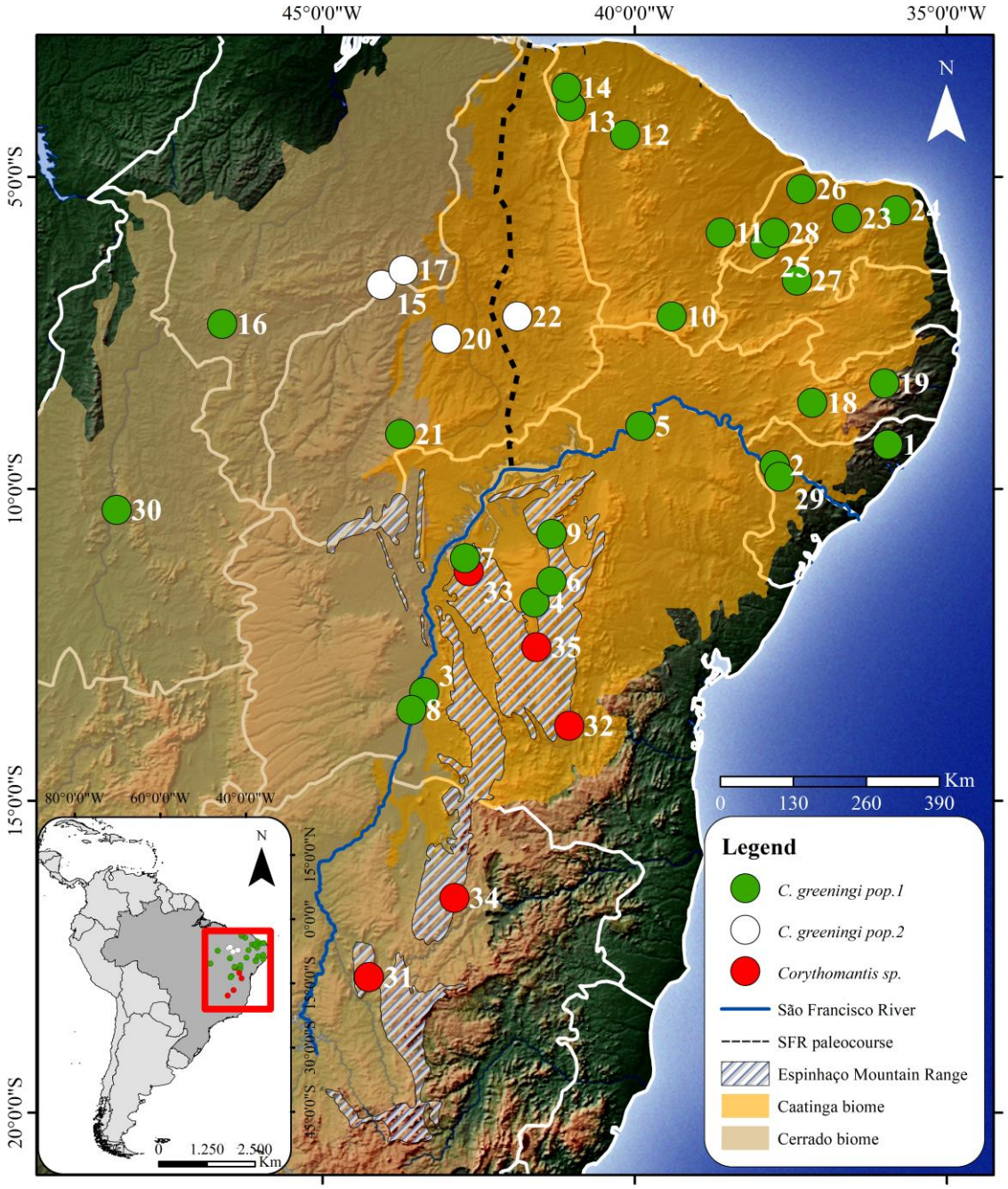

Figure 1: Distribution map of samples within Caatinga and Cerrado boundaries. The blue line shows the current São Francisco River and the dashed black line shows its Paleocourse. Each circle color corresponds to a specific population and locality numbers are described in Table S1.

2.2 Data treatment

We manually edited all sequences with Geneious 8.1.9 and aligned sequences with MUSCLE algorithm in MEGA X 10.0.4 (Kumar et al., 2018). For alignments with gaps, we used Gblocks (Talavera and Castresana, 2007) with default options and parameter values to obtain consistent sequences. Later, we used the PHI test

to check for recombination in nuclear data in SPLITSTREE4 (Huson and Bryant, 2006). Ambiguities and heterozygous specimens were treated with the algorithm Phase (Stephens et al., 2001) in DnaSP 5.1 (Librado and Rozas, 2009) using default settings.

2.3 Population assignments

To test if the genetic structure of *C. greeningi* is associated to landscape features and geological events, we used two Bayesian population assignment approaches. GENELAND detects population structure through variation in allele frequencies and geographic information, grouping samples that minimize departures from Hardy-Weinberg and linkage equilibrium, allowing the use of geographic coordinates besides molecular data. We tested our dataset using GENELAND package 4.0.5 (Guillot et al., 2005) in R 3.5.1 (R Core Team 2019) using the whole mitochondrial dataset and the nuclear data subset. The first analysis we performed contained the mtDNA, nuDNA, and geographic coordinates for specimens whilst the second analysis contained only nuDNA and geographic coordinates. For both analysis our parameters were 20 runs from one to six populations (k) of 5×10^5 MCMC chain sampled every 5×10^3 generations and a burn in of 2×10^2. Next, we ran another population assignment test in BAPS 5.0 (Corander and Marttinen, 2006), which treats allele frequencies and divergent genetic groups in population as random values of allele frequencies and number of genetically diverged groups within populations. To generate the mixture results, we used the same nuDNA dataset described above and performed the clustering with linked loci evaluating one to six populations (k). As our mixture obtained value of $k>2$, we ran the admixture with a minimum of one individual per population, 100 iterations, up to 200 individuals for each population and 10 iterations for each reference individual.

2.4 Lineage delimitation

We tested the validation of the populations recovered in population assignment using the species/lineage delimitation Bayesian Phylogenetics and Phylogeography (BPP) 3.3 (Flouri et al., 2018) with all nuclear loci dataset. We used four configuration scenarios, with three independent runs for each, 2×10^5 generations

and 4 x 10^4 burn-in and thinning every two generations. The parameter sets we used for each model were: large ancestral population with deep divergences, $\Theta \sim G(1, 10)$ and $\tau 0 \sim G(1, 10)$; large ancestral population with recent divergences $\Theta \sim G(1, 10)$ and $\tau 0 \sim G(2, 2000)$; small ancestral population and deep divergences $\Theta \sim G(2, 2000)$ and $\tau 0 \sim G(1, 10)$; and small ancestral population and recent divergences $\Theta \sim G(2, 2000)$ and $\tau 0 \sim G(2, 2000)$.

2.5 Mitochondrial gene tree, haplotype reconstruction and summary statistics

We used jModelTest 2.1.7 (Posada, 2008) using the Bayesian Information Criterion (BIC) to select the best evolutionary model for each mitochondrial gene fragment. The best-fit substitution model were TrNef+G (16S) and HKY+G (COI). We reconstructed a mitochondrial gene tree with 16S and COI combined in BEAST 1.8.4 (Drummond et al., 2012) using a strict clock, Yule process tree prior, and 10^7 generations sampled at every 10^4 generations. The convergence of all MCMC runs was evaluated in Tracer v1.5 (Rambaut and Drummond, 2007), and stationarity assessed by Effective Sample Size (ESS) for each parameter with values>200. We generated a consensus tree in TreeAnnotator 1.8.4 (Drummond et al., 2012) excluding as burn in the first 2 x 10^3 trees. We visualized the final consesnsu tree in FigTree 1.4.2 and used *Trachycephalus typhonius* as an outgroup when necessary.

We constructed a haplotype network for all loci by median joining network (Bandelt et al., 1994) in PopArt 1.7 (Leigh and Bryant, 2015), highlighting the populations identified in the population assignment with different colors. We calculated summary statistics in DnaSP 5.1 (Librado and Rozas, 2009) for all loci in each population, including number of segregating sites and haplotypes, haplotype diversity, standard deviation of haplotype diversity, nucleotide diversity, Tajima's D and its p value. Pairwise genetic distances (uncorrected p-distance) between populations were generated in MEGA X 10.0.4 (Kumar et al., 2018).

2.5 Diversification scenarios in Corythomantis

Our second hypothesis state that Pleistocene climactic fluctuation (PCF) affected the species' demographic history, and our third hypothesis states that the

divergence between populations are associated to geological events. To test possible outcomes in the evolutionary history of *Corythomantis*, we constructed diversification scenarios (models) based on previous results of structured populations, demographic change, phylogenetic relationships and haplotype sharing between populations (see Supplementary File for demographic changes and population divergence details). By integrating all these results, we built six diversification scenarios: (i) gene flow between population one and two and recent population expansion in population one (model 1); (ii) gene flow from population one to population two and recent population expansion in population one (model 2); (iii) gene flow from population two to population one and recent population expansion in population one (model 3); (iv) divergence without gene flow and recent population expansion in population one (model 4); (v) founder effect of population two from population one and population expansion in population one (model 5); (vi) founder effect of population one from population two (model 5). All models included the mitochondrial gene tree topology.

We performed 100,000 simulations for each model using the R package "pipemaster" (Gehara et al., in prep.; available at www.github.com/gehara/PipeMaster). The simulated datasets emulated the empirical dataset, i.e., the same number of genes, individuals per population, and sequence size per gene. Parameters were set as minimum and maximum values assuming a uniform prior distribution. Model support was calculated for each model using "postpr" function in R package "abc" (Csilléry et al., 2012). We performed the rejection and multinomial logistic regression methods to compare the models (tolerance rate = 0.001 and 0.01, respectively). We used a principal component analysis (PCA) to summarize simulated and empirical datasets and check if the simulated datasets produce statistics similar to the empirical dataset.

2.7 Ecologic niche modeling

We tested the potential distribution of *C. greeningi* for current period and along different scenarios of climatic fluctuations over the last 130 kya (Mid-Holocene, Last Glacial Maximum and Last Inter-Glacial). Then we identify stability areas based on all four results. We used records from our tissue samples localities, complemented with literature, with a total of 78 records (Table S3 and S4). We used R package spThin (Aiello-Lammens et al., 2015) to reduce spatial sampling bias, establishing 15 km of

minimal distance between records. Our final dataset consisted of 58 records for modeling. Worldclim 2.0 (Fick and Hijmans, 2017) (available at www.worldclim.org) allow present and past projections, so we downloaded 19 bioclimatic variables in a resolution of 2.5 arc-minutes for all periods, except LIG which was available at 30 arc-seconds, later rescaled to match previous periods. We did not tested the potential distribution of *Corythomantis* sp. due to low number of sample points.

We loaded all 19 bioclimatic variables, altitude and distribution records of *C. greeningi* in R 3.5.1 (R Core Team 2019). We tested colinearity among variables with Pearson's correlation coefficient, with a threshold of 0.75 and maintained those relevant for the biology of the species. Our dataset of bioclimatic variables was composed of: annual mean temperature, temperature annual range, annual precipitation, precipitation seasonality, precipitation of warmest quarter, and precipitation of coldest quarter. With bootstrap method we used 25% of records to test the model in 20 replicates for each model with Maxent 3.3.3 algorithm (Phillips et al., 2006) and final results consisted of models with acceptable values of area under curve (AUC > 0.9). We constructed binary maps for each projection with "Equal training sensitivity and specificity logistic threshold" values and stacked binary maps to predict the stability area for *C. greeningi* along PCF.

2.8 Background similarity

Our third hypothesis also states that ecological traits are responsible for population structure. The Background Similarity Test use ecological niche models extracted from populations to infer if their distribution segregate or overlap more from each other than expected by chance. Indexes of Schoener's D statistics and Hellinger's based I statistics measure the degree of similarity, ranging from absence of niche overlap (0) to identical niches (1) (Warren et al., 2008). To test the background similarity, we produced a minimum convex polygon around localities according to population assignment. For population one and Espinhaço population we used 25 points and five points, respectively, to produce its MPC and complemented with additional literature records located inside the polygon, totaling 52 points for population one and eight for Espinhaço population. We used four points for population two and a central additional point. We downloaded 19 bioclimatic variables from Worldclim 2.0 (Fick and

Hijmans, 2017) and tested the colinearity among variables with Pearson's correlation coefficient ($r > 0.75$) and maintained variables relevant to *Corythomantis*' biology: Annual mean temperature, temperature seasonality, temperature annual range, annual precipitation, precipitation seasonality, precipitation of driest quarter, precipitation of warmest quarter, and precipitation of coldest quarter. Then we used Phyloclim package 0.9.5 to pair test background similarity between populations with Maxent 3.3.3 algorithm (Phillips et al., 2006) using 100 replications. Previous analysis showed populations one and two belong to a single species (*C. greeningi*), while Espinhaço population represent another species (*Corythomantis* sp., see results). So we tested the background similarity between populations one and two, and another test between *C. greeningi* and *Corythomantis* sp.

3 Results

3.1 Population assignments

Population assignment tests recovered three populations for *Corythomantis greeningi* with minor differences. One population consistently gathered specimens from five localities within the Espinhaço Mountain Range (EMR) between the states of Bahia and Minas Gerais, and is henceforth referred to as Espinhaço population. The remaining localities were grouped in two different populations: Population one consists of the most widespread, which includes most localities of the distribution of *C. greeningi*, from Palmas in Tocantins State within the Cerrado domain to the eastern boundaries of Caatinga; Population two is sympatric with population one, but restricted to four localities in an area of 12,544 m^2 from the boundaries of Maranhão State to the mid portion of Piauí State. All populations are represented in Figure 1. Some localities were assigned to populations one or two, depending on the analysis (BAPS or GENELAND, see Supporting information for detail). Due to the proximity of these localities, we decided to maintain these four localities as population two (Figure 2).

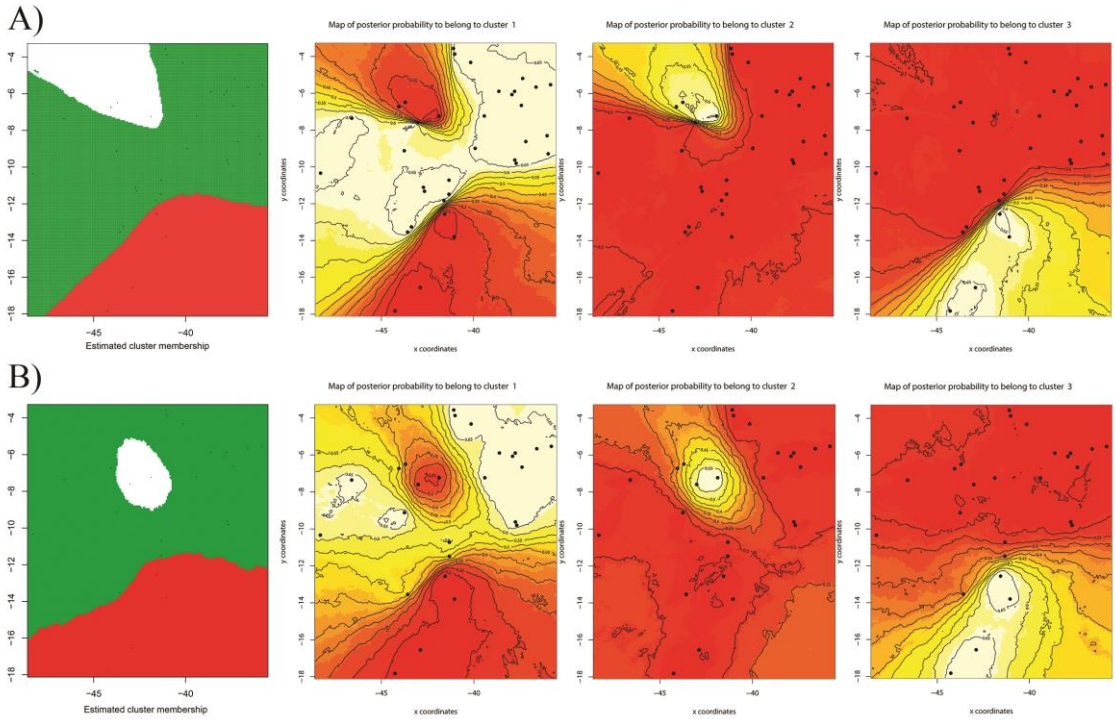

Figure 2: Graphical representation of the populations recovered in GENELAND. Analysis with both mtDNA and nuDNA combined (A) and only nuDNA (B) data, showing the spatial delimitation of all populations, and population one (left column), population two (mid column) and Espinhaço population (right column), respectively. Warmer colors represent higher probabilities of localities assigned to those populations. Black lines show delimitation support.

3.2 Haplotype reconstruction, species delimitation, genetic data and gene tree

Haplotype networks showed a clear separation of the Espinhaço population from populations one and two for all genes. Espinhaço population are exclusive and separated by several mutation steps (3–51) from populations one and two. As for populations one and two, all genes show shared haplotypes without a clear separation from populations (Figure 3). Mitochondrial genes covered all localities and totaled 23 (16S) and 35 (COI) haplotypes with 11 and 20 exclusive haplotypes, respectively. In 16S, two haplotypes (H1 and H6) are widely distributed in 14 and nine localities, respectively. H1 gathered exclusively localities from population one, while H6 contains localities from populations one and two. As for COI, it showed only one widely distributed haplotype (H1) in nine localities, all allocated in population one.

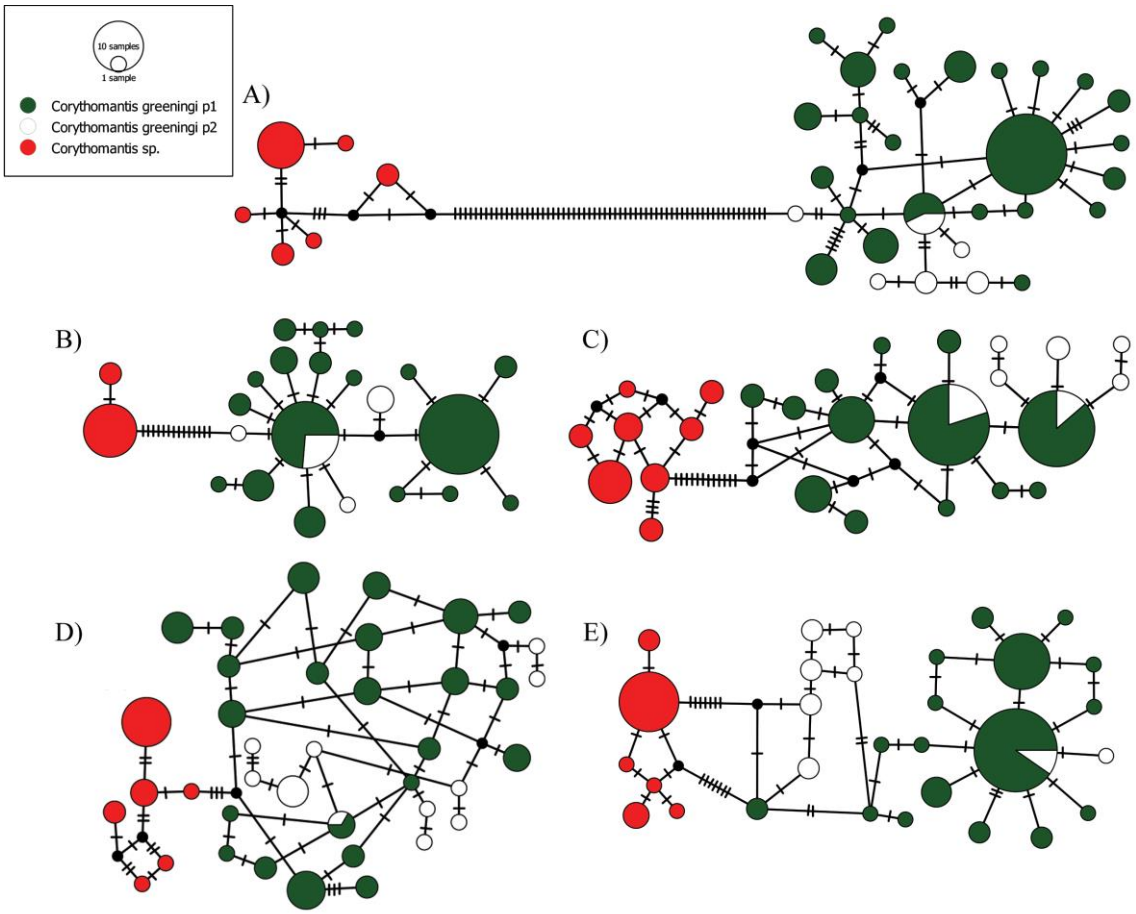

Figure 3: Haplotype network from neighbor-joining analyses for all genes of *Corythomantis*. COI (A), 16S (B), βfib (C), RPL3 (D) and Tyrosinase (E). Colors represent each recovered population, as green for population one and white for population two of *Corythomantis greeningi* whilst red represent Espinhaço population. The size of circles represent the haplotype frequency.

We tested the validity of all populations with the consensus localities in BPP. All four models and 12 runs in BPP obtained congruent results supported by a high posterior probability (pp = 1) and reinforce the presence of three populations. The consensus mitochondrial gene tree support two monophyletic lineage of *Corythomantis* with high support (pp=1; Figure 4). One lineage gathered localities comprising both population one and population two. The second lineage comprised only five localities distributed along the EMR, the same region detected in the population assignment tests assigned to Espinhaço population. Although the specimen from Gameleira do Assuruá was not assigned to the Espinhaço population in population assignment, it has only one sequence for COI gene and yet, was clustered with other specimens from EMR in the mitochondrial gene tree. We tested the pairwise distance of COI sequence from Gameleira do Assuruá with other specimens from EMR and the divergence was of

0.3%. When compared to populations one and two, sequence divergence was of 13%. Likewise, we compared the genetic divergence between populations for all loci and the variance ranged from 0.4% to 13% (Table 1). When we combine the lack of shared haplotypes and the number of mutational steps between lineages, genetic distance between lineages, and geographic distribution, we believe populations one and two represent the nominal *C. greeningi*, while the Espinhaço population is actually a cryptic species and will be treated as *Corythomantis* sp. henceforth.

Table 1: Sequence divergence with uncorrected p-distance mean values between the three recovered populations for all five loci of *Corythomantis*. (E) Espinhaço population, (P1) population one, and (P2) population two.

	Between populations			Within populations		
	E x P1	E x P2	P1 x P2	E	P1	P2
16S	0.0303	0.0249	0.0081	0	0	0
COI	0.1316	0.1281	0.008	0	0.01	0.01
Bfib	0.0354	0.0379	0.0048	0	0	0
RPL3	0.021	0.0236	0.01	0.01	0.01	0.01
Tyr	0.0269	0.0235	0.0114	0	0.01	0

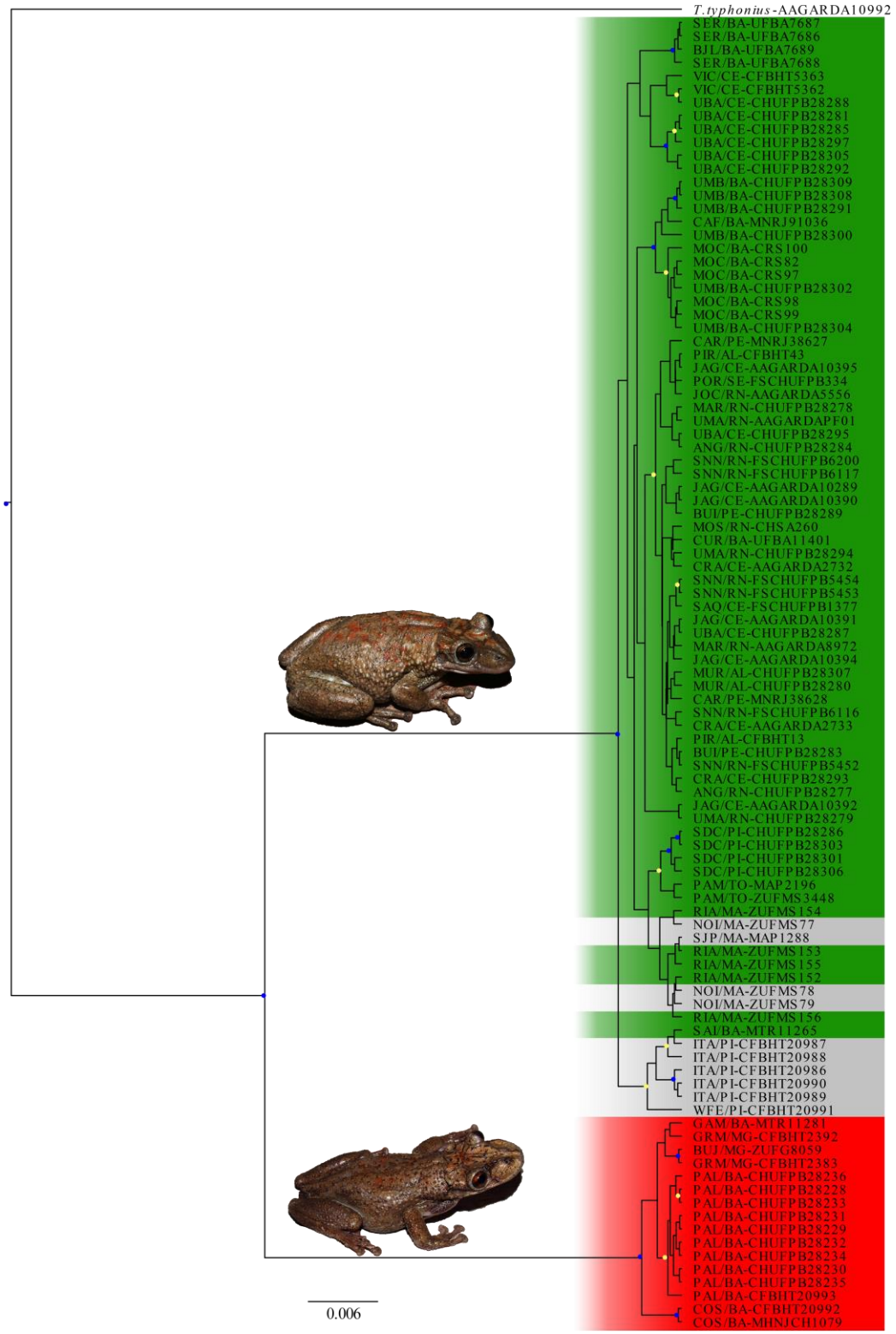

Figure 4: Consensus bayesian mitochondrial gene tree for all samples of *Corythomantis* across its distribution. Red bar represents specimens from the Espinhaço Mountain Range, while green and gray bars are populations 1 and 2 recovered in the population assignments, respectively. Node values of posterior probabilities (pp) are represented by circles: blue (pp = 1), yellow (0.99 > pp >0.91), and orange (0.89 > pp > 0.80). Nodes without circles have posterior probabilities below 0.79.

With specimens of our dataset assigned to populations and species (Table S1, supporting information), we provide the summary statistics for each population. Our dataset comprised 2482 base pairs (bp): 534 bp for 16S, 511 bp for COI (1145 bp of mtDNA, 45.13% of total), 458 for βfib, 418 for RPL3, and 451 for Tyr (1337 bp of nuDNA, 53.87% of total). PHI Test showed no evidence for recombination in nuclear data (p = 0.5015 for βfib, p = 0.2028 for RPL3 and p = 0.9315 for Tyr). The highest variance in our dataset comparing both species was observed in COI with 88 segregation sites, followed by βfib (35), 16S (34), Tyr (25) and RPL3 (23). Haplotype and nucleotide diversity are higher in populations of *C. greeningi* for most genes. The neutrally test of Tajima's D showed no significance for all loci and populations. Full genetic statistics of each loci for all populations are described in Table 2.

Table 2: Summary statistics information for the sequenced genes in *C. greeningi* (populations one and two) and *Corythomantis* sp. (Espinhaço population). Number of base pairs (bp), number of sequences used (N), segregating sites (S), number of haplotypes (h), haplotype diversity (Hd), standard deviation of haplotype diversity (SDHd), nucleotide diversity (pi), Tajima's D (D) and its main p value. (*) Phased sequences.

Locus	bp	N	S	h	Hd	SDHd	pi	D	p value
Espinhaço population									
16S	534	14	1	2	0.254	0.135	0.0004	-0.3414	P>0.1
COI	511	15	11	5	0.583	0.12	0.0045	-0.5154	P>0.1
βfib*	458	22	8	8	0.855	0.049	0.0049	0.1881	P>0.1
RPL3*	419	18	9	5	0.58	0.109	0.0057	0.2525	P>0.1
Tyr*	451	24	4	5	0.551	0.114	0.0025	0.3085	P>0.1
Population 1									
16S	534	59	18	18	0.803	0.039	0.0039	-1.3591	P>0.1
COI	511	72	31	24	0.845	0.039	0.0057	-1.5778	P>0.05
βfib*	458	55	12	13	0.812	0.03	0.0041	-0.83	p>0.1
RPL3*	419	50	11	23	0.953	0.008	0.0078	1.0819	P>0.1
Tyr*	451	54	15	17	0.752	0.045	0.0034	-1.5098	P>0.1
Population 2									
16S	534	10	4	4	0.711	0.117	0.0025	-0.2188	P>0.1
COI	511	10	8	7	0.933	0.052	0.0045	-0.1781	P>0.1
βfib*	458	14	5	7	0.845	0.074	0.0033	-0.0502	P>0.1
RPL3*	419	14	10	11	0.934	0.051	0.0074	-0.0292	P>0.1
Tyr*	451	14	9	8	0.923	0.044	0.0083	1.2585	P>0.1

3.3 Ecologic niche modeling

The potential distribution for *C. greeningi* (populations one and two) generated by Maxent for current climate was congruent with the known distribution for the species (AUC = 0.97; Figure 5A), except for minor blotches at northern South America. Past projections showed minor fluctuations in the potential distribution at mid-Holocene (Figure 5B) where the species was slightly wider distributed. During Last Glacial Maximum (Figure 5C), it maintains the distribution pattern from current and mid-Holocene, with minor contraction in Northeast Brazil. However, Last Inter-Glacial projection (Figure 5D) shows a broader distribution expansion for the species from Northeast Brazil to Central-West portions. The climatic surface generated with the sum of binary maps from all models (Figure 5E) shows the North and East of Northeast Brazil as a stable region for *C. greenini* during PCF.

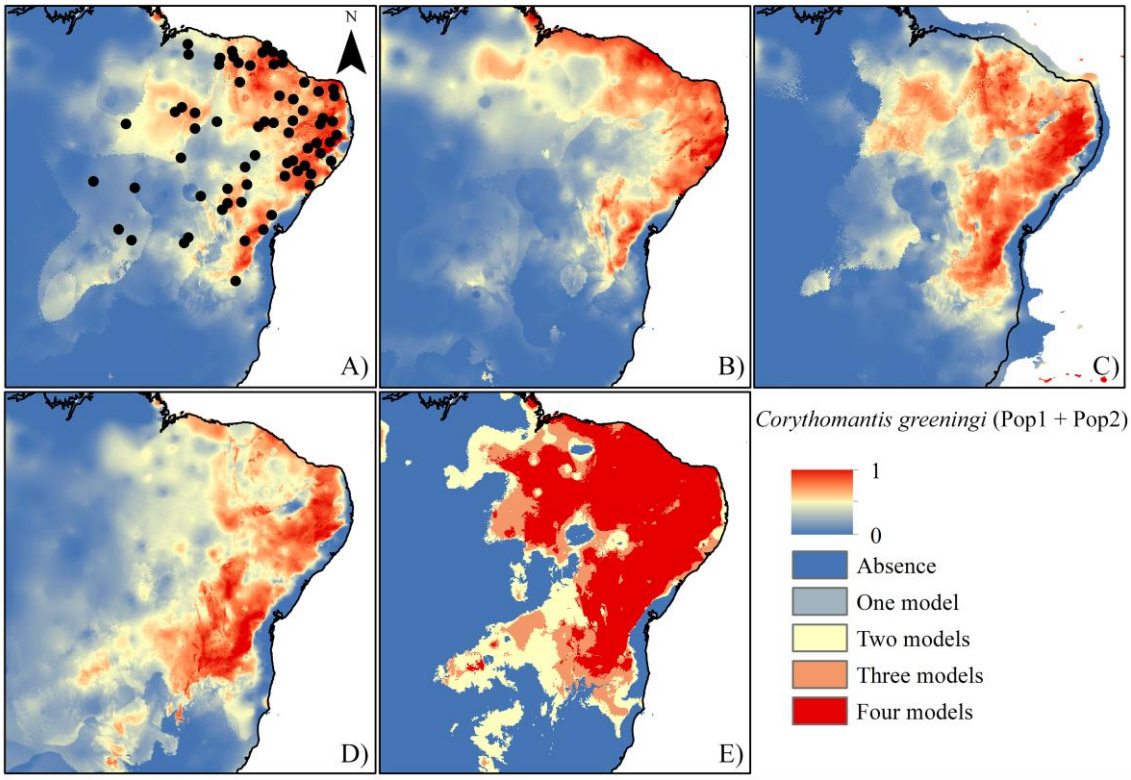

Figure 5: Ecologic Niche Modeling for *C. greeningi*. The recovered potential distribution in four periods are (A) current, (B) mid-Holocene (6 kya), (C) Last Glacial Maximum (21 kya) and (D) Last Inter-Glacial (120 kya). Stability area across periods (E) generated with a four models consensus. Black dots represent occurrence points. Warmer coloration indicates higher probability of occurrence based on the selected bioclimatic data.

3.4 Diversification scenarios in Corythomantis

ABC found a higher posterior probability for model 5, which predicts a founder effect of population 1 from population 2 and bidirectional gene flow (Figure 6). The divergence between *C. greeningi* and *Corythomantis* sp. was during Pliocene at 3,641,857 ya (95% HPD interval 1,205,905–5,892,083). Divergence between *C. greeningi*'s population one and two, followed by demographic expansion of population one dated from Late Pleistocene at 500,617 ya (95% HPD interval 114,727–972,652). This model was recovered for both rejection and mnlogistic regression methods with posterior probabilities of 0.59 and 0.99, respectively (Table 3). All the other models had a lower posterior probability. PCA analyses showed that the simulated dataset produced summary statistics similar to the observed dataset (Figure S3–S4).

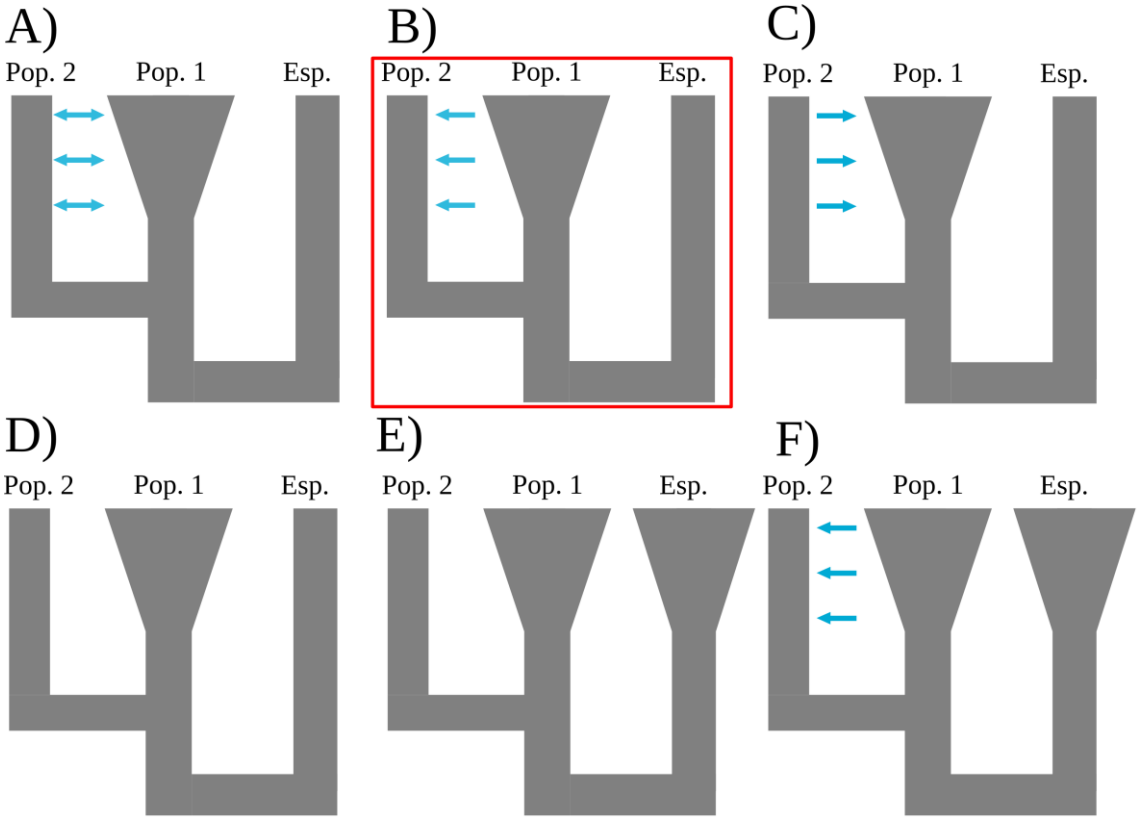

Figure 6: Schematic representation of the six models tested using approximate Bayesian computation. a–e represents distinct diversification scenario of divergence scenarios among population 1 (P1), population 2 (P2) and *Corythomantis* sp. (C). The direction of the arrows indicates the migration direction. The best-supported model is marked by a red box.

Table 3. Posterior probabilities of model comparison using approximate Bayesian computation (ABC). The best-fit model is highlight in bold. A tolerance of 0.01 and 0.1 were used in the comparisons for the rejection and Mnlogistic, respectively.

Model	Method	
	Rejection	**Mnlogistic**
Model 1	0.1117	0.0000
Model 2	0.0900	0.0012
Model 3	0.1000	0.0005
Model 4	0.0000	0.0003
Model 5	0.0000	0.0000
Model 6	**0.5983**	**0.9980**

3.5 Background similarity between C. greeningi *and* Corythomantis *sp.*

Background comparison rejected the null hypothesis that environmental niche models more similar than expected by chance. Either comparisons of population one vs population two and *C. greeningi* vs *Corythomantis* sp., showed D and I indices metrics were statistically lower ($p < 0.05$) than the null distribution (Figure 7).

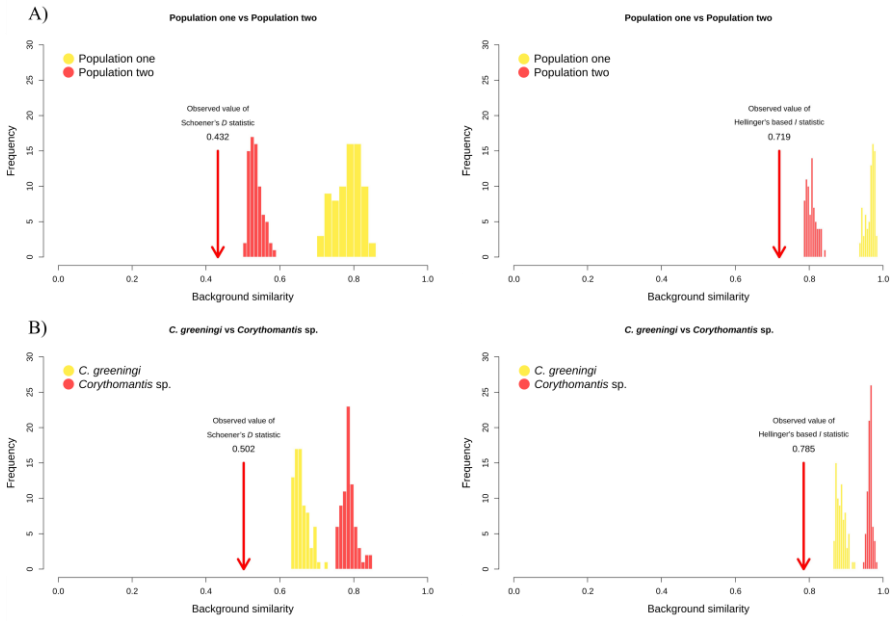

Figure 7: Background similarity test in *Corythomantis*. Comparisons are between population one and population two (A) and between the species *C. greeningi* and *Corythomantis* sp. (B). The right column shows Schoener's D statistic values while the

left column show Hellinger's based I statistic. Observed values are shown as red arrows and null distribution is shown as bar histogram.

4. Discussion

4.1. Diversification of the genus Corythomantis

Contrary to our prediction, genetic diversity within Corythomantis was not structured according to river basins. Instead, genetic structure is associated to altitude and a zone of climatic stability, supporting our first hypothesis. According to De Queiroz (2007), species are lineages evolving without gene flow, as our results show. The lineage correspondent to the formerly described *C. greeningi* is widely spread in lowlands of Caatinga and northern Cerrado biome, while *Corythomantis* sp. inhabits only the EMR from Chapada Diamantina in Bahia state to northern Minas Gerais state. Rodríguez et al. (2015) show that genetic structure is associated to topographic complexity, where flat and homogeneous habitats tend to show lower genetic diversification if compared to forests. This directly apply for Caatinga biome, as it presents fewer elevated plateaus and relictual forests if compared to other biomes (Sampaio, 1995).

Water dependency, low dispersion, fidelity to breeding sites or specific habitats and microhabitats (philopatry) are the main features expected to restrict amphibians' distribution (Beebee, 2005; Reading et al., 1991). That applies for some Neotropical frog species with restricted geographic distribution and different life traits (Gehara et al., 2014, 2013; Menezes et al., 2016; Thomé et al., 2016). An increasing number of studies have shown amphibian species with broader distribution ranges, most of them from the Caatinga and Cerrado biomes in South American Diagonal of Open Formations (DOF) (Brusquetti et al., 2019; Mângia et al., 2020; Prado et al., 2012; Thomé et al., 2016), but also distributed across large spans in the Amazon basin (Garda and Cannatella, 2007). Widespread species usually are generalist, highly dispersive and tolerant to habitat changes (Brown et al., 1996). *Corythomantis* breed specifically in rocky river streams, with tadpoles adapted to lotic waters (Jared et al., 1999; Juncá et al., 2008). Similar to our species, the lizard *Phyllopezus pollicaris* is distributed throughout the DOF and is strongly associated to rocky outcrops. Molecular evidence showed this lizard has eight deep genetic breaks, including candidate species within its

distribution, with more than one species associated to the Caatinga biome (Werneck et al., 2012). We show that the genus *Corythomantis* present both patterns of wide distribution and genetic breaks associated to a region.

The nominal *C. greeningi* is a widespread species from the DOF. Yet, its lineage is divided into two populations (population one and two). Population one follows the species broad distribution in Caatinga and Cerrado biomes. As for population two, is in a small transitional region from Caatinga to Cerrado where was climactic stable during Pleistocene, and sympatric with population one. The course of São Francisco River (SFR) changed during Quaternary, and its paleocourse drained northward to equatorial Atlantic Ocean, with speculated course where today is the Piauí River (Mabesoone 1994). These events might explain the retention of a ancestral population in that area, since three localities from population two are on the west margin of Piauí River. Both population share haplotypes and our mitochondrial gene tree grouped most specimens from population two in a single clade, but mixed with one specimen from population one, while two individuals from population two were grouped with specimens from population one. Introgression between populations is evident due shared haplotypes and might hamper a proper population segregation (Harrison and Larson, 2014). The frog *Pleurodema diplolister* show similar geographic distribution and population structure with *C. greeningi*. Thomé et al. (2016) recovered three populations for *P. diplolister*, one broader distributed throughout the Caatinga, a second population in Cerrado, and a third restricted to Chapada Diamantina, with shared haplotypes, which suggests introgression between populations.

Corythomantis sp. is restricted to the EMR and the population assignment was congruent with the mitochondrial tree result, assigning the same individuals as the third population (Espinhaço population). This undescribed species is supported not only by several genetic evidences, but also in morphology and advertisement call (Marques et al. In. Prep.), also corroborating our third hypothesis that isolated populations would present interpecific differences. Over the last decades, phylogenetic studies have unveiled several cryptic species attributed to a nominal taxon (Fouquet et al., 2016, 2007; Gehara et al., 2014, 2013; Lanna et al., 2018; Prado et al., 2012; Sabbag et al., 2018; Werneck et al., 2012). Patterns of speciation processes associated to mountain ranges are reported in other studies, as Gehara et al. (2013) uncovered cryptic lineages of *Ischnocnema guentheri* distributed along Serra do Mar chain; Prado et al. (2012)

found that the treefrog *Boana albopunctata* is associated to Chapada dos Guimarães; and Sabbag et al. (2018) observed genetic structure in *Thoropa* spp. in montane rocky areas from Atlantic forest. The EMR is a hotspot for speciation of several organisms (Bitencourt and Rapini, 2013; Echternacht et al., 2011; Thomé et al., 2016; Werneck, 2011), and surprisingly for frogs, it harbors 15 of the 21 endemic species from Caatinga biome (Garda et al., 2018; Mângia et al., 2018).

4.2 Divergence times and species limits

Speciation events attributed to mountain ranges are usually a consequence of two scenarios: mountains as vicariant barriers inhibiting gene flow or population isolation by altitude. The uplift of Central Brazilian Plateau is an example of the former scenario, and date from Miocene around 7–5 Mya (Del'Arco and Bezerra, 1989). This uplift was a major vicariant barrier for several species from the DOF, promoting divergent lineages with divergence times concordant with this vicariant barrier (Oliveira et al., 2018; Recoder et al., 2014; Werneck et al., 2012). Hypothesis on organisms isolated by altitude claim that these species were widespread and a climatic or tectonic events shifted part of their distribution upward, hence becoming isolated by a physical or climatic barrier, restricting gene flow, as observed in few species complexes across mountain ranges (Barres et al., 2019; Gehara et al., 2013; McCormack et al., 2009; Sabbag et al., 2018; Thomé et al., 2016). *Corythomantis* sp. inhabits the EMR from Bahia state in the localities of Gameleira do Assuruá (940 m above sea level), Palmeiras (750 m), and Contendas do Sincorá (315 m), to Minas Gerais state in the localities of Grão Mogol (847 m), Buritizeiro (655 m), Buenópolis (885 m), Leme do Prado (569 m), and Três Marias (546 m), the southermost location at East margin of SFR. The northern portion of the EMR is located within Caatinga biome, but its prevalent vegetation habitat are "*campos rupestres*", characteristics of Cerrado vegetation (Alves et al., 2014). The EMR climate consists of a orographic regime, with prevalence of precipitation and humidity, contrary as observed in the harsh Caatinga areas (Magalhães et al., 2015; Sampaio, 1995). Such discrepancy in climate regimes and habitat conditions might result in gene flow interruption in sister species (Hua and Wiens, 2010). Therefore, segregation between *Corythomantis* species apparently is a result of ecological divergence rather than a physical barrier isolation alone.

Overall, our data show that the geographic distribution of *C. greeningi* encompasses localities at altitudes until ~500 m, with few exceptions in Ibiapaba Plateau, Ceará state (587–772 meters asl) and in Catimbau Valley, Pernambuco state (800 meters asl). These records show that altitude alone does not explain the EMR lineage diversification, as *C. greeningi* reaches the extreme North of EMR in three localities of Caatinga-like vegetation: Santo Inácio, Umburanas, Morro do Chapéu and Cafarnaum, in altitudes of 500–900 meters asl and are genetically, morphologically and acoustically different from *Corythomantis* sp. (Marques et al., In. Prep.). Our results show a pattern of speciation concordant with isolation by altitude. ABC estimated a divergence between *Corythomantis* species from late Miocene to Pleistocene. This period is concordant with the final uplift of the EMR date from early Pleistocene, which occurred around 4–2 Mya (Colli, 2005; Porzecanski and Cracraft, 2005). The EMR mean altitude range between 800–1000 m, with peaks with altitude >1500 m asl and "campos rupestres" are more frequent at >900 m asl (Bitencourt and Rapini, 2013; Echternacht et al., 2011). We believe that the uplift of EMR isolated a group of an ancestral population on a mountain peak, hence restricting gene flow between specimens from peaks and lowlands. The isolated population was later distributed in similar habitats and climactic conditions over the EMR, now distinguished from lowland individuals (Figure 9). Therefore, it might explain species lack of shared haplotypes, low nucleotide diversity, divergence time and geographic distribution observed in *Corythomantis* sp. inhabiting elevated habitats of "*campos rupestres*" rocky outcrops in EMR, while *C. greeningi* is distributed over Caatinga lowlands and the North of Cerrado.

4.3 Demographic inferences in *Corythomantis* species

Our results from population assignments for *C. greeningi*, ecological niche modeling and demographic history inferred with ABC suggest climatic Pleistocene cycles significantly affected *Corythomantis* species. Population assignment showed a second population of *C. greeningi* in a small region between the northern Cerrado and the Caatinga. Palinological data show that region (known as Serra Geral de Goiás) was stable during Pleistocene (Costa et al., 2017). In addition, most localities of population two are on the west margin of the SFR paleocourse. Such features might have limited this relictual population in this climactic stable area. Estimates suggests the uplift of

Serra Grande and Ibiapaba changed the paleocourse of SFR to its current direction during Mindel glaciation at ~400 kya during middle Pleistocene (Mabesoone, 1994). Our ABC analysis showed a founder effect from population two to population one, with divergence at ~500 kya with wide 95% HPD confidence range. We also detected an increase of effective population size in population one, whilst population two remained stable and gene flow among them, as suggested by shared haplotypes and low genetic distance (Figure 3; Table 1), a possible result of change in SFR paleocourse and PCF. Other studies have found genetic structure associated to SFR paleocourse as in the lizards *T. semitaeniatus* and *Lygodactylus klugei* (Lanna et al., 2020; Werneck et al., 2015). Gene flow between populations of *C. greeningi* possibly shows an ongoing parapatric speciation scenario. Similar to *C. greeningi*, the Cerrado-distributed and mountain-associated *Ameivula xacriaba* was the source of a dispersion into the Caatinga that resulted in speciation with gene flow with its sister species *Ameivula ocellifera* (Oliveira et al., 2015).

Several wet and dry periods during the Pleistocene resulted in alternated events of expansion and retraction of forested biomes and open and dry biomes (Heine, 2000; Pennington et al., 2000; Wang et al., 2004). Past climatic data show cooler and dry periods favored the expansion of open and dry biomes, and relictual forest patches remained, whilst wet and hot periods allowed forested biomes to expand and even interconnect the Amazon and the Atlantic forest affecting species diversification (Batalha-Filho et al., 2013; Haffer, 1969; Thomé et al., 2016; Werneck, 2011). Such events led to refugees for forest species during Pleistocene and were crucial for the diversification of many organisms' groups, as extensively described in many studies (Cantidio and Souza, 2019; Carnaval et al., 2009; Cazé et al., 2016). Thus, it is expected that species from open vegetation habitats have benefited by these dry periods during PCF. However, a similar pattern of forest refugees for species of open areas its is still unclear. Among frog species, such pattern was observed by (Thomé et al., 2016) as they also detected population structure for *Pleurodema diplolister* in northern Cerrado, attributed to expansion and retraction of biomes during PCF. Novel evidence suggests expansion of Atlantic forest and contraction of Caatinga during last glacial maximum (Silveira et al., 2019). Past potential distribution of *C. greeningi* show congruence to respective climate conditions over 130 kya, as we observe a distribution contraction in last glacial maximum compared to last interglacial. Phylogeographic studies on

Neotropics have attributed PCF as the main event for Caatinga species expansion (Caetano et al., 2008; Oliveira et al., 2015; this study; Thomé et al., 2016; Werneck et al., 2015), as we recovered a population expansion for population one after divergence with population two, during Late Pleistocene. Although these studies estimate with a single species evolutionary history, they are concordant with Gehara et al. (2017) which simulated information from 14 Caatinga species of frogs, lizards and snakes with different phylogenetic traits and found a congruent pattern of demographic coexpansion during Late Pleistocene (~400 kya).

Conclusions

Our results showed two highly divergent lineages of *Corythomantis*, where the widespread *C. greeningi* actually hid an undescribed species restricted to the EMR. Nonetheless, the main distribution of *C. greeningi* encompasses lowlands on the whole Caatinga and the North of Cerrado. Therefore, *C. greeningi* is another widespread Neotropical species from the DOF, contrary to what is expected from a saxicolous amphibian species. Within its distribution, the species is structured in two populations associated to past climate and vicariant events. The former restricted population from Caatinga-Cerrado ecotone is a result of a climatic stable region, whilst the broader population expansion was favored by PCF.

We also showed that *Corythomantis* sp. probably diverged in due to changes in landscape during early Pliocene. Our data indicate it does not exchange gene flow with *C. greeningi* and maintained a constant population size during Quaternary. The new species inhabits the EMR and compose another endemic species to this mountain range along with 15 others. Our results endorse affirmations that the EMR is a hotspot for species diversification where possibly more undescribed species and require legal and conservation actions to protect its biota. Future inquiries should focus on migration between populations and species to increase its evolutionary history.

Acknowledgements

We thank herpetological collections curators and their staff for providing tissue samples. RM thanks Coordenação de Aperfeiçoamento de Pessoal de Nível

Superior (CAPES) for the doctoral fellowship (Process number 1489595). AAG thanks Conselho Nacional de Desenvolvimento Científico e Tecnológico (CNPq) for financial support (310942/2018-7, 206958/2017-0, 431433/2016-0 and #552031/2011-9). CFBH thanks Fundação de Amparo à Pesquisa do Estado de São Paulo (FAPESP proc #2013/50741-7) and CNPq (research fellowship 306623/2018-8) for financial support. We thank Instituto Chico Mendes de Conservação da Biodiversidade for provide the specimen collection permit (SISBIO 33402-1).

References

McCormack, J.E., Huang, H., Knowles, L.L., 2009. Sky Islands, in: Gillespie, R.G., Clague, D.A. (Eds.), Encyclopedia of Islands. Berkeley, CA: University of California Press, pp. 839–843.

Magalhães, A.P., Barros, L.F., Felippe, M.F., 2015. Southern Serra do Espinhaço: the impressive plateau of quartzite ridges, in: Vieira, B., Salgado, A., Santos, L. (Eds.), Landscapes and landforms of Brazil. Dordrecht: Springer, pp. 359–370.

Aiello-Lammens, M.E., Boria, R.A., Radosavljevic, A., Vilela, B., Anderson, R.P., 2015. spThin: An R package for spatial thinning of species occurrence records for use in ecological niche models. Ecography (Cop.). 38, 541–545. https://doi.org/10.1111/ecog.01132

Alves, R., Silva, N., Oliveira, J., Medeiros, D., 2014. Circumscribing campo rupestre – megadiverse Brazilian rocky montane savanas. Brazilian J. Biol. 74, 355–362. https://doi.org/10.1590/1519-6984.23212

Amaral, F.R., Albers, P.K., Edwards, S. V., Miyaki, C.Y., 2013. Multilocus tests of Pleistocene refugia and ancient divergence in a pair of Atlantic Forest antbirds (Myrmeciza). Mol. Ecol. 22, 3996–4013. https://doi.org/10.1111/mec.12361

Avise, J.C., 2009. Phylogeography: Retrospect and prospect. J. Biogeogr. 36, 3–15. https://doi.org/10.1111/j.1365-2699.2008.02032.x

Bandelt, H.-J., Forster, P., Rohl, A., 1994. Median-Joining Networks for Inferring Intraspecic Phylogenies. Mol. Biol. 16, 37–48. https://doi.org/10.1093/oxfordjournals.molbev.a026036

Barres, L., Batalha-Filho, H., Schnadelbach, A.S., Roque, N., 2019. Pleistocene climatic changes drove dispersal and isolation of *Richterago discoidea* (Asteraceae), an endemic plant of campos rupestres in the central and eastern Brazilian sky islands. Bot. J. Linn. Soc. 189, 132–152. https://doi.org/10.1093/botlinnean/boy080

Batalha-Filho, H., Fjeldså, J., Fabre, P.-H., Miyaki, C.Y., 2013. Connections between the Atlantic and the Amazonian forest avifaunas represent distinct historical events. J. Ornithol. 154, 41–50. https://doi.org/10.1007/s10336-012-0866-7

Beebee, T.J.C., 2005. Conservation genetics of amphibians. Heredity (Edinb). 95, 423–427. https://doi.org/10.1038/sj.hdy.6800736

Bitencourt, C., Rapini, A., 2013. Centres of endemism in the espinhaço range: Identifying cradles and museums of asclepiadoideae (apocynaceae). Syst. Biodivers. 11, 525–536. https://doi.org/10.1080/14772000.2013.865681

Blotto, B.L., Lyra, M.L., Cardoso, M.C.S., Trefaut Rodrigues, M., R. Dias, I., Marciano-Jr, E., Dal Vechio, F., Orrico, V.G.D., Brandão, R.A., Lopes de Assis, C., Lantyer-Silva, A.S.F., Rutherford, M.G., Gagliardi-Urrutia, G., Solé, M., Baldo, D., Nunes, I., Cajade, R., Torres, A., Grant, T., Jungfer, K.-H., da Silva, H.R., Haddad, C.F.B., Faivovich, J., 2020. The phylogeny of the Casque-headed treefrogs (Hylidae: Hylinae: Lophyohylini). Cladistics 1–37. https://doi.org/10.1111/cla.12409

Boulenger, G.A., 1896. Descriptions of new batrachians in the British Museum. Ann. Mag. Nat. Hist. 17, 401–406.

Brown, J.H., Stevens, G.C., Kaufman, D.M., 1996. The geographic range: size, shape, boundaries, and internal structure. Annu. Rev. Ecol. Syst. 27, 597–623. https://doi.org/10.1146/annurev.ecolsys.27.1.597

Brusquetti, F., Netto, F., Baldo, D., Haddad, C.F.B.B., 2019. The influence of Pleistocene glaciations on Chacoan fauna: Genetic structure and historical demography of an endemic frog of the South American Gran Chaco. Biol. J. Linn. Soc. 126, 404–416. https://doi.org/10.1093/biolinnean/bly203

Caetano, S., Prado, D., Pennington, R.T., Beck, S., Oliveira-Filho, A., Spichiger, R., Naciri, Y., 2008. The history of Seasonally Dry Tropical Forests in eastern South America: Inferences from the genetic structure of the tree *Astronium urundeuva* (Anacardiaceae). Mol. Ecol. 17, 3147–3159. https://doi.org/10.1111/j.1365-294X.2008.03817.x

Cantidio, L.S., Souza, A.F., 2019. Aridity, soil and biome stability influence plant ecoregions in the Atlantic Forest, a biodiversity hotspot in South America. Ecography 42,1887–1898. https://doi.org/10.1111/ecog.04564

Carnaval, A.C., Hickerson, M.J., Haddad, C.F.B., Rodrigues, M.T., Moritz, C., 2009. Stability predicts genetic diversity in the Brazilian Atlantic forest hotspot. Science (80-.). 323, 785–789. https://doi.org/10.1126/science.1166955

Cazé, A.L.R., Mäder, G., Nunes, T.S., Queiroz, L.P., de Oliveira, G., Diniz-Filho, J.A.F., Bonatto, S.L., Freitas, L.B., 2016. Could refuge theory and rivers acting as barriers

explain the genetic variability distribution in the Atlantic Forest? Mol. Phylogenet. Evol. 101, 242–251. https://doi.org/10.1016/j.ympev.2016.05.013

Colli, G.R., 2005. As origens e a diversificação da herpetofauna do Cerrado, in: Scariot, A., Souza-Silva, J.C., Felfili, J.M. (Eds.), Cerrado: Ecologia, Biodiversidade e Conservação. Ministerio do Meio Ambiente, Brasilia, pp. 247–264. https://doi.org/10.1590/s0103-63512006000100003

Colli, G.R., Bastos, R.P., de Araujo, A.F.B., 2002. The character and dynamics of the Cerrado herpetofauna, in: Oliveira, P.S., Marquis, R.J. (Eds.), The Cerrados of Brazil: Ecology and Natural History of a Neotropical Savanna. Columbia University Press, New York, pp. 223–241.

Corander, J., Marttinen, P., 2006. Bayesian identification of admixture events using multilocus molecular markers. Mol. Ecol. 15, 2833–2843. https://doi.org/10.1111/j.1365-294X.2006.02994.x

Costa, G.C., Burbrink, F.T., Colli, G.R., Martinez, P.A., Garda, A.A., São-Pedro, V.A., Mesquita, D.O., Oliveira, E.F., Gehara, M., 2017. Climatic suitability, isolation by distance and river resistance explain genetic variation in a Brazilian whiptail lizard. Heredity (Edinb). 120, 251–265. https://doi.org/10.1038/s41437-017-0017-2

Csilléry, K., François, O., Blum, M., 2012. Approximate Bayesian Computation (ABC) in R: A Vignette. 202.162.217.53 1–21.

De Queiroz, K., 2007. Species concepts and species delimitation. Syst. Biol. 56, 879–886. https://doi.org/10.1080/10635150701701083

Drummond, A.J., Suchard, M.A., Xie, D., Rambaut, A., 2012. Bayesian phylogenetics with BEAUti and the BEAST 1.7. Mol. Biol. Evol. 29, 1969–1973. https://doi.org/10.1093/molbev/mss075

Echternacht, L., Trovó, M., Oliveira, C.T., Pirani, J.R., 2011. Areas of endemism in the Espinhaço Range in Minas Gerais, Brazil. Flora Morphol. Distrib. Funct. Ecol. Plants 206, 782–791. https://doi.org/10.1016/j.flora.2011.04.003

Fick, S.E., Hijmans, R.J., 2017. WorldClim 2: new 1-km spatial resolution climate surfaces for global land areas. Int. J. Climatol. 37, 4302–4315. https://doi.org/10.1002/joc.5086

Flouri, T., Jiao, X., Rannala, B., Yang, Z., 2018. Species Tree Inference with BPP Using Genomic Sequences and the Multispecies Coalescent. Mol. Biol. Evol. 35, 2585–2593. https://doi.org/10.1093/molbev/msy147

Fonseca, E.M., Gehara, M., Werneck, F.P., Lanna, F.M., Colli, G.R., Sites, J.W., Rodrigues, M.T., Garda, A.A., 2018. Diversification with gene flow and niche divergence in a lizard species along the South American “diagonal of open formations.” J. Biogeogr. 45, 1688–1700. https://doi.org/10.1111/jbi.13356

Fouquet, A., Martinez, Q., Zeidler, L., Courtois, E.A., Gaucher, P., Blanc, M., Lima, J.D., Souza, S.M., Rodrigues, M.T., Kok, P.J.R., 2016. Cryptic diversity in the Hypsiboas semilineatus species group (Amphibia, Anura) with the description of a new species from the eastern Guiana Shield. Zootaxa 4084, 79–104. https://doi.org/10.11646/zootaxa.4084.1.3

Fouquet, A., Vences, M., Salducci, M.-D., Meyer, A., Marty, C., Blanc, M., Gilles, A., 2007. Revealing cryptic diversity using molecular phylogenetics and phylogeography in frogs of the Scinax ruber and Rhinella margaritifera species groups. Mol. Phylogenet. Evol. 43, 567–582. https://doi.org/10.1016/j.ympev.2006.12.006

Funk, W.C., Murphy, M.A., Hoke, K.L., Muths, E., Amburgey, S.M., Lemmon, E.M., Lemmon, A.R., 2016. Elevational speciation in action? Restricted gene flow associated with adaptive divergence across an altitudinal gradient. J. Evol. Biol. 29, 241–252. https://doi.org/10.1111/jeb.12760

Garda, A.A., Cannatella, D.C., 2007. Phylogeny and biogeography of paradoxical frogs (Anura, Hylidae, Pseudae) inferred from 12S and 16S mitochondrial DNA. Mol. Phylogenet. Evol. 44, 104–114. https://doi.org/10.1016/j.ympev.2006.11.028

Garda, A.A., Lion, M.B., Lima, S.M. de Q., Mesquita, D.O., Araujo, H.F.P. de, Napoli, M.F., 2018. Os animais vertebrados do Bioma Caatinga. Cienc. Cult. 70, 29–34. https://doi.org/10.21800/2317-66602018000400010

Gehara, M., Canedo, C., Haddad, C.F.B., Vences, M., 2013. From widespread to microendemic: Molecular and acoustic analyses show that *Ischnocnema guentheri* (Amphibia: Brachycephalidae) is endemic to Rio de Janeiro, Brazil. Conserv. Genet. 14, 973–982. https://doi.org/10.1007/s10592-013-0488-5

Gehara, M., Crawford, A.J., Orrico, V.G.D., Rodríguez, A., Lötters, S., Fouquet, A., Barrientos, L.S., Brusquetti, F., De La Riva, I., Ernst, R., Urrutia, G.G., Glaw, F., Guayasamin, J.M., Hölting, M., Jansen, M., Kok, P.J.R., Kwet, A., Lingnau, R., Lyra, M., Moravec, J., Pombal, J.P., Rojas-Runjaic, F.J.M., Schulze, A., Señaris, J.C., Solé, M., Rodrigues, M.T., Twomey, E., Haddad, C.F.B., Vences, M., Köhler, J., 2014. High levels of diversity uncovered in a widespread nominal taxon: Continental phylogeography of the neotropical tree frog *Dendropsophus minutus*. PLoS One 9, e103958. https://doi.org/10.1371/journal.pone.0103958

Gehara, M., Garda, A.A., Werneck, F.P., Oliveira, E.F., da Fonseca, E.M., Camurugi, F., Magalhães, F. de M., Lanna, F.M., Sites, J.W., Marques, R., Silveira-Filho, R., São Pedro, V.A., Colli, G.R., Costa, G.C., Burbrink, F.T., 2017. Estimating synchronous demographic changes across populations using hABC and its application for a herpetological community from northeastern Brazil. Mol. Ecol. 26, 4756–4771. https://doi.org/10.1111/mec.14239

Geurgas, S.R., Rodrigues, M.T., 2010. The hidden diversity of Coleodactylus amazonicus (Sphaerodactylinae, Gekkota) revealed by molecular data. Mol. Phylogenet. Evol. 54, 583–593. https://doi.org/10.1016/j.ympev.2009.10.004

Godinho, L.B., Moura, M.R., Feio, R.N., 2013. New records and geographic distribution of Corythomantis greeningi Boulenger, 1896 (Amphibia: Hylidae). Check List 9, 148–150. https://doi.org/10.15560/9.1.148

Graham, C.H., Ron, S.R., Santos, J.C., Schneider, C.J., Moritz, C., 2004. Integrating phylogenetics and environmental niche models to explore speciation mechanisms in dendrobatid frogs. Evolution (N. Y). 58, 1781. https://doi.org/10.1554/03-274

Guillot, G., Estoup, A., Mortier, F., Cosson, J.F., 2005. A spatial statistical model for landscape genetics. Genetics 170, 1261–1280. https://doi.org/10.1534/genetics.104.033803

Haffer, J., 1969. Speciation in Amazonian Forest Birds. Science (80-.). 165, 131–138.

Harrison, R.G., Larson, E.L., 2014. Hybridization, introgression, and the nature of species boundaries. J. Hered. 105, 795–809. https://doi.org/10.1093/jhered/esu033

Heine, K., 2000. Tropical South America during the Last Glacial Maximum: Evidence from glacial, periglacial and fluvial records. Quat. Int. 72, 7–21. https://doi.org/10.1016/S1040-6182(00)00017-3

Hua, X., Wiens, J.J., 2010. Latitudinal variation in speciation mechanisms in frogs. Evolution (N. Y). 64, 429–443. https://doi.org/10.1111/j.1558-5646.2009.00836.x

Huson, D.H., Bryant, D., 2006. Application of Phylogenetic Networks in Evolutionary Studies. Mol. Biol. Evol. 23, 254–267. https://doi.org/10.1093/molbev/msj030

Jared, C., Antoniazzi, M.M., Katchburian, E., Toledo, R.C., Freymüller, E., 1999. Some aspects of the natural history of the casque-headed tree frog Corythomantis greeningi Boulenger (Hylidae). Ann. des Sci. Nat. - Zool. Biol. Anim. 105–115. https://doi.org/10.1016/s0003-4339(00)86975-0

Juncá, F.A., Carneiro, M.C.L., Rodrigues, N.N., 2008. Is a dwarf population of Corythomantis greeningi Boulenger, 1896 (Anura, Hylidae) a new species? Zootaxa 1686, 48–56.

Kumar, S., Stecher, G., Li, M., Knyaz, C., Tamura, K., 2018. MEGA X: Molecular evolutionary genetics analysis across computing platforms. Mol. Biol. Evol. 35, 1547–1549. https://doi.org/10.1093/molbev/msy096

Lanna, F.M., Gehara, M., Werneck, F.P., Fonseca, E.M., Colli, G.R., Sites, J.W., Rodrigues, M.T., Garda, A.A., 2020. Dwarf geckos and giant rivers: the role of the São Francisco River in the evolution of Lygodactylus klugei (Squamata: Gekkonidae) in the semi-arid Caatinga of north-eastern Brazil. Biol. J. Linn. Soc. 129, 88–98. https://doi.org/10.1093/biolinnean/blz170

Lanna, F.M., Werneck, F.P., Gehara, M., Fonseca, E.M., Colli, G.R., Sites, J.W., Rodrigues, M.T., Garda, A.A., 2018. The evolutionary history of *Lygodactylus lizards* in the South American open diagonal. Mol. Phylogenet. Evol. 127, 638–645. https://doi.org/10.1016/j.ympev.2018.06.010

Leigh, J.W., Bryant, D., 2015. POPART: Full-feature software for haplotype network construction. Methods Ecol. Evol. 6, 1110–1116. https://doi.org/10.1111/2041-210X.12410

Librado, P., Rozas, J., 2009. DnaSP v5: A software for comprehensive analysis of DNA polymorphism data. Bioinformatics 25, 1451–1452. https://doi.org/10.1093/bioinformatics/btp187

Lynch, J.D., Duellman, W.E., 1997. Frogs of the Genus Eleutherodactylus (Leptodactylidae) in Western Ecuador: Systematics, Ecology, and Biogeography. Univ. Kansas, Nat. Hist. Museum Spec. Publ. 23, 1–236. https://doi.org/10.2307/1447320

Magalhães, I.L.F., Oliveira, U., Santos, F.R., Vidigal, T.H.D.A., Brescovit, A.D., Santos, A.J., 2014. Strong spatial structure, Pliocene diversification and cryptic diversity in the Neotropical dry forest spider Sicarius cariri. Mol. Ecol. 23, 5323–5336. https://doi.org/10.1111/mec.12937

Mângia, S., Faria, E., Diego, O., Santana, J., Paiva, F., Antonio, A., 2020. Revising the taxonomy of Proceratophrys Miranda-Ribeiro , 1920 (Anura : Odontophrynidae) from the Brazilian semiarid Caatinga : Morphology , calls and molecules support a single widespread species 1–22. https://doi.org/10.1111/jzs.12365

Mângia, S., Koroiva, R., Nunes, P.M.S., Roberto, I.J., Ávila, R.W., Sant'Anna, A.C., Santana, D.J., Garda, A.A., 2018. A New Species of Proceratophrys (Amphibia: Anura: Odontophrynidae) from the Araripe Plateau, Ceará State, Northeastern Brazil. Herpetologica 74, 255–268. https://doi.org/10.1655/Herpetologica-D-16-00084.1

Marshall, J.C., Bastiaans, E., Caccone, A., Camargo, A., Morando, M., Niemiller, M.L., Pabijan, M., Russello, M.A., Sinervo, B., Sites Jr., J.W., Vences, M., Werneck, F.P., Valero, K.C.W., Steinfartz, S., 2018. Mechanisms of speciation in reptiles and amphibians: A synopsis. PeerJ Prepr. 1–47. https://doi.org/10.7287/peerj.preprints.27279v1

Menezes, L., Canedo, C., Batalha-Filho, H., Garda, A.A., Gehara, M., Napoli, M.F., 2016. Multilocus phylogeography of the treefrog *Scinax eurydice* (Anura, Hylidae) reveals a plio-pleistocene diversification in the atlantic forest. PLoS One 11, 1–20. https://doi.org/10.1371/journal.pone.0154626

Nascimento, F.F., Lazar, A., Menezes, A.N., Durans, A. da M., Moreira, J.C., Salazar-Bravo, J., DAndrea, P.S., Bonvicino, C.R., 2013. The Role of Historical Barriers in

the Diversification Processes in Open Vegetation Formations during the Miocene/Pliocene Using an Ancient Rodent Lineage as a Model. PLoS One 8. https://doi.org/10.1371/journal.pone.0061924

Navas, C., Jared, C., Antoniazzi, M.M., 2002. Water economy in the casque-headed tree-frog Corythomantis greeningi (Hylidae): role of behaviour, skin, and skull skin co-ossification. J Zool 257: 525–532.

Oliveira, E.F., Gehara, M., São-Pedro, V.A., Costa, G.C., Burbrink, F.T., Colli, G.R., Rodrigues, M.T., Garda, A.A., 2018. Phylogeography of Muller's termite frog suggests the vicariant role of the Central Brazilian Plateau. J. Biogeogr. 45, 2508–2519. https://doi.org/10.1111/jbi.13427

Oliveira, E.F., Mesquita, D.O., Chen, X., Gehara, M., Garda, A.A., Zaher, H., Arias, F.J., Burbrink, F.T., Santos, R.M.L., Costa, G.C., Rodrigues, M.T., São-Pedro, V.A., Colli, G.R., Myers, E.A., 2015. Speciation with gene flow in whiptail lizards from a Neotropical xeric biome. Mol. Ecol. 24, 5957–5975. https://doi.org/10.1111/mec.13433

Osborne, O.G., Batstone, T.E., Hiscock, S.J., Filatov, D.A., 2013. Rapid Speciation with Gene Flow Following the Formation of Mt. Etna. Genome Biol. Evol. 5, 1704–1715. https://doi.org/10.1093/gbe/evt127

Patton, J.L., Silva, M.N.F. Da, Malcolm, J.R., 1994. Gene Genealogy and Differentiation Among Arboreal Spiny rats (Rodentia: Echimyidae) of the Amazon Basin: A Test of the Riverine Barrier Hypothesis. Evolution (N. Y). 48, 1314. https://doi.org/10.2307/2410388

Pennington, R.T., Prado, D.E., Pendry, C.A., 2000. Neotropical seasonally dry forests and Quaternary vegetation changes. J. Biogeogr. 27, 261–273. https://doi.org/10.1046/j.1365-2699.2000.00397.x

Phillips, S.J., Anderson, R.P., Schapire, R.E., 2006. Maximum entropy modeling of species geographic distributions. Ecological Modelling, 190, 231–259. https://doi.org/10.1016/j.ecolmodel.2005.03.026

Porzecanski, A.L., Cracraft, J., 2005. Cladistic analysis of distributions and endemism (CADE): Using raw distributions of birds to unravel the biogeography of the South American aridlands. J. Biogeogr. 32, 261–275. https://doi.org/10.1111/j.1365-2699.2004.01138.x

Posada, D., 2008. jModelTest: Phylogenetic model averaging. Mol. Biol. Evol. 25, 1253–1256. https://doi.org/10.1093/molbev/msn083

Prado, C.P.A., Haddad, C.F.B., Zamudio, K.R., 2012. Cryptic lineages and Pleistocene population expansion in a Brazilian Cerrado frog. Mol. Ecol. 21, 921–941. https://doi.org/10.1111/j.1365-294X.2011.05409.x

Reading, C.J., Loman, J., Madsen, T., 1991. Breeding pond fidelity in the common toad, *Bufo bufo*. J. Zool. 225, 201–211. https://doi.org/10.1111/j.1469-7998.1991.tb03811.x

Recoder, R.S., Werneck, F.P., Teixeira, M., Colli, G.R., Sites, J.W., Rodrigues, M.T., 2014. Geographic variation and systematic review of the lizard genus Vanzosaura (Squamata, Gymnophthalmidae), with the description of a new species. Zool. J. Linn. Soc. 171, 206–225. https://doi.org/10.1111/zoj.12128

Rodríguez, A., Börner, M., Pabijan, M., Gehara, M., Haddad, C.F.B., Vences, M., 2015. Genetic divergence in tropical anurans: deeper phylogeographic structure in forest specialists and in topographically complex regions. Evol. Ecol. 29, 765–785. https://doi.org/10.1007/s10682-015-9774-7

Sabbag, A.F., Lyra, M.L., Zamudio, K.R., Haddad, C.F.B., Feio, R.N., Leite, F.S.F., Gasparini, J.L., Brasileiro, C.A., 2018. Molecular phylogeny of Neotropical rock frogs reveals a long history of vicariant diversification in the Atlantic forest. Mol. Phylogenet. Evol. 122, 142–156. https://doi.org/10.1016/j.ympev.2018.01.017

Sampaio, E.V.S.B., 1995. Overview of the Brazilian caatinga, in: Bullock, S.H., Mooney, H.A., Medina, E. (Eds.), Seasonally Dry Tropical Forests. Cambridge University Press, Cambridge, pp. 35–63. https://doi.org/10.1017/CBO9780511753398.003

Silveira, M.H.B., Mascarenhas, R., Cardoso, D., Batalha-Filho, H., 2019. Pleistocene climatic instability drove the historical distribution of forest islands in the northeastern Brazilian Atlantic Forest. Palaeogeogr. Palaeoclimatol. Palaeoecol. 527, 67–76. https://doi.org/10.1016/j.palaeo.2019.04.028

Stephens, M., Smith, N.J., Donnelly, P., 2001. A new statistical method for haplotype reconstruction from population data. Am. J. Hum. Genet. 68, 978–89. https://doi.org/10.1086/319501

Talavera, G., Castresana, J., 2007. Improvement of phylogenies after removing divergent and ambiguously aligned blocks from protein sequence alignments. Syst. Biol. 56, 564–577. https://doi.org/10.1080/10635150701472164

Thomé, M.T.C., Sequeira, F., Brusquetti, F., Carstens, B., Haddad, C.F.B., Rodrigues, M.T., Alexandrino, J., 2016. Recurrent connections between Amazon and Atlantic forests shaped diversity in Caatinga four-eyed frogs. J. Biogeogr. 43, 1045–1056. https://doi.org/10.1111/jbi.12685

Vences, M., Wake, D.B., 2007. Speciation, species boundaries and phylogeography of amphibians. Amphib. Biol. 7, 2613–2660.

Wang, X., Auler, A.S., Edwards, R.L., Cheng, H., Cristalli, P.S., Smart, P.L., Richards, D.A., Shen, C.-C., Edwards, R.L., 2004. Wet periods in northeastern Brazil over

the past 210 kyr linked to distant climate anomalies. Nature 432, 2767–2769. https://doi.org/10.1038/nature03067

Warren, D. L., Glor, R.E., Turelli, M., 2008. Environmental niche equivalency versus conservatism: Quantitative approaches to niche evolution. Evolution, 62, 2868–2883. https://doi.org/10.1111/j.1558- 5646.2008.00482.x

Werneck, F.P., 2011. The diversification of eastern South American open vegetation biomes: Historical biogeography and perspectives. Quat. Sci. Rev. 30, 1630–1648. https://doi.org/10.1016/j.quascirev.2011.03.009

Werneck, F.P., Gamble, T., Colli, G.R., Rodrigues, M.T., Sites, J.W., 2012. Deep diversification and long-term persistence in the south american “dry diagonal”: Integrating continent-wide phylogeography and distribution modeling of geckos. Evolution (N. Y). 66, 3014–3034. https://doi.org/10.1111/j.1558-5646.2012.01682.x

Werneck, F.P., Leite, R.N., Geurgas, S.R., Rodrigues, M.T., 2015. Biogeographic history and cryptic diversity of saxicolous Tropiduridae lizards endemic to the semiarid Caatinga. BMC Evol. Biol. 15, 1–24. https://doi.org/10.1186/s12862-015-0368-3

#

Molecular Phylogenetics and Evolution

Past São Francisco River course, altitude isolation, and ecological traits as the evolutionary history plot for *Corythomantis greeningi* Boulenger 1896 (Anura, Hylidae) in dry biomes of Neotropical Region

Ricardo Marques, Emanuel M. da Fonseca, Leandro A. da Silva, Diego J. Santana, Amanda S. F. Lantyer-Silva, Célio F. B. Haddad & Adrian A. Garda

Supporting Information (appendix S1)

Laboratory protocols

We extracted DNA from tissue samples from liver and muscle using an adapted protocol from Brufold et al. (1992). To generate Polymerase Chain Reaction (PCR) mixes, we standardized a mix with 7.5 µl of Taq Polymerase Master Mix Red Ampliqon, 0.36 µl for primers (forward and reverse) and (BSA), 2-3 µl of extracted DNA and complemented with Miliq, totaling a mix of 15 µl. We used a specific cycle for each locus as described in Table S1. The respective primer for each locus and the source material are described in Table S1. We followed standard PCR techniques to amplify portions of DNA and PCR cycles for all loci are described in Table S2. Purification and sequencing of DNA were performed in Macrogen Inc.

Table S1: Respective locus, its source material, primer label and sequence fragment for all five loci.

Locus	**Reference**	**Primer**	**Sequence 5’ → 3’**
16S	Palumbi et al., 1991	16SA-L	CGCCTGTTTATCAAAAACAT
		16SB-H	CCGGTCTGAACTCAGATCACGT
COI	Folmer et al. 1994	dgLCO1490	GGTCAACAAATCATAAAGAYATYGG
		dgHCO2198	TAAACTTCAGGGTGACCAAARAAYCA
β-fib	Prychitko & Moore 1997	B17U	GGAGAAAACAGGAAATGACAATTCAC
		B17L	TCCCATATATCTGCCATTAGGGTT
RPL3	Pinho et al., 2010	RPL3-5F	TGTACAGGTCAAGTGTTATC
		RPL3-6RA	ATGCCAGTTAAAAATCAGACC
Tyr	Bossuyt & Milinkovitch 2000	TyrC	GGCAGAGGAWCRTGCCAAGATGT
		TyrG	TGCTGGCRTCTCTCCARTCCCA

Table S2: Detailed PCR cycles for all five loci with the respective temperature and duration of each stage. (*) Touchdown.

Cycle stage	16S	COI	βfib	RPL3	Tyr
Initial denaturation	94º C, 3 min	94º C, 5 min	95º C, 5 min	92º C, 5 min	94º C, 2 min
Number of cycles	10* + 35	35	38-45	40	35
Denaturation	94º C, 50 s	94º C, 40 s	94º C, 35 s	92º C, 30 s	94º C, 30 s
Annealing	60º C* + 50º C 1 min	48º C, 40 s	56º C, 35 s	55º C, 30 s	58º C, 30 s
Extension	72º C, 1 min	72º C, 40 s	68º C, 35 s	72º C, 1:30 min	72º C, 1 min
Final extension	72º C, 5 min	72º C, 7 min	68º C, 7 min	72º C, 5 min	72º C, 6 min

Population assignment ambiguities

We performed two different approaches for population assignment with Geneland and BAPS. The result from each analysis presented minor differences. BAPS assigned the localities of Itaiueira, Nova Iorque and Wall Ferraz to population two. One specimen from Nova Iorque and the specimen from São João dos Patos were assigned to population one. As for Geneland results, Wall Ferraz was the only locality assigned as population two in both datasets (mitochondrial+nuclear and nuclear alone). In nuclear alone result, Itaiueira was assigned to population two, while Nova Iorque was assigned to population one with 49% (against 35% to be assigned in population two), Itaiueira assigned to population two with 54%, and São João dos Patos was almost ambiguous (41% chance to be assigned in population one and 39% in population two). The combination of mitochondrial and nuclear loci in Geneland produced a result with Itaiueira assigned to population one with 47% (against 36% of population two), Nova Iorque assigned to population two with 56% and São João dos Patos assigned to population two with 59%. Considering the divergence of populations was recent (see divergence time results in the main text), all population assignment results and the geographic location of these four localities, we allocated them in population two.

Historical demography

Bayesian Skyline Plot uses coalescence to estimate past demographic history from single locus data (Drummond et al., 2005). We inferred the adequate substitution model for each population in jModelTest 2.1.7 (Posada, 2008). We conducted a run of 5×10^7 generations sampled every 5×10^4 steps for population one, and 3×10^7 generations for population two and Espinhaço population, sampled every 3×10^4 steps under the Coalescent Bayesian Skyline prior with strict clock for all populations. We set mutation rate at 7×10^{-9} subs/site/years (SD of 10^{-9}) for 16S and 1.5×10^{-8} subs/site/years (SD of $5 \times 10^{-$

^{9}) for COI under normal prior distribution. To check the convergence of runs, values of effective sample size (>200) and generate the plot figure we used Tracer 1.5 (Rambaut and Drummond 2007).

Our mitochondrial Bayesian skyline plot showed population one effective population size was stable during Late Pleistocene, with an expansion around 40 kya, despite Tajima's D indications of population expansion were not significant. Both population two and Espinhaço population showed demographic stability according to 95 % HPD interval (Figure S1).

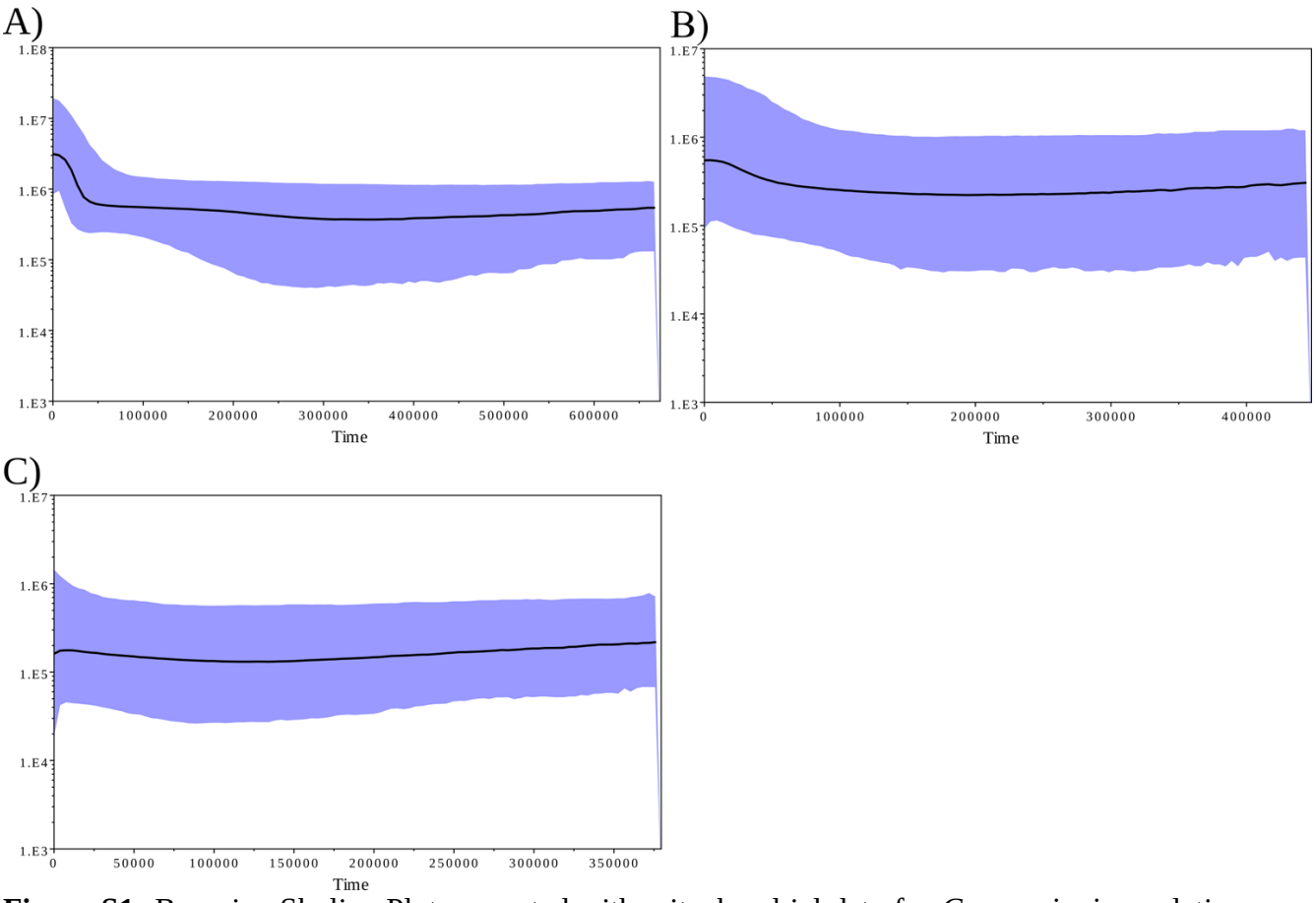

Figure S1: Bayesian Skyline Plot generated with mitochondrial data for *C. greeningi* populations one (A) and two (B), and *Corythomantis* sp. (C). The y-axis is the effective population size, the x-axis is the time scale in years read from the present (left) to the past (right). The black line shows the median population size and the confidence intervail is in blue (95% HPD).

Populations divergences

We estimate divergence time in populations of *C. greeningi*, we reconstructed phylogenetic relationships using *BEAST (Heled and Drummond, 2012) in BEAST 1.8.4 to produce a dated multispecies coalescent species tree. We assigned alleles according to population assignment results. Our dataset have two mitochondrial genes, so we conducted three independent runs to check for a congruent

divergence time: one run with 16S and nuclear data, a second run with COI and nuclear data, and a third run with concatenated mitochondrial genes and nuclear data. Each run was conducted with 3×10^8 generations, sampled every 3×10^4 steps under the Yule speciation process prior with uncorrelated lognormal relaxed clock. We calibrated the *BEAST mitochondrial mutation rate at 7.35×10^{-3} mutation/site/My for 16S and 1.47×10^{-2} mutation/site/My for COI (Gehara et al., 2014; Vences et al., 2005). We calibrated the molecular clock with uniform prior for mtDNA *ucld.mean* parameter (16S, 8.7×10^{-3} upper and 5.1×10^{-3} lower; COI, 1.74×10^{-2} upper and 1.22×10^{-2} lower). For the concatenated mtDNA, we used a mean mutation rate of 0.011025 mutation/site/My, molecular clock with uniform prior *ucld.mean* parameter (5.1×10^{-3} upper and 1.74×10^{-2} lower). As for nuDNA *ucld.mean* we set lognormal prior distribution at default options. We checked the convergence of runs and ESS values (>200) in Tracer 1.5 (Rambaut and Drummond, 2007) and calculated the maximum clade credibility tree in TreeAnnotator (Drummond et al., 2012) excluding 20% of trees as burn-in. We produced the graphic visualization of all trees in DensiTREE 2.2.5 (Bouckaert and Heled, 2014).

The resulting Bayesian coalescent-based species tree recovered in *BEAST shows the same monophyletic group as the concatenated species tree, also with high support (pp = 1). *BEAST estimated the divergence of Espinhaço population for early Pleistocene at 1.91 Mya (0.81–3.27 Mya 95% highest posterior density interval). A much shallower branch show the divergence between *C. greeningi* populations one and two for late Pleistocene, estimated for 0.12 Mya (0.08–0.18 My 95% highest posterior density interval) (Figure S2).

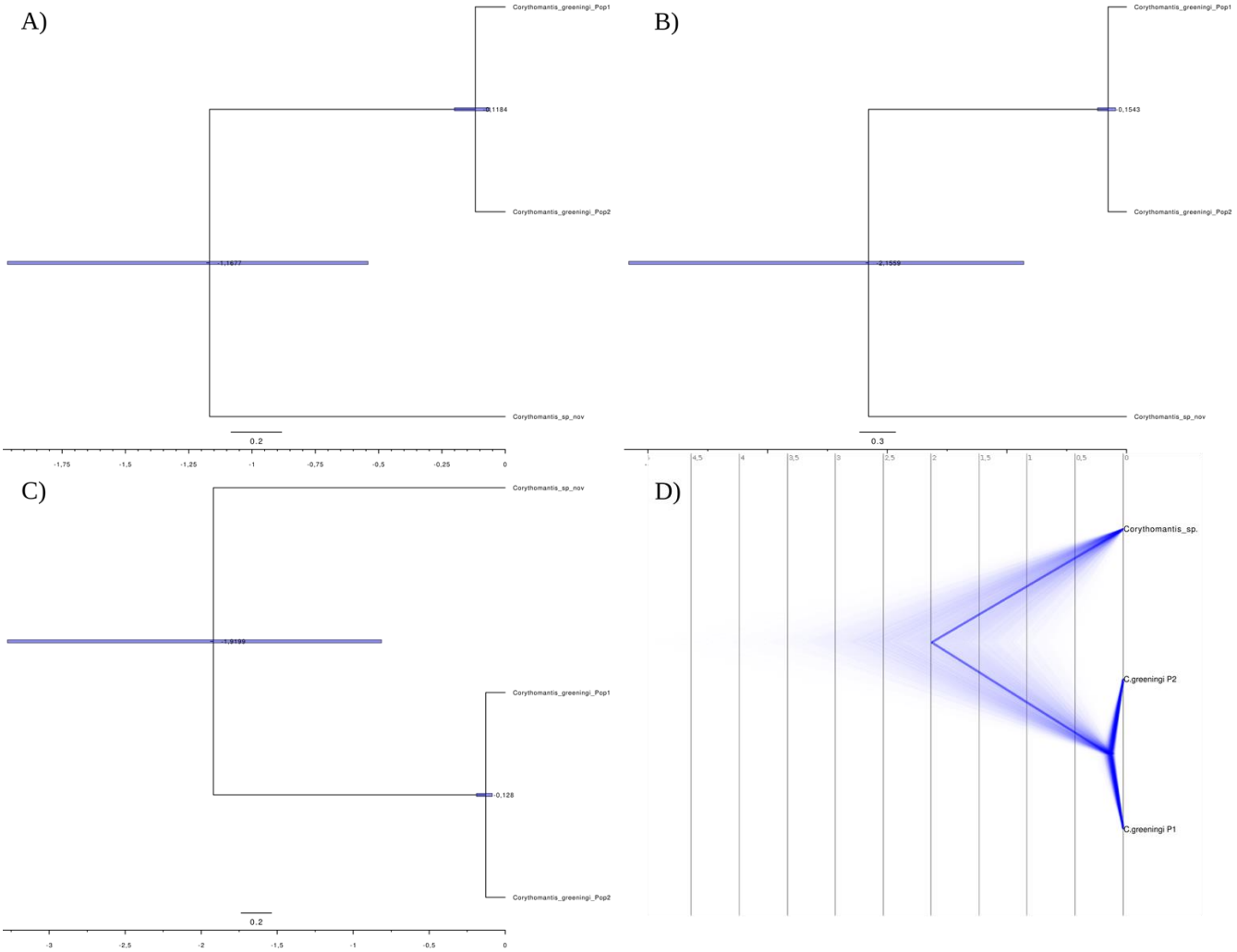

Figure S2: Divergence time estimated in *BEAST with different datasets. (A) 16S and nuclear data, (B) COI and nuclear data, and (C) concatenated mitochondrial data and nuclear data. (D) shows DensiTree plot showing all possible dates for this inference. X-axis show the timescale in millions of years and the blue bars are the 95% HPD.

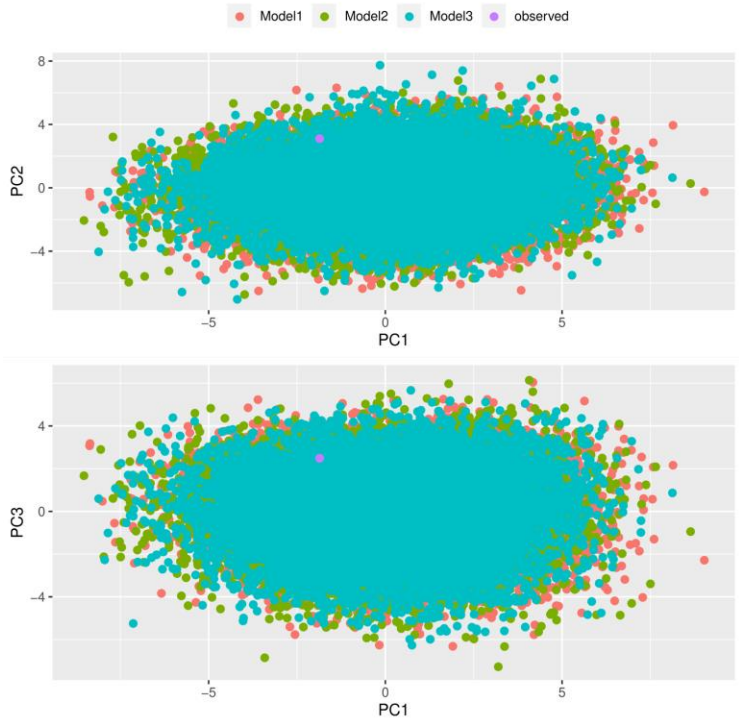

Figure S3: Principal Components Analysis plots (PC1 X PC2 and PC1 X PC3) derived from the simulated and observed data derived from models 1, 2, and 3.

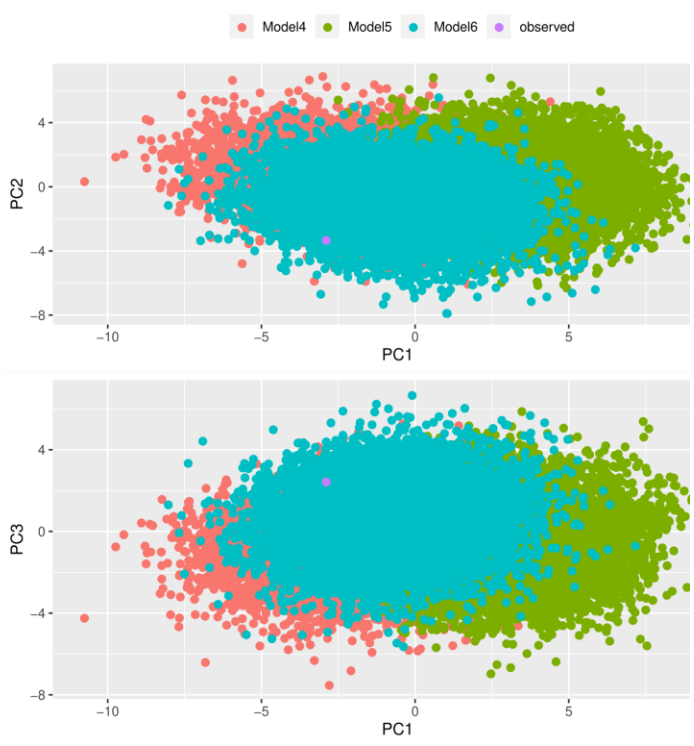

Figure S4: Principal Components Analysis plots (PC1 X PC2 and PC1 X PC3) derived from the simulated and observed data derived from models 4, 5, and 6.

Table S3: List of samples used for molecular data from *Corythomantis greeningi* (Cg), *Corythomantis* sp. (Csp) and *Trachycephalus typhonius* (Tt). Respective Genbank deposit number for each gene, the main locality and its acronym, respective state and coordinates.

Species	Voucher	Genbank number					Municipality (map number)	Acronym	State	Latitude	Longitude	Population assignment
		16S	COI	B-Fibrin	RPL3	Tyrosinase						
Cg	AAGARDA 10434	X	X	X	X	X	Angicos (23)	ANG	RN	-5.661667	-36.6005	population one
Cg	AAGARDA 10435	X	X				Angicos (23)	ANG	RN	-5.661667	-36.6005	population one
Cg	UFBA 7689	X	X				Bom Jesus da Lapa (3)	BJL	BA	-13.259676	-43.371156	population one
Cg	AAGARDA 8261	X	X				Buíque (18)	BUI	PE	-8.621092	-37.157249	population one
Cg	AAGARDA 8690	X	X				Buíque (18)	BUI	PE	-8.621092	-37.157249	population one
Csp	ZUFG 8059	X	X	X		X	Buenópolis (31)	BUJ	MG	-17.827385	-44.260984	Espinhaço
Cg	MNRJ 91036		X				Cafarnaum (4)	CAF	BA	-11.822516	-41.603087	population one
Cg	MNRJ 38627		X				Caruaru (19)	CAR	PE	-8.308974	-36.000401	population one
Cg	MNRJ 38628		X				Caruaru (19)	CAR	PE	-8.308974	-36.000401	population one
Csp	CFBH 20992	X	X	X	X	X	Contendas do Sincorá (32)	COS	BA	-13.799572	-41.047927	Espinhaço
Csp	MHNJCH 1079		X				Contendas do Sincorá (32)	COS	BA	-13.799572	-41.047927	Espinhaço
Cg	AAGARDA 2732	X	X	X	X	X	Crato (10)	CRA	CE	-7.234167	-39.409167	population one
Cg	AAGARDA 2733	X	X	X	X	X	Crato (10)	CRA	CE	-7.234167	-39.409167	population one
Cg	AAGARDA 2734	X	X				Crato (10)	CRA	CE	-7.234167	-39.409167	population one
Cg	UFBA 11401	X	X				Curaçá (5)	CUR	BA	-8.991663	-39.90584	population one
Csp	MTR 11281		X				Gameleira do Assuruá (33)	GAM	BA	-11.321393	-42.658672	Espinhaço
Csp	CFBH 2383	X	X	X	X	X	Grão Mogol (34)	GRM	MG	-16.559167	-42.889444	Espinhaço
Csp	CFBH 2392	X	X	X		X	Grão Mogol (34)	GRM	MG	-16.559167	-42.889444	Espinhaço
Cg	CFBH 20986	X	X				Itaueira (20)	ITA	PI	-7.595597	-43.016559	population two
Cg	CFBH 20987	X	X				Itaueira (20)	ITA	PI	-7.595597	-43.016559	population two
Cg	CFBH 20988	X	X				Itaueira (20)	ITA	PI	-7.595597	-43.016559	population two
Cg	CFBH 20989	X	X	X	X	X	Itaueira (20)	ITA	PI	-7.595597	-43.016559	population two
Cg	CFBH 20990	X	X	X	X	X	Itaueira (20)	ITA	PI	-7.595597	-43.016559	population two
Cg	AAGARDA 10390	X	X				Jaguaribe (11)	JAG	CE	-5.892705	-38.622015	population one
Cg	AAGARDA 10391	X	X				Jaguaribe (11)	JAG	CE	-5.892705	-38.622015	population one
Cg	AAGARDA 10392	X	X	X	X	X	Jaguaribe (11)	JAG	CE	-5.892705	-38.622015	population one
Cg	AAGARDA 10289	X	X	X	X	X	Jaguaribe (11)	JAG	CE	-5.892705	-38.622015	population one
Cg	AAGARDA 10394	X	X	X	X	X	Jaguaribe (11)	JAG	CE	-5.892705	-38.622015	population one
Cg	AAGARDA 10395	X	X				Jaguaribe (11)	JAG	CE	-5.892705	-38.622015	population one
Cg	AAGARDA 5556	X	X	X	X	X	João Câmara (24)	JOC	RN	-5.534793	-35.815058	population one

Cg	AAGARDA 8972	X	X				Martins (25)	MAR	RN	-6.069882	-37.911158	population one
Cg	AAGARDA 9538	X	X	X	X	X	Martins (25)	MAR	RN	-6.069882	-37.911158	population one
Cg	UFBA-CRS 82	X	X				Morro do Chapéu (6)	MOC	BA	-11.483056	-41.333056	population one
Cg	UFBA-CRS 97	X	X				Morro do Chapéu (6)	MOC	BA	-11.483056	-41.333056	population one
Cg	UFBA-CRS 98	X	X				Morro do Chapéu (6)	MOC	BA	-11.483056	-41.333056	population one
Cg	UFBA-CRS 99	X	X	X			Morro do Chapéu (6)	MOC	BA	-11.483056	-41.333056	population one
Cg	UFBA-CRS 100	X	X				Morro do Chapéu (6)	MOC	BA	-11.483056	-41.333056	population one
Cg	CHSA 260	X	X				Mossoró (26)	MOS	RN	-5.19508	-37.330004	population one
Cg	AAGARDA 12101	X	X				Murici (1)	MUR	AL	-9.289364	-35.943575	population one
Cg	AAGARDA 12102	X	X				Murici (1)	MUR	AL	-9.289364	-35.943575	population one
Cg	ZUFMS 77	X	X	X	X	X	Nova Iorque (15)	NOI	MA	-6.729822	-44.056644	population two
Cg	ZUFMS 78	X	X	X	X	X	Nova Iorque (15)	NOI	MA	-6.729822	-44.056644	population two
Cg	ZUFMS 79	X	X	X	X	X	Nova Iorque (15)	NOI	MA	-6.729822	-44.056644	population two
Csp	AAGARDA 6985	X	X	X	X	X	Palmeiras (35)	PAL	BA	-12.537891	-41.574944	Espinhaço
Csp	AAGARDA 6986	X	X		X	X	Palmeiras (35)	PAL	BA	-12.537891	-41.574944	Espinhaço
Csp	AAGARDA 7019	X	X	X	X	X	Palmeiras (35)	PAL	BA	-12.537891	-41.574944	Espinhaço
Csp	AAGARDA 7092	X	X	X		X	Palmeiras (35)	PAL	BA	-12.537891	-41.574944	Espinhaço
Csp	AAGARDA 6981	X	X	X	X	X	Palmeiras (35)	PAL	BA	-12.537891	-41.574944	Espinhaço
Csp	AAGARDA 6982	X	X				Palmeiras (35)	PAL	BA	-12.537891	-41.574944	Espinhaço
Csp	AAGARDA 6983	X	X	X	X	X	Palmeiras (35)	PAL	BA	-12.537891	-41.574944	Espinhaço
Csp	AAGARDA 6984	X	X	X	X	X	Palmeiras (35)	PAL	BA	-12.537891	-41.574944	Espinhaço
Csp	AAGARDA 7018	X	X	X	X	X	Palmeiras (35)	PAL	BA	-12.537891	-41.574944	Espinhaço
Cg	CFBH 20993	X	X				Palmeiras (35)	PAL	BA	-12.537891	-41.574944	Espinhaço
Cg	ZUFMS 3448	X	X		X		Palmas (30)	PAM	TO	-10.339223	-48.302834	population one
Cg	MAP 2196	X					Palmas (30)	PAM	TO	-10.339223	-48.302834	population one
Cg	CFBH 13	X	X	X	X	X	Piranhas (2)	PIR	AL	-9.623333	-37.756667	population one
Cg	CFBH 43	X	X	X		X	Piranhas (2)	PIR	AL	-9.623333	-37.756667	population one
Cg	FSCHUFPB 334	X	X	X		X	Poço Redondo (29)	POR	SE	-9.806582	-37.683604	population one
Cg	ZUFMS 152	X	X	X	X	X	Riachão (16)	RIA	MA	-7.356583	-46.610374	population one
Cg	ZUFMS 153	X	X	X	X	X	Riachão (16)	RIA	MA	-7.356583	-46.610374	population one
Cg	ZUFMS 154	X	X				Riachão (16)	RIA	MA	-7.356583	-46.610374	population one
Cg	ZUFMS 155	X	X	X	X	X	Riachão (16)	RIA	MA	-7.356583	-46.610374	population one
Cg	ZUFMS 156	X	X				Riachão (16)	RIA	MA	-7.356583	-46.610374	population one
Cg	MTR 11265		X				Santo Inácio (7)	SAI	BA	-11.111598	-42.716633	population one
Cg	FSCHUFPB 1377	X	X	X		X	Santa Quitéria (12)	SAQ	CE	-4.325321	-40.152648	population one

Cg	AAGARDA 11361	X	X				Caracol (21)	SDC	PI	-9.121454	-43.756846	population one
Cg	AAGARDA 11488	X	X	X	X	X	Caracol (21)	SDC	PI	-9.121454	-43.756846	population one
Cg	AAGARDA 11489	x	X	X	X	X	Caracol (21)	SDC	PI	-9.121454	-43.756846	population one
Cg	AAGARDA 11490	X	X	X	X	X	Caracol (21)	SDC	PI	-9.121454	-43.756846	population one
Cg	UFBA 7686	X	X				Serra do Ramalho (8)	SER	BA	-13.543214	-43.577956	population one
Cg	UFBA 7687	X	X				Serra do Ramalho (8)	SER	BA	-13.543214	-43.577956	population one
Cg	UFBA 7688	X	X	X		X	Serra do Ramalho (8)	SER	BA	-13.543214	-43.577956	population one
Cg	MAP 1288	X	X	X	X	X	São João dos Patos (17)	SJP	MA	-6.493789	-43.703992	population two
Cg	FSCHUFPB 5452	X	X				Serra Negra do Norte (27)	SNN	RN	-6.660708	-37.399937	population one
Cg	FSCHUFPB 5453	X	X	X	X	X	Serra Negra do Norte (27)	SNN	RN	-6.660708	-37.399937	population one
Cg	FSCHUFPB 5454	X	X				Serra Negra do Norte (27)	SNN	RN	-6.660708	-37.399937	population one
Cg	FSCHUFPB 6116	X	X	X	X	X	Serra Negra do Norte (27)	SNN	RN	-6.660708	-37.399937	population one
Cg	FSCHUFPB 6117	X	X	X	X	X	Serra Negra do Norte (27)	SNN	RN	-6.660708	-37.399937	population one
Cg	FSCHUFPB 6200	X	X				Serra Negra do Norte (27)	SNN	RN	-6.660708	-37.399937	population one
Cg	AAGARDA 10664	X	X				Ubajara (13)	UBA	CE	-3.869213	-41.019178	population one
Cg	AAGARDA 10681	X	X	X	X	X	Ubajara (13)	UBA	CE	-3.869213	-41.019178	population one
Cg	AAGARDA 10919	X	X				Ubajara (13)	UBA	CE	-3.869213	-41.019178	population one
Cg	AAGARDA 10888	X	X	X	X	X	Ubajara (13)	UBA	CE	-3.869213	-41.019178	population one
Cg	AAGARDA 10620	X	X				Ubajara (13)	UBA	CE	-3.869213	-41.019178	population one
Cg	AAGARDA 10889	X	X	X	X	X	Ubajara (13)	UBA	CE	-3.869213	-41.019178	population one
Cg	AAGARDA 10920	X	X	X	X	X	Ubajara (13)	UBA	CE	-3.869213	-41.019178	population one
Cg	AAGARDA 10921	X	X				Ubajara (13)	UBA	CE	-3.869213	-41.019178	population one
Cg	AAGARDA PF01	X	X	X	X	X	Umarizal (28)	UMA	RN	-5.897975	-37.764576	population one
Cg	AAGARDA 9293	X	X	X	X	X	Umarizal (28)	UMA	RN	-5.897975	-37.764576	population one
Cg	AAGARDA 9294	X	X		X	X	Umarizal (28)	UMA	RN	-5.897975	-37.764576	population one
Cg	AAGARDA 12343	X	X	X	X		Umburanas (9)	UMB	BA	-10.724189	-41.329788	population one
Cg	AAGARDA 12344	X	X	X	X	X	Umburanas (9)	UMB	BA	-10.724189	-41.329788	population one
Cg	AAGARDA 12345	X	X				Umburanas (9)	UMB	BA	-10.724189	-41.329788	population one
Cg	AAGARDA 12346	X	X				Umburanas (9)	UMB	BA	-10.724189	-41.329788	population one
Cg	AAGARDA 12347	X	X				Umburanas (9)	UMB	BA	-10.724189	-41.329788	population one
Cg	AAGARDA 12348	X	X				Umburanas (9)	UMB	BA	-10.724189	-41.329788	population one
Cg	CFBH 5362	X	X	X	X	X	Viçosa do Ceará (14)	VIC	CE	-3.566667	-41.091389	population one
Cg	CFBH 5363	X	X	X	X	X	Viçosa do Ceará (14)	VIC	CE	-3.566667	-41.091389	population one
Cg	CFBH 20991	X	X	X	X	X	Wall Ferraz (22)	WFE	PI	-7.236828	-41.879941	population two

Tt	AAGARDA 10992	X	X		X	X	Ubajara (13)		-	CE	-3.869213	-41.019178	-

Table S4: Additional distribution records of *Corythomantis greeningi* used in the Ecological Niche Modeling and its respective source material.

Latitude	Longitude	Locality	State	Biome	Source material
-9.261944	-37.937778	Água Branca	Alagoas	Caatinga	Pombal et al. 2012
-9.278524	-35.728936	Flexeiras	Alagoas	Atlantic Forest	Almeida et al. 2016
-9.606767	-37.258193	Monteirópolis	Alagoas	Caatinga	Almeida et al. 2016
-9.522645	-37.304366	Olho D'água das Flores	Alagoas	Caatinga	Almeida et al. 2016
-9.383143	-37.252957	Santana do Ipanema	Alagoas	Caatinga	Almeida et al. 2016
-9.960589	-36.980403	Traipu	Alagoas	Caatinga	Almeida et al. 2016
-10.5075	-40.3214	Campo Formoso	Bahia	Caatinga	SpeciesLink
-9.595833	-40.419167	Carnaíba do Sertão	Bahia	Caatinga	Pombal et al. 2012
-15.53	-40.912222	Encruzilhada	Bahia	Atlantic Forest	Sazima & Cardoso 1980
-12.1	-39.03	Feira de Santana	Bahia	Caatinga	Juncá et al. 2008
-10.068334	-38.346944	Jeremoabo	Bahia	Caatinga	Pombal et al. 2012
-13.435278	-40.432222	Maracás	Bahia	Caatinga	Pombal et al. 2012
-11.429722	-40.603056	Miguel Calmon	Bahia	Caatinga	Pombal et al. 2012
-9.398056	-38.221389	Paulo Afonso	Bahia	Caatinga	Pombal et al. 2012
-14.2672	-43.1619	Palmas de Monte Alto	Bahia	Caatinga	SpeciesLink
-12.85	-39.4666	Serra da Jiboia	Bahia	Atlantic Forest	Freitas et al. 2018
-7.301082	-38.937875	Milagres	Ceará	Caatinga	SpeciesLink
-4.389097	-40.719013	Planalto da Ibiapaba	Ceará	Caatinga	Loebmann & Haddad 2010
-3.717256	-38.643405	Caucaia	Ceará	Caatinga	Roberto & Loebmann 2016
-5.178399	-40.686637	Crateús	Ceará	Caatinga	Roberto & Loebmann 2016
-3.763432	-38.50048	Fortaleza	Ceará	Caatinga	Roberto & Loebmann 2016
-4.170815	-40.765231	Guaraciaba do Norte	Ceará	Caatinga	Roberto & Loebmann 2016
-4.260424	-38.926192	Guaramiranga	Ceará	Caatinga	Roberto & Loebmann 2016
-4.162577	-38.463542	Pacajus	Ceará	Caatinga	Roberto & Loebmann 2016
-3.938391	-38.603726	Pacatuba	Ceará	Caatinga	Roberto & Loebmann 2016
-4.22847	-38.923794	Pacoti	Ceará	Caatinga	Roberto & Loebmann 2016
-3.609285	-38.978888	São Gonçalo do Amarante	Ceará	Caatinga	Roberto & Loebmann 2016
-3.275302	-39.274665	Trairi	Ceará	Caatinga	Roberto & Loebmann 2016
-3.631772	-39.505232	Uruburetama	Ceará	Caatinga	Roberto & Loebmann 2016
-13.399722	-46.321667	São Domingos	Goiás	Cerrado	Pombal et al. 2012

-3.738611	-43.360278	Chapadinha	Maranhão	Cerrado	Sazima & Cardoso 1980
-3.206389	-43.387778	Urbano Santos	Maranhão	Cerrado	Pombal et al. 2012
-7.221944	-35.873056	Campina Grande	Paraíba	Caatinga	Pombal et al. 2012
-7.192778	-37.928611	Piancó	Paraíba	Caatinga	Pombal et al. 2012
-7.366389	-36.516389	São João do Cariri	Paraíba	Caatinga	Vieira et al. 2007
-7.058056	-36.366667	Soledade	Paraíba	Caatinga	Pombal et al. 2012
-7.503611	-39.723611	Exu	Pernambuco	Caatinga	Pombal et al. 2012
-8.882221	-36.496391	Garanhuns	Pernambuco	Atlantic Forest	Pombal et al. 2012
-8.35778	-36.697777	Pesqueira	Pernambuco	Caatinga	Carvalho 1941
-7.926667	-35.650278	Salgadinho	Pernambuco	Caatinga	Carvalho 1941
-7.813333	-38.1475	Santa Cruz da Baixa Verde	Pernambuco	Caatinga	Silva et al. 2010
-6.776932	-43.022601	Floriano	Piauí	Cerrado	Sazima & Cardoso 1980
-4.273056	-41.776667	Parque Nacional Sete Cidades	Piauí	Caatinga	Pombal et al. 2012
-4.42272	-41.4586	Pedro II	Piauí	Caatinga	SpeciesLink
-3.928056	-41.709167	Piracuruca	Piauí	Caatinga	Godinho et al. 2013
-4.273889	-41.776667	Piripiri	Piauí	Caatinga	Pombal et al. 2012
-5.899167	-35.764167	São Paulo do Potengi	Rio Grande do Norte	Caatinga	Pombal et al. 2012
-10.541667	-37.058333	Refúgio Mata do Junco	Sergipe	Atlantic forest	Morato et al. 2011
-10.679995	-46.150545	Estação Ecológica Serra Geral	Tocantins	Cerrado	Valdujo et al. 2011
-12.83752	-46.992533	Taipas do Tocantins	Tocantins	Cerrado	Voucher UFG 9066-67

References

Almeida, J. P. F. A., Nascimento, F. A. C., Torquato, S., Lisboa, B. S., Tiburcio, I. C. S., Palmeira, C. N. S., … Mott, T. (2016). Amphibians of Alagoas State, northeastern Brazil. Herpetology Notes, 9, 123–140.

Bossuyt, F. & Milinkovitch, M.C. 2000. Convergent adaptive radiations in Madagascan and Asian ranid frogs reveal covariation between larval and adult traits. Proceedings of the National Academy of Sciences, 97(12), 6585-6590.

Carvalho, A.L. 1941. Notas sôbre os gêneros Corythomantis Boulenger e Aparasphenodon Miranda Ribeiro. Papéis Avulsos do Departamento de Zoologia 1(14): 101-110.

Folmer O, Black M, Hoeh W, Lutz R, Vrijenhoek R (1994) DNA primersfor amplification of mitochondrial cytochrome coxidase subunit I fromdiverse metazoan invertebrates.Molecular Marine Biology and Biotech-nology,3, 294–299.

Godinho, L. B., Moura, M. R., & Feio, R. N. (2013). New records and geographic distribution of Corythomantis greeningi Boulenger, 1896 (Amphibia: Hylidae). Check List, 9(1), 148–150. https://doi.org/10.15560/9.1.148

Juncá, F.A., M.C.L. Carneiro and N.N. Rodrigues. 2008. Is a dwarf population of Corythomantis greeningi Boulenger, 1896(Anura, Hylidae) a new species? Zootaxa 1686: 48-56.

Loebmann, D., & Haddad, C. F. B. (2010). Amphibians and reptiles from a highly diverse area of the Caatinga domain: composition and conservation implications. Biota Neotropica, 10(3), 227–256. https://doi.org/10.1590/s1676-06032010000300026

Morato, S. A. A., de Lima, A. M. X., Staut, D. C. P., Faria, R. G., de Souza-Alves, J. P., Gouveia, S. F., … da Silva, M. J. (2011). Amphibians and reptiles of the refúgio de vida silvestre mata do junco, municipality of Capela, state of sergipe, northeastern Brazil. Check List, 7(6), 756–762.

Palumbi S.R., Martin A., Romano S., McMillan W.O., Stice L. & Grabowski G. 1991. The Simple Fool's Guide to PCR, Version 2.0. Privately published document compiled by S. Palumbi, Dept. Zoology. Honululu: Univ. Hawaii.

Pinho, C., Rocha, S., Carvalho, B.M., Lopes, S., Mourão, S., Vallinoto, M., Brunes, T.O., Haddad, C.F.B., Gonçalves, H., Sequeira, F. & Ferrand, N. 2010 New primers for the amplification and sequencing of nuclear loci in a taxonomically wide set of reptiles and amphibians. Conservation Genetic Resources, 2, 181–185

Pombal, J.P.Jr., V.A. Menezes, A.F. Fontes, I. Nunes, C.F.D. Rocha and M. Van-Sluys. 2012. A second species of the casque-headed frog genus Corythomantis (Anura:Hylidae) from northeastern Brazil, the distribution of C.greeningi , and comments on the genus. Boletim do Museu Nacional, Nova Série, Zoologia 530: 1-14.

Prychitko, T.M. & Moore, W.S. 1997. The utility of DNA sequences of an intron from the b-fibrinogen gene in phylogenetic analysis of woodpeckers (Aves: Picidae). Molecular Phylogenetics and Evolution, 8, 193–204.

Roberto, I. J., & Loebmann, D. (2016). Composition, distribution patterns, and conservation priority areas for the herpetofauna of the state of Ceará, northeastern Brazil. Salamandra, 52(2), 134–152. https://doi.org/10.1111/geb.12053

Sazima, I. and A.J. Cardoso. 1980. Notas sobre a distribuição de Corythomantis greeningi Boulenger, 1896 e Aparasphenodon brunoi Miranda-Ribeiro, 1920 (Amphibia, Hylidae). Iheringia, Série Zoologia 55: 3-7.

Silva, G.L., E.M. Santos and J.P. Gomes. 2010. Predação de ovos de Corythomantis greeningi Boulenger, 1896 (Anura, Hylidae) por Solenopsis invicta Buren, 1972 (Formicidae: Myrmicinae). Biotemas 23(4): 153-156.

Valdujo, P.H., A. Camacho, R.S. Recoder, M. Teixeira-Jr, J.M.B. Ghellere, T. Mott, P.M.S. Nunes, C. Nogueira and M.T. Rodrigues. 2011. Anfíbios da Estação Ecológica Serra Geral do Tocantins, região do Jalapão, Estados do Tocantins e Bahia. Biota Neotropica 11(1): 251-262.

Vieira, W.L.S., C. Arzabe and G.G. Santana. 2007. Composição e distribuição espaço-temporal de Anuros no Cariri Paraibano, Nordeste do Brasil. Oecologia Brasiliensis 11(3): 383-396.

Capítulo III

Ida e volta da monotipia: Uma nova espécie do cabeça-de-capacete *Corythomantis* Boulenger 1896 (Anura, Hylidae) da Cadeia de Montanhas do Espinhaço, Brasil

Manuscrito aceito no periódico Herpetologica

There and Back Again From Monotypy: A New Species of the Casque-headed *Corythomantis* Boulenger 1896 (Anura, Hylidae) from the Espinhaço Mountain Range, Brazil

RICARDO MARQUES[1,4], CÉLIO F. B. HADDAD[2], AND ADRIAN A. GARDA[1, 3]

[1] Programa de Pós-Graduação em Ciências Biológicas (Zoologia), Centro de Ciências Exatas e da Natureza, Departamento de Sistemática e Ecologia, Universidade Federal da Paraíba; João Pessoa, PB 58051-900, Brazil

[2] Universidade Estadual Paulista (UNESP), Departamento de Zoologia e Centro de Aquicultura (CAUNESP), Instituto de Biociências, Rio Claro, São Paulo, Brasil

[3] Departamento de Botânica e Zoologia, Centro de Biociências, Universidade Federal do Rio Grande do Norte, Lagoa Nova, Natal, RN, Brazil

[4] CORRESPONDENCE: rcdmarquess@gmail.com

ABSTRACT: The genus *Corythomantis* was monotypic for over 100 years, encompassing only the species *C. greeningi*. In 2012 a second species, *C. galeata*, was described, but this species was recently reassigned to *Nyctimantis*, rendering *Corythomantis* once again monotypic. The geographic distribution of *C. greeningi* covers the Caatinga and Cerrado biomes from northeast Brazil, with a western limit in Tocantins state and a southward limit in Minas Gerais state. Here we demonstrate the existence of a second species of *Corythomantis* through molecular, acoustic, and morphological data. The new species differs in morphology from *C. greeningi* in head shape and tibia coloration. The new species has an advertisement call with shorter duration 0.18 ± 0.011 s (0.11–0.21 s), higher pulse rate 97.42 ± 5.63 (66.43–117.27 pulses/s), and different acoustic structure. Molecular data of mitochondrial DNA show that the genetic divergence from *C. greeningi* range from 2.88 % in 16S to 14.06 % in COI. The new species geographic distribution is restricted to the Espinhaço Mountain Range in elevations from 315 to 930 meters above sea level.

Key words: Bahia state; *Corythomantis "espinhaço"*; Endemism center; Larval morphology; Lophyohylini; Minas Gerais state

THE CAATINGA is an exclusively Brazilian biome, but nevertheless the least studied region in this country. It was for long considered species poor, with low levels of endemism as a result of its harsh climate, sharing most of its species with neighboring biomes (Vanzolini et al. 1989; Rodrigues 2003; Leal et al. 2005). Recent studies, however, provided a contrasting scenario and have shown that it actually harbors a significant number of endemic species for all vertebrate groups, likely being one of the most diverse semiarid regions in the world (Garda et al. 2018). This region extends from northeastern Brazil to northern Minas Gerais state in southeastern Brazil. The vegetation is composed of xerophytic and open vegetation (i.e. reduced canopy cover) that encompasses a mosaic of different physiognomies adapted to low levels of annual rainfall and high solar radiation (Prado 2003; Silva et al. 2017). It lies in between the tropical Amazon and Atlantic rainforests, composing the South American

diagonal of open formations, along with the Cerrado and Chaco biomes (Werneck 2011). Though this environment seems harsh for water-dependent biota, the last compilation for amphibian richness list 98 species for Caatinga biome, of which 39 are hylids (Garda et al. 2017).

The family Hylidae is the second richest in number of species within Anura (Frost 2019). Among the several morphological types within the family, the tribe Lophyohylini comprises 88 species of frogs with ossified heads popularly known as Casque-headed treefrogs (Faivovich et al. 2005; Frost 2019; Blotto et al. 2020). Members of this tribe share a synapomorphy of at least four posterior labial tooth rows during larvae stage. In Brazil, this clade is represented by species of the genera *Corythomantis* Boulenger, 1896, *Dryaderces* Jungfer et al. 2013, *Itapotihyla* Faivovich et al. 2005, *Nyctimantis* Boulenger, 1882, *Osteocephalus* Steindachner, 1862, *Phyllodytes* Wagler, 1830, *Tepuihyla* Ayarzagüena et al. 1993, and *Trachycephalus* Tschudi, 1838 (Blotto et al. 2020).

For over one hundred years, the genus *Corythomantis* was monotypic and comprised only *Corythomantis greeningi* Boulenger, 1896, an inhabitant of xeric environments associated with temporary rocky streams within the Caatinga and nearby localities in the Cerrado. In the phylogenetic hypothesis of Faivovich et al. (2005), *C. greeningi* is sister to *Nyctimantis siemersi*, *Nyctimantis brunoi*, and *Nyctimantis rugiceps*. The species was described from a single specimen deposited in the British Museum of London but with uncertain type locality, assigned only as “from Brazil”. That remained until Condit (1964) assign the type locality of *C. greeningi* to “Brazil: Espírito Santo”, which is unlikely given that the distribution of *C. greeningi* does not reach the state of Espírito Santo. Therefore, the type locality for *C. greeningi* remain unknown. Then, Pombal et al. (2012) described a second species for the genus, *C. galeata* from Morro do Chapéu, Bahia state, through morphological data comparison. Recently, however, Blotto et al. (2020), while reconstructing the phylogeny of Lophyohylini, showed this species is in fact more related to *Nyctimantis*. Therefore, *Corythomantis* is now once again a monotypic genus.

Herein, we describe a second species of the genus *Corythomantis* from the Espinhaço Mountain Range from the Brazilian states of Bahia and Minas Gerais using molecular, acoustic, and morphological data.

MATERIALS AND METHODS

Fieldwork and Institutional Abbreviations

As a result of multiple field surveys over the last 10 years in the Caatinga, we were able to gather specimens, tissues, tadpoles, and calls across the distribution of *Corythomantis greeningi* in northeastern Brazil. During an expedition to Chapada Diamantina, at the northern part of the Espinhaço Mountain Range in municipality of Palmeiras (12.560672 S, 41.561242 W, WGS84, 770 m a.s.l.), state of Bahia, we collected a few highly distinct individuals of *Corythomantis greeningi* (Magalhães et al. 2015). The type specimens and tissue samples of the new species were deposited in the following Brazilian collections: Universidade Federal da Paraíba, Paraíba (CHUFPB), Universidade Estadual Paulista, Rio Claro, São Paulo (CFBH), Universidade Estadual de Campinas, Campinas, São Paulo (ZUEC-AMP), and Universidade Federal de Viçosa, Viçosa, Minas Gerais (MZUFV). We followed Sabaj (2016) for institutional abbreviations. Institutions or collections not listed in that compilation are: Universidade Federal do Semi-Árido, Mossoró, Rio Grande do Norte, Brazil (CHSA), Universidade Federal de Goiás, Goiânia, Goiás, Brazil (UFG), and Coleção de Anfíbios e Répteis from Universidade Federal do Rio Grande do Norte, Natal, Rio Grande do Norte (AAGARDA). The type series and specimens used for comparison are listed in Appendix.

Bioacoustics

We recorded only the holotype at the type locality with a Marantz PMD 661 recorder and a Sennheiser 66 directional microphone, and analyzed a total of 278 advertisement calls. Because the species inhabits streams, several recordings contained intense background noise in the same frequency as the species' call. Therefore, we used only those with minimal background noise. For comparisons we obtained recordings from four *C. greeningi* from three

localities and analyzed a total of 199 advertisement calls. Recordings were normalized at 0 dB in Audacity v2.2.1 before analyzed in Raven Pro v1.5 and audio spectrograms were constructed using the following parameters: Hann window type, Fast Fourier Transform (FFT) window with 128 points and 50 % overlap. Calls are structured in two distinct groups, one with several low amplitude, individualized pulses and another with concatenated (very short intervals that make pulses overlap), high amplitude pulses, similar to those observed in Juncá et al. (2008). To account for the two groups (low amplitudes/high intervals and high amplitudes/low intervals), we separated calls in group A and group B. As call variables we used call duration, dominant frequency, pulses per call, pulse duration, pulse rate, pulse intervals, pulses in the first part of call, duration of first part of call, dominant frequency in the first part of call, pulses in the second part of call, duration of first part of call and dominant frequency in the second part of call. Terminology followed Köller et al. (2017). All recordings we used are deposited in the following collections: Sound Files from the Universidade Federal do Rio Grande do Norte (ASUFRN), Amphibian Sound Library of the MHNBA (SUFBA) at Universidade Federal da Bahia (UFBA), and Jacques Vielliard Neotropical Sound Library (FNJV) at Universidade Estadual de Campinas (UNICAMP).

Molecular Data

We gathered tissue samples from *Corythomantis greeningi* and the new species available at Universidade Federal do Rio Grande do Norte (AAGARDA), Universidade Estadual Paulista (CFBH), and from donations and loans from several herpetology collections to cover the broad distribution of the genus. We gathered 18 samples of the new species distributed in four localities. For *C. greeningi* we gathered 23 samples from 13 localities. We extracted genomic DNA from liver or muscle tissues using saline protocol (Bruford et al. 1992). We amplified targeted gene fragments with polymerase chain reactions (PCR) for two mitochondrial genes (16S ribosomal DNA and Cytochrome Oxydase I — COI henceforth). For 16S we used the primer pair from Palumbi et al. (1991) (16Sa/16Sb) and for COI we used dgLCO1490/dgHCO2198 primer pair from Folmer et al. (1994). PCR mixes consisted of 7.5

µL Ampliqon Taq DNA Polimerase Master Mix Red, each primer at 0.36 µL, 0.36 µL of Bovine Serum Albumin, and 2 µL of template DNA, in a total reaction volume of 15 µL. PCR cycling program condition for 16S was 94ºC for 3 min, followed by 10 touchdown cycles of 94ºC for 50s, annealing temperature at 60ºC for 1 min, 72ºC for 1 min, then 35 regular cycles at 50ºC of annealing temperature, and a 5 min final extension at 72ºC. COI PCR cycling program was 94ºC for 5 min, 35 cycles of 94ºC for 40 s, 48ºC for 40 s, 72ºC for 40 s, and a final extension of 72ºC for 7 min. Sequences were manually edited in Geneious v9.1.4 and aligned with MUSCLE algorithm in MegaX v10.0.04 (Kumar et al. 2018). We also used MegaX to calculate the genetic divergence between *Corythomantis* species for both genes. The resulting total length of sequences alignment were 534 bp for 16S and 611 bp for COI.

To test the phylogenetic relationships of the new species respect to other Lophyohylini, we produced a mitochondrial gene tree with our sequence dataset for *Corythomantis* and additional sequences of species from the tribe available in GenBank (Table 1). We used *Boana raniceps* as an outgroup. We removed gaps in the alignment with the default options and parameters of Gblocks (Talavera and Castresana 2007). Since COI is a coding gene, we concatenated genes in one alignment and divided into four partitions, one for 16S and three corresponding to each codon position in COI (COI1, COI2, and COI3). We used PartitionFinder2 (Lanfear et al. 2016) to estimate evolutionary rate heterogeneity among partitions with the greedy algorithm, linked branch lengths, and Bayesian Information Criterion to find the best partitioning scheme model of nucleotide substitution. PartitionFinder2 suggested four partitions: 16S partition as HKY+I+G, and COI1, COI2 and COI3 as HKY, TRN+G and TRN+G, respectively, as the best-fit model of nucleotide substitution. We estimated the gene tree in BEAST v1.8.4 (Drummond et al. 2012) set to 10^7 generations, sampled every 10^3 steps under the Birth-Death Process tree prior and strict clock. We considered the analysis adequate when convergence values of effective sample size (ESS) were above 200 in Tracer v1.6 (Drummond and Rambaut 2007). We calculated the maximum

clade credibility tree in TreeAnnotator (Drummond et al. 2012) excluding 2000 trees as burn-in.

Morphology

We measured morphometric variables with a Mitutoyo digital caliper (+/- 0.01 mm) following measurements from Garda et al. (2010): snout-vent length (SVL), head length (HL), head width (HW), commissure of the mouth to the tip of the snout (CMS), eye-nostril distance (END), eye-snout distance (ESD), nostril-snout distance (NSD), interorbital distance (IOD), internasal distance (IND), tympanum diameter (TD), eye diameter (ED), elbow-finger III length (EFIII), hand length (HaL), thigh length (ThL), tibia length (TL), and foot length (FL). For the comparisons between *C. greeningi* and the new species, we sexed specimens by the occurrence of nuptial pads and vocal slits in males to avoid variation due to sexual dimorphism. We followed Luna et al. (2018) for nuptial pads terminology.

We used morphometric measurements to test if (1) there are differences between the new species and *C. greeningi* and (2) if there is sexual dimorphism between males and females of the new species. First, we explored the data with a Principal Component Analysis (PCA) and tested if there were differences between species through a Procrustes MANOVA with geomorph package v3.0.7 (Adams and Otárola-Castillo 2013) in R v3.4.4 (R core Team 2015) for all mature males of the new species and *C. greeningi*. For both tests we first used all morphometric measurements. In a second run, we considered that the head of *Corythomantis* is co-ossified and reduce misleading measurements, so we used only the following head measurements: Head length, head width, commissure of the mouth to the tip of the snout, eye-nostril distance, eye-snout distance, and nostril-snout distance. Examined specimens of *Corythomantis* are listed in the Appendix.

Tadpoles

We collected tadpoles along with adult specimens from Palmeiras, state of Bahia (Lots CHUFPB 28775 and 30501). Tadpoles could be easily attributed to the genus *Corythomantis* based on their coloration, peculiar oral formula, and total teeth row number (Juncá et al.

2008). In northeast Brazil, only tadpoles of *Bokermanohyla* have more than 10 tooth rows, but can be distinguished from tadpoles of *Corythomantis* by its coloration (Magalhães 2014). We used a Leica EZ4 stereo microscope for morphological measurements, following Altig and McDiarmid (1999) for these variables: total length, body length, body width, body height, tail length, tail height, dorsal fin height, ventral fin height, internostril distance, interorbital distance, eye diameter, nostril diameter, eye nostril distance, nostril-snout distance, eye-snout distance, snout-spiracle distance, spiracle-vent distance, and oral disc width. We determined the stages of the tadpoles by using Gosner's (1960) table.

SPECIES DESCRIPTION

*Corythomantis **"espinhaço"*** sp. nov.

(Figs. 1–4, Tables 2–4)

Corythomantis greeningi: Godinho et al. 2013:149, in part.

Corythomantis greeningi: Magalhães et al. 2015:248.

Holotype.—CHUFPB 28228, adult male (Fig. 1), collected at Chapada Diamantina National Park, municipality of Palmeiras, Bahia state (-12.537891 S, -41.574944 W, WGS84, 750 m above sea level [a.s.l.]), on 24 January 2013 by F. M. Magalhães, W. P. Silva, T. B. Costa, D. O. Laranjeiras, and C. N. S. Palmeira.

Paratopotypes.—CHUFPB 28229–33 (adult males), CHUFPB 28234–36 (adult females) collected with the holotype, CHUFPB 30489 and 30491 (adult males) and CHUFPB 30494 and 30496 (adult females) (Fig. 2) collected on 08 February 2020, by R. Marques, A. A. Garda, F. M. Magalhães, and A. F. Silva-Neta, CFBH 30147 (adult male) collected on 17 November 2011, by M. T. C. Thomé, F. Brusquetti, K. Zamudio, and H. Greene.

Paratypes.—CFBH 30089 (adult female) collected at Contendas do Sincorá municipality, Bahia state (-13.799572 S, -41.047927 W, 315 m a.s.l.), on 15 November 2011, by M. T. C. Thomé, F. Brusquetti, K. Zamudio, and H. Greene. CFBH 10211 (male), CFBH 10212 and10213 (females) collected at Grão Mogol municipality, Minas Gerais state (-

16.559167 S, -42.889444 W, 884 m a.s.l.), on the 2 December 2005, by L. F. Toledo and O. G. S. Araújo. MZUFV 11705 (adult male), MZUFV 11706 (adult female) collected at Buritizeiro municipality, Minas Gerais state (-17.404073 S, -45.060422 W, 655 m a.s.l.), on the 13 November 2011, by L. B. Godinho. ZUEC-AMP 20083 (adult female) collected at Três Marias municipality, Minas Gerais state (-18.206399 S, -45.241699 W, 547 m a.s.l.), on the 26 November 2012, by M. A. Passos, D. S. Rodrigues, and R. Martins.

Diagnosis.—The new species is assigned to the genus *Corythomantis* due to the combined presence of rhomboidal pupil, brown iris, vomerine teeth, heavily co-ossified skull bones, projecting labial borders, vocal sac single, median, and subgular (Boulenger 1896), and molecular data. The new species can be diagnosed by the following combination of traits: (1) medium size (SVL of males 59.8–74.4 mm, n = 11, SVL of females 58.2–89.5 mm, n = 10); (2) snout rounded in dorsal and ventral views, obtuse in lateral view; prominent ridges on *canthus rostralis*; spinose processes often present on ridges, around the snout and upper eyelid; prominent crest divided by a notch; (3) dorsal region with small tubercles on body extending to the flanks; flank region with few tubercles; arms and legs with short and few tubercles; tubercles absent on the head; ventral skin granular; (4) males have dark epidermal projections in the nuptial pad on thenar portion of finger I and inner portion of finger II, reaching the inner portion of finger III in a few specimens; (5) dorsal coloration brownish fading towards ventral region, with irregular short brown lines and red spots; ventral region cream; (7) advertisement call consisting of one-pulsed note with a duration from 0.11 to 0.21 s, pulse rate from 66.43 to 117.27 pulses/s, first group of the call with 7–9 pulses and second group with 7–12 pulses.

Comparison with other species.—*Corythomantis "espinhaço"* differs from *C. greeningi* in coloration of the inguinal region and legs. *Corythomantis greeningi* has a blotched pattern in the inguinal region and ventral and inner portion of the tibia with brownish spots, all absent in *C. "espinhaço"* (Fig. 3). The nostril-snout distances of the new species are slightly longer with 19.87 % of head length in males (NSD 3.4–5.5 mm) and 19.80 % of head

length in females (NSD 2.8–6.7 mm) than in *C. greeningi* with 16.25 % of head length in males (NSD 2.4–4.6 mm) and 17.27 % of head length in females (NSD 2.2–5.7 mm). In dorsal view the snout of *C. "espinhaço"* is rounder than that of *C. greeningi*, which looks narrower. *Corythomantis "espinhaço"* has sharp ridges in the *canthus rostralis*, while ridges are smoother in *C. greeningi* (Fig. 4). Both species also diverge in advertisement call parameters. Call duration in *C. "espinhaço"* is 41.9 % shorter (0.11–0.21 s in *C. "espinhaço"* vs. 0.27–0.38 s in *C. greeningi*) and pulse rate is higher (66.43–117.27 pulse/s in *C. "espinhaço"* vs. 47.68–72.95 pulse/s in *C. greeningi*). Despite the similar number of pulses in the advertisement calls of both species (17 to 22 pulses/call), species share the same call structure with a call divided in two groups of pulses. *Corythomantis "espinhaço"* has a low number of pulses in group one (7–9) and a high number of pulses in group two (7–12) while *C. greeningi* has high number of pulses in group one (9–16) and low number of pulses in group two (2–9). Molecular data show that the genetic distance between the new species and *C. greeningi* ranges from 2.88 % to 14.06 %. Our Procustes MANOVA values were significant for differences between species for mature males using all morphometric measurements ($p = 0.015$) and for head measurements ($p < 0.001$).

Description of the holotype.—Adult male with slender body. Dorsal skin of body covered with small tubercles up to the posterior part of the head; dorsal skin of limbs with less prominent tubercles, granular skin on ventral portion of body and limbs. Head longer than wide (9.5 % longer); head length 34.62 % of SVL; snout rounded in dorsal and ventral views and highly obtuse in lateral view; projecting labial border; single vocal sac, subgular; posterior portion of the head with a visible crest divided by a notch. *Canthus rostralis* with prominent ridges; *canthus rostralis* converges to the tip of snout between nostrils; loreal region concave. Frontoparietal ridges strongly developed; spinose processes mainly present around and under the snout, on the crest at posterior portion of head, rarely on the upper eyelid, frontoparietal, and on the *canthus rostralis*. Nostrils rounded and directed dorsolaterally. Tympanic annuli distinct; tympanum medium sized and rounded; one

distinctive supratympanic fold. Iris brownish; pupil horizontally elliptical; eye directed anterolaterally; small ridge before eye; eye large; ED 23.29 % of HL; nictitating membrane transparent. Tongue large and subcircular; a pair of vomerine teeth row not in contact, perpendicular to head length, between and posterior to choanae, with eight teeth on each one; choanae nearly oblique; small vocal slits, slit shaped, located laterally from the base of the tongue. Forearm robust; arm slender; fingers medium sized, moderately robust; unwebbed fingers; thenar portion of finger I, inner portion of finger II, and first phalanx of finger III with nuptial pads; nuptial pads composed of dark colored papillary epidermal projections; each finger contains a distal subarticular ovoid tubercle; fingers with smaller proximal tubercles; supranumerary tubercles absent; palmar tubercles slightly developed; small sized finger discs, nearly round; thumb disc smaller than the other digits; diameter of finger discs not larger than the diameter of tympanum; relative finger lengths III > IV > II > I. Legs moderately slender; ventral portion of thick highly granular; ventral portion of tibia smooth; foot 38.21 % of SVL; moderately robust and medium sized toes; rounded subarticular tubercle on each toe; rounded supernumerary tubercles; ovoid inner metatarsal tubercle; toe discs small and rounded; disc of first toe smaller than the others; relative toe lengths IV > III > V > II > I; foot webbing formula I1½ — 2½II1½ — 3^{+}III1^{+}½ — 2^{-}IV2^{-} — 1^{-}V. Cloacal opening directed posteroventrally, above the midlevel of the thigs; cloacal flap short.

Measurements of the holotype (mm).—SVL, 63.4; HL, 21.9; HW, 19.9; CMS, 17.9; TD, 3.4; ED, 5.1; END, 6.7; ESD, 10.7; NSD, 4.0; IOD, 8.5; IND, 4.3; EFIII, 27.6; HaL, 16.7; ThL, 26.4; TL, 27.6; FL, 24.2.

Color in life of the holotype.—Dorsal background brownish, maculated with faded irregular short brown lines and red spots of irregular shapes. Dorsum of the head follows the same coloration as dorsal background, with stronger brown blotches. Dorsal coloration fades towards the flank region, becoming light brownish. A brown stripe from axillary region towards inguinal region divides the flank and ventral regions. Gular region whitish with brown blotches. Ventral region whitish. Coloration of inguinal and ventral regions, hidden

surfaces of thighs, and inner portion of tibia whitish without blotches, darkening towards the dark dorsum coloration. Nuptial pads of dark coloration.

Color in preservative of the holotype.—Dorsal background of body and head dark brown with few lighter brown blotches. Flank region light brownish, separated from the ventral region by a brownish stripe from the axillary region towards the inguinal region. Gular region cream with brown blotches. Ventral region cream. Coloration of inguinal and ventral regions, and inner portion of tibia cream without blotches.

Variation.— Only males from Palmeiras, Bahia state, have a longitudinal stripe from the axillary region to the inguinal region, between the flank and ventral regions. Sexual dimorphism is not evident, with females (SVL 58.2–89.5 mm, n = 10) slightly larger than males (11.2 %, SVL 59.8–74.4 mm, n = 11) considering the mean SVL size. Males show more tubercles on dorsal skin, while female show smoother skins with fewer tubercles (see Fig. 2). Vomerine tooth rows can be in contact or not, and teeth number varies in males (5–11) and females (8–11). Large females (SVL 82.8–89.5) showed stronger development of *Canthus rostralis* and crests. Foot webbing formula follow $I1^{-}$–2^{+} — 2½II1½ — 3^{+}III1^{+}½ — 2^{-}IV2^{-} — 1^{-}V. Our Procustes MANOVA was not significant for sexual dimorphism using all measurements (p = 0.51) or head measurements (p = 0.09). Measurements of the type series are listed in Table 2.

Advertisement call.—The analysis of 278 advertisement calls from the holotype of *Corythomantis "espinhaço"* showed that they consist of a one pulsed note with a duration of 0.18 ± 0.01 s (0.11–0.21 s) and a pulse rate of 97.42 ± 5.63 pulses/s (66.43–117.27 pulses/s). Two groups can be distinguished in the note: the first group consists of 7.95 ± 0.37 pulses (7–9) and begins in low amplitude, lacking frequency modulation; the second group consists of 9.93 ± 1.35 (7–12) concatenated pulses of higher amplitude. The dominant frequency in group one was consistently 750 Hz, while in group two was 1097.72 ± 97.68 Hz (750–1125 Hz) (Table 3 and Fig. 5).

Geographic Distribution.—The new species is distributed along the northern Espinhaço Mountain Range, from mid parts of Bahia state, where this mountain range ends, southwards to northern Minas Gerais states at altitudes varying from 315 to 940 m a.s.l. The known distribution for *Corythomantis "espinhaço"* are Gameleira do Assuruá, Palmeiras, and Contendas do Sincorá in Bahia state and Grão Mogol, Buritizeiro, Buenópolis (Serra do Cabral State Park), Leme do Prado, and Três Marias in Minas Gerais state. The municipalities of Cristália and Montes Claros in Minas Gerais state are potential records for the species (see discussion; Fig. 6).

Etymology.—The specific epithet of the new species will refer to an ornament used by the Aimoré native ethnic group which inhabited the states of Bahia, Minas Gerais, and Espírito Santo.

Natural history.—*Corythomantis "espinhaço"* inhabits mostly higher elevations ranging from 860 to 930 meters above sea level, with Contendas do Sincorá as the lowest location (315 m a.s.l.). The region in the north of Minas Gerais state is a mosaic of Cerrado and open areas of Caatinga, where the species inhabits rocky areas with streams. A couple of specimens from Buritizeiro in Minas Gerais state were collected in a bromeliad on a margin of a stream (Godinho et al. 2013). Specimens from Palmeiras in Bahia state (CHUFPB 28228–28236) were collected in a rocky stream that flows from a small human made dam next to a dirt road (Fig. 7). Frogs were reproductive as males were calling beneath rocks and within the vegetation around the stream, from where we obtained the advertisement call described above and several tadpoles in different stages. Other specimens were observed in January in axillary amplexus and one female (CHUFPB 28235) contained eggs. Two additional females (CHUFPB 30494 and 30496) collected in February 2020 also presented eggs. A fourth female (ZUEC AMP 20083) with eggs from Três Marias in Minas Gerais state was collected in November 2012. Tadpoles inhabit rocky streams and can be found in the flowing water or water ponds on rocks. They cling to the rock with their oral apparatus and scrape its surface to feed on algae. When threatened, they seek deeper portions of ponds, if

available, or release the rock and let the water flow carry them. The municipality of Palmeiras is located within the Chapada Diamantina, which consists of a mountainous region with a range of ecosystems such as rocky outcrop fields, streams, and gallery forests. The region is also characterized by areas of Caatinga or Cerrado, but specimens were collected at a site mostly characterized by Cerrado vegetation. Ontogenetic variation is evident as we observed that head structures are more developed and evident in larger specimens, specifically in ridges of the *canthus rostralis*, supratympanic folds, and crests.

External morphology of the tadpole.—We obtained two tadpole lots from the type locality with a wide range of developmental stages (CHUFPB 28775 and 30501). We also obtained tadpoles from Grão Mogol (UFMG 1902) and Leme do Prado (UFMG 1461), Minas Gerais state (Table 4). In stage 36, tadpoles of *C. "espinhaço"* from the type locality (n = 5) shows oval body in dorsal view and depressed in profile (Fig. 8A–B). Body length is 39.6 % of total length; body 1.3 times wider than high. Snout rounded in dorsal and ventral views; end of body not as round as snout; snout protruding downward in profile; eye dorsally oriented; nostril oval, dorsolaterally located and anterolaterally oriented, closest to eye than to snout. Unique and short spiracle, directed upward, located after midbody on left side, below eye line; spiracle opening is rounded, narrower than basal region. Vent tube medial, attached to ventral fin and not longer than it. Tail musculature reaching the tip of tail; tail musculature width 38.41 % of body width. Dorsal fin originating at the end of body, slightly higher than ventral fin and reaching maximum height at midpoint. Indistinct neuromasts on body and tail. Anteroventral oral disc broad with a diameter 79.17 % of body width (Fig. 8C); anterior and posterior labium without folds; dark labial tooth with labial tooth row formula (LTRF) 6–7(6–7)/9–10(1); first tooth row in the posterior jaw with a small gap in the middle; tooth row interruption in A-6–7 wider than in P-1; teeth size on anterior and posterior labial tooth rows diminish reaching the border of both labium. Oral apparatus not emarginate; papillae around the oral disc in one row, without gap; lower labium smaller than upper labium; papillae longer than wide and in similar size in both labia. Jaw sheaths pigmented; wide serrated jaw sheath,

arc-shaped upper jaw sheath and V-shaped lower jaw sheath; upper jaw with keratinized non-serrate lateral processes (Fig. 8D). Tadpoles showed little variation in LTRF: stages 27–30 presented 6(6)/6–9(1), tadpoles at stages 31–37 presented 6–7(6–7)/8–10(1), and tadpoles at stage 40 presented 7(7)/9(1).

Tadpole coloration.—Tadpoles are more pigmentated at higher developmental stages. Live tadpoles from stage 31 onward show brownish body coloration with darker brown spots, becoming transparent towards the venter. Eyes are brownish as in adult specimens. Margin of oral disc slightly pigmented. Spiracle transparent. Tail musculature cream with darker pigmentation leaving several small cream blotches. Upper and lower fins creamy colored and also transparent with few dark blotches (Fig.8E). Tadpoles at lower stages (27–30) preserved in formalin 10 % show cream coloration and from the snout to the region before spiracle and along the tail musculature, with few brownish spots, mainly on the edges of the body; belly region is transparent in dorsal, ventral, and lateral profile views; dorsal and ventral fins are transparent. Preserved tadpoles in more advanced stages show the same coloration as in life, but faded.

Phylogenetic analysis.—Our Bayesian mitochondrial gene tree recovered a monophyletic group that places *C. "espinhaço"* and *C. greeningi* as sister species with high support (PP = 1) and places the genus *Corythomantis* as a sister taxon with *Itapotihyla langsdorfii* and *Trachycephalus* spp. although with low support (PP = 0.86) (Fig. 9). Genetic divergence with uncorrected p-distance between *C. greeningi* and *C. "espinhaço"* sp. nov. were of 2.88–3.69 % for 16S and 12.42–14.06 % for COI (Table S1).

DISCUSSION

Corythomantis "espinhaço" is a novel species of the genus *Corythomantis* as indicated by molecular and phenotypic evidence and distributed throughout the northern Espinhaço Mountain Range in Brazil. The species is present in Chapada Diamantina, the northernmost portion of this mountain range, which harbors many other endemic species (Bitencourt and

392 Rapini 2013; Fernandes and Hamdan 2014; Thomé et al. 2016; Silva and Souza 2018), which
393 makes it an intriguing speciation zone, where more undescribed species and the evolutionary
394 processes responsible for such diversification are yet to be unveiled. This new discovery
395 further endorses the distinctiveness of this region, which now harbors 16 of the 21 Caatinga's
396 endemic frogs (Garda et al. 2018; Mângia et al. 2018). Likewise, the region has many
397 endemic lizards (Rodrigues et al. 2009; Arias et al. 2014), amphisbaenians (Costa et al. 2015),
398 snakes (Passos et al. 2013; Fernandes and Hamdan 2014), and plants (Bitencourt and Rapini
399 2013). Even with such potential, only six public protected areas are found in the region, and
400 do not cover the whole mosaic of habitats and their biodiversity (MMA 2005). Therefore,
401 many authors already pointed out that the Chapada Diamantina region as a priority target for
402 conservation (e.g. Tabarelli and Silva 2003; Bitencourt and Rapini 2013; Antongiovanni et al.
403 2018). We reinforce the need for a significant expansion of conservation actions to protect the
404 majority of this unique biota.
405 Our data shows that *C. "espinhaço"* and *C. greeningi* do not occur in sympatry.
406 *Corythomantis "espinhaço"* is distributed along the Espinhaço Mountain Range from Bahia to
407 Minas Gerais, whilst *C. greeningi* inhabits most lowlands from northeast Brazil. However, the
408 closest records between both species are in Bahia state, in the municipalities of Santo Inácio
409 (530 m a.s.l.) for *C. greeningi* and Gameleira do Assuruá (940 m a.s.l.) for *C. "espinhaço"*,
410 which are 24 km apart. Such proximity might indicate that the distribution of both species
411 overlaps at some point. The distribution map for *C. greeningi* produced by Godinho et al.
412 (2013) includes four localities in Minas Gerais state: Grão Mogol, Buritizeiro, Cristália, and
413 Montes Claros. Our data show that the species found in Grão Mogol and Buritizeiro are
414 actually *C. "espinhaço"*. Because we do not have molecular, acoustic, or morphological data
415 for Cristália and Montes Claros, we cannot attest whether they are actually *C. "espinhaço"*.
416 Cristália and Montes Claros are high elevation localities, with 760 m and 660 m above sea
417 level, respectively. Cristália is 17 km south of Grão Mongol, while Montes Claros is 100 km
418 west. We accessed specimens from Buritizeiro and we could attest they are *C. "espinhaço"* by

419 the outlining sharper ridges in the *canthus rostralis*, rounded snout, and tibia coloration
420 pattern. Buritizeiro is the farthest from Grão Mogol (250 km west) and is 126 km northwest
421 from Parque Estadual Serra do Cabral. Therefore, we believe the records on municipalities of
422 Cristália and Montes Claros are actually *C. "espinhaço"* and the geographic distribution of the
423 new species mostly restricted to high altitudes of Espinhaço Mountain Range and its
424 surroundings whilst *C. greeningi* is distributed throughout the northeastern region, but also
425 reaching the northern region of Brazil in the municipality of Palmas in Tocantins state (Silva
426 et al. 2014).
427 The advertisement calls are clearly distinct among *Corythomantis* species. Juncá et al.
428 (2008) first investigated possible differences in *C. greeningi* advertisement calls. They
429 compared two localities in the state of Bahia (in Morro do Chapéu and Feira de Santana
430 municipalities) and their results indicated no differences between these localities. We obtained
431 acoustic, morphological, and molecular data from Morro do Chapéu, and all indicate that
432 specimens from this area are not different from the other populations of *C. greeningi*. Juncá et
433 al. (2008) also reported the external morphology of the tadpole of *C. greeningi*. The tadpoles
434 of *C. "espinhaço"* do not differ from the description provided by Juncá et al. (2008), except
435 the first posterior teeth row, which has a gap in the tadpoles of *C. "espinhaço"*. However, we
436 also analyzed tadpoles of *C. greeningi* from Morro do Chapéu, Bahia state and Nova Iorque,
437 Maranhão state and they have gaps in the first posterior teeth row. *Corythomantis "espinhaço"*
438 shows higher numbers of labial tooth rows than described by Juncá et al. (2008), but these
439 numbers overlap with some specimens of *C. greeningi*. We observed neuromasts lines on the
440 body of tadpoles of *C. greeningi* but not in tadpoles of *C. "espinhaço"* (Fig. 8E). Such
441 characteristic was not described in Juncá et al. (2008) and might be a distinctive feature
442 among these species. Further investigation on internal oral morphology might also distinguish
443 the tadpole of both species.
444 Males and females did not differ statistically in morphometric measurements, but
445 could be distinguished based on qualitative traits. The lack statistical differences between

446 males and females can be a consequence of low number of specimens for comparative
447 purposes, with 21 specimens for the new species (11 males and 10 females). Indeed,
448 superficial differences can emerge when small number of individuals and/or localities are
449 used, as is evident from the comparisons among two populations of *Corythomantis* with
450 contrasting adult body sizes (Juncá et al. 2008). These populations, both within the
451 distribution defined herein for *C. greeningi*, have contrasting body sizes (which mostly
452 overlap with the ranges described here for *C. greeningi*) but no significant differences in
453 tadpoles, calls, or other external morphology characters (Juncá et al. 2008). Body size, indeed,
454 is highly liable, being significantly influenced by larval life history and environmental
455 characteristics (Werner 1986).
456 However, morphological differences between *Corythomantis* species are significant in
457 head measurements and leg color patterns. Morphological measurements differed
458 significantly between males of *C. "espinhaço"* and *C. greeningi*, reinforcing the visual
459 differences in nostril-snout distance and snout shape, longer and rounder, respectively, in *C.*
460 *"espinhaço"*. In addition, spots at the inguinal region and ventral and inner portions of the
461 tibia in specimens of *C. "espinhaço"* are absent in specimens from three localities, while *C.*
462 *greeningi* from 13 localities within a wide distribution range showed an ontogenetic variation
463 in this feature. Juveniles showed faded or very low quantity of spots and adults were highly
464 marked. Nevertheless, we show that in the absence of genetic or acoustic data, both head
465 structure and tibia coloration should be sufficient to identify the new species based on
466 morphology alone. We had access to a photograph of the holotype of *C. greeningi* (BMNH
467 1947.2.25.97), deposited in the British Museum of London, for which the type locality is set
468 as “from Brazil” in Boulenger (1896). Photographs show its head shape is obtuse in dorsal
469 view, and blotches on the legs are also visible. Therefore, we conclude that we correctly
470 applied the name *C. greeningi*.
471 Complementary lines of evidence support *C. "espinhaço"* is a distinct species from *C.*
472 *greeningi*. Despite its resemblance to *C. greeningi*, it is easily distinguished from it based on

morphology, advertisement calls, geographic distribution, and molecular data. Further research should compare if these species also diverge in ecological traits. If we consider the IUCN Red List parameters (IUCN Standards and Petitions Working Group 2019), we believe that the new species has similar characteristics to others classified as Data Deficient. Our data show that the new species is endemic to the Espinhaço Mountain Range from central Bahia to northern Minas Gerais state, like many other species amphibians and reptiles from the region. (Rodrigues et al. 2009; Arias et al. 2014; Fernandes and Hamdan 2014; Costa et al. 2015; Garda et al. 2018). The distributions of both species do not overlap, as *C. greeningi* inhabits mostly Caatinga lowlands and a few Cerrado localities. The addition of *C. "espinhaço"* to the Espinhaço Mountain Range highlights the importance of this region as a center of endemism, demanding public and conservation actions to protect its unique biodiversity.

Acknowledgments.—We thank the herpetological collections curators and their staff for providing access to tissue samples and voucher specimens. We are also in debt with S. Mângia, T. Mott, H. Batalha-Filho, M. Bernardino, the editor, and two anonymous reviewers for their comments on earlier versions of the manuscript. We also thank J. Streicher and G. Bittencourt-Silva for the photographs of the holotype of *C. greeningi* housed in the British Museum. RM thanks Coordenação de Aperfeiçoamento de Pessoal de Nível Superior (CAPES) for the doctoral fellowship (Process number 1489596). AAG thanks Conselho Nacional de Desenvolvimento Científico e Tecnológico (CNPq) for financial support (310942/2018-7, 206958/2017-0, 431433/2016-0 and #552031/2011-9). CFBH thanks Fundação de Amparo à Pesquisa do Estado de São Paulo (FAPESP proc #2013/50741-7) and CNPq (research fellowship 306623/2018-8) for financial support. We thank Instituto Chico Mendes de Conservação da Biodiversidade for provide the specimen collection permit (SISBIO 33402-1).

LITERATURE CITED

Altig, R., and R.W. McDiarmid. 1999. Body plan. Development and morphology. Pp. 24–51 in Tadpoles: The Biology of Anuran Larvae (McDiarmid, R.W., and R. Altig, eds.). The University of Chicago Press, USA.

Antongiovanni, M., E.M. Venticinque and C.R. Fonseca. 2018. Fragmentation patterns of the Caatinga drylands. Landscape Ecology 33:1353–1367. DOI: https://doi.org/10.1007/s10980-018-0672-6

Arias, F., C.M. Carvalho, H. Zaher and M.T. Rodrigues. 2014. A new species of *Ameivula* (Squamata, Teiidae) from southern Espinhaço Mountain Range, Brazil. Copeia 2014:95–105.

Bitencourt, C., and A. Rapini. 2013. Centres of endemism in the Espinhaço range: identifying cradles, and museums of Asclepiadoideae (Apocynaceae). Systematic Biodiversity 11:525–536.

Blotto, B.L., M.L. Lyra, M.C. Cardoso, M.T. Rodrigues, I.R. Dias, E. Marciano-Jr, F. Dal Vechio, V.G. Orrico, R.A. Brandão, C. Lopes de Assis, A.S. Lantyer-Silva, M.G. Rutherford, G. Gagliardi-Urrutia, M. Solé, D. Baldo, I. Nunes, R. Cajade, A. Torres, T. Grant, K.-H. Jungfer, H.R. da Silva, C.F.B. Haddad and J. Faivovich. 2020. The phylogeny of the Casque-headed treefrogs (Hylidae: Hylinae: Lophyohylini). Cladistics: 1–37.

Boulenger, G.A. 1896. Descriptions of new batrachians in the British Museum. Annals and Magazine of Natural History Series 17:401–406.

Bruford, M.W., O. Hanotte, J.F.Y. Brookfield and T. Burke. 1992. Single-locus and multilocus DNA fingerprint. Pp. 225–270 in Molecular Genetic Analysis of Populations (Hoelzel, A.R., ed.). IRL Press, USA.

Condit, J.M. 1964. A list of the types of hylid frogs in the collection of the British Museum (Natural History). Journal of the Ohio Herpetological Society 4:85–98.

Costa, H.C., F.C. Resende, M. Teixeira Junior, F.D. Vechio and C.A. Clemente. 2015. A new *Amphisbaena* (Squamata: Amphisbaenidae) from Southern Espinhaço Range, southeastern Brazil. Anais da Academia Brasileira de Ciências 87:891–901. DOI: http://dx.doi.org/10.1590/0001-3765201520140088

Drummond, A.J., and A. Rambaut. 2007. BEAST: Bayesian evolutionary analysis sampling trees. BMC Evolutionary Biology 7: 214. DOI: https://doi.org/10.1186/1471-2148-7-214

Drummond, A.J., M.A. Suchard, X. Dong and A. Rambaut. 2012. Bayesian phylogenetics with BEAUti and the BEAST 1.7. Molecular Biology and Evolution 29:1969–1973. DOI: https://doi.org/10.1093/molbev/mss075

Faivovich, J., C.F.B. Haddad, P.C.A. Garcia, D.R. Frost, J.A. Campbell and W.C. Wheeler. 2005. Systematic review of the frog family Hylidae, with special reference to Hylinae: phylogenetic analysis and taxonomic revision. Bulletin of the American Museum of Natural History 294:1–240.

Fernandes, D.S., and B. Hamdan. 2014. A new species of *Chironius* Fitzinger, 1826 from the state of Bahia, Northeastern Brazil (Serpentes: Colubridae). Zootaxa, 3881:563–575.

Folmer, O., M. Black, W. Hoeh, R. Lutz and R. Vrijenhoek. 1994. DNA primers for amplification of mitochondrial cytochrome coxidase subunit I from diverse metazoan invertebrates. Molecular Marine Biology and Biotechnology 3:294–299.

Frost, D.R. 2019. Amphibian species of the world: An online reference, Version 6.0. Available at http://research.amnh.org/herpetology/amphibia/index.html. Accessed on 6 May 2019. American Museum of Natural History, USA.

Garda, A.A., and D.C. Cannatella. 2007. Phylogeny and biogeography of paradoxical frogs (Anura, Hylidae, Pseudae) inferred from 12S and 16S mitochondrial DNA. Molecular Phylogenetics and Evolution 44:104–114.

Garda, A.A., D.J. Santana and V.A. São-Pedro. 2010. Taxonomic characterization of Paradoxical frogs (Anura, Hylidae, Pseudae): Geographic distribution, external morphology, and morphometry. Zootaxa 2666:1–28.

Garda, A.A., M.G. Stein, R.B. Machado, M.B. Lion, F.A. Juncá and M.F. Napoli. 2017. Ecology, biogeography, and conservation of amphibians of the Caatinga. Pp. 133–150 in Caatinga: The Largest Tropical Dry Forest Region in South America (Silva, J.M.C., I.R. Leal and M. Tabarelli, M., eds.). Springer, USA.

Garda, A. A., M.B. Lion, S.M.Q. Lima, D.O. Mesquita, H.F.P. Araujo and M.F. Napoli. 2018. Os animais vertebrados da Caatinga. Ciência e Cultura 70:29–34.

Godinho, L.B., M.R. Moura and R.N. Feio. 2013. New records and geographic distribution of *Corythomantis greeningi* Boulenger, 1896 (Amphibia: Hylidae). Checklist 9:148–150.

Gosner, K.L. 1960. A simplified table for staging anuran embryos and larvae with notes on identification. Herpetologica 16:183–190.

International Union For Conservation Of Nature – IUCN. 2019. Guidelines for Using the IUCN Red List Categories and Criteria, Version 14.0. Available at https://www.iucnredlist.org/resources/redlistguidelines. Accessed on 6 September 2019. Prepared by the Standards and Petitions Committee.

Juncá, F.A., M.C.L. Carneiro and N.N. Rodrigues. 2008. Is a dwarf population of *Corythomantis greeningi* Boulenger, 1896 (Anura, Hylidae) a new species? Zootaxa 1686:48–56.

Jungfer, K.H., J. Faivovich, J.M. Padial, S. Castroviejo-Fisher, M.M. Lyra, B.V.M. Berneck, P.P. Iglesias, P.J.R. Kok, R.D. MacCulloch, M.T. Rodrigues, V.K. Verdade, C.P. Torres Gastello, J.C. Chaparro, P.H. Valdujo, S. Reichle, J. Moravek, V. Gvoždík, G. Gagliardi-Urrutia, R. Ernst, I. De la Riva, D.B. Means, A.P. Lima, J.C. Señaris, W.C. Wheeler and C.F.B. Haddad. 2013. Systematics of spiny-backed treefrogs (Hylidae: *Osteocephalus*): An Amazonian puzzle. Zoologica Scripta 42:351–380.

Köhler, J., M. Jansen, A. Rodríguez, P.J.R. Kok, L.F. Toledo, M. Emmrich, F. Glaw, C.F.B. Haddad, M.O. Rödel and M. Vences. 2017. The use of bioacoustics in anura taxonomy: Theory, terminology, methods and recommendations for best practice. Zootaxa 4251:001–124.

Kumar, S., G. Stecher, M. Li, C. Knyaz and K. Tamura. 2018. MEGA X: Molecular Evolutionary genetics analysis across computing platforms. Molecular Biology and Evolution 35:1547–1549. DOI: https://doi.org/10.1093/molbev/msy096

Lanfear, R., P.B. Frandsen, A.M. Wright, T. Senfeld and B. Calcott. 2016. PartitionFinder 2: New methods for selecting partitioned models of evolution for molecular and morphological phylogenetic analyses. Molecular Biology and Evolution 34:772–773. DOI: https://doi.org/10.1093/molbev/msw260

Leal I. R., J.M.C. Silva, M. Tabarelli and T.E. Lancher Jr. 2005. Changing the course of biodiversity conservation in the Caatinga of Northeastern Brazil. Conservation Biology 19:701–706.

Lyra, M.L., C.F.B. Haddad and A.M.L. Azeredo-Espin. 2017. Meeting the challenge of DNA barcoding Neotropical amphibians: Polymerase chain reaction optimization and new COI primers. Molecular Ecology Resources 17:966–980.

Luna, M.C., R.W. McDiarmid and J. Faivovich. 2018. From erotic excrescences to pheromone shots: structure and diversity of nuptial pads in anurans. Biological Journal of the Linnean Society 124: 403–446.

Magalhães, F.M. 2014. Morfologia Larval e sua Importância para a Sistemática e Taxonomia de Anfíbios Anuros. Masters Dissertation, Universidade Federal do Rio Grande do Norte, Brazil.

Magalhães, F.M., D.O. Laranjeiras, T.B. Costa, F.A. Juncá, D.O. Mesquita, D.L. Röhr, W.P. Silva, G.H.C. Vieira and A.A. Garda. 2015. Herpetofauna of protected areas in the Caatinga IV: Chapada Diamantina National Park, Bahia, Brazil. Herpetology Notes 8:243–261.

604 Mângia, S., R. Koroiva, P.M.S. Nunes, I.J. Roberto, R.W. Ávila, A.C. Sant'Anna, D.J.
605 Santana and A.A. Garda. 2018. A new species of *Proceratophrys* (Amphibia: Anura:
606 Odontophrynidae) from the Araripe Plateau, Ceará State, Northeastern Brazil.
607 Herpetologica 74:255–268.
608 Palumbi S.R., A. Martin, S. Romano, W.O. McMillan, L. Stice and G. Grabowski 1991. The
609 Simple Fool's Guide to PCR, Version 2.0. Privately Published Document Compiled by
610 S. Palumbi, Dept. Zoology. Honululu: Univ. Hawaii.
611 Passos, P., M. Teixeira Jr, R.S. Recoder, M.A. Sena, F.D. Vechio, H.B.A. Pinto, S.H.S.T.
612 Mendonça, J. Cassimiro and M.T. Rodrigues. 2013. A new species of *Atractus*
613 (Serpentes: Dipsadidae) from Serra do Cipó, Espinhaço Range, Southeastern Brazil,
614 with proposition of a new species group to the genus. Papéis Avulsos de Zoologia
615 53:75–85. DOI: http://dx.doi.org/10.1590/S0031-10492013000600001
616 Pombal Jr., J.P., V.A. Menezes, A.F. Fontes, I. Nunes, C.F.D. Rocha and M.V. Sluys. 2012. A
617 second species of the casque-headed frog genus *Corythomantis* (Anura: Hylidae) from
618 northeastern Brazil, the distribution of *C. greeningi*, and comments on the genus.
619 Boletim do Museu Nacional Zoologia 530:1–14.
620 Prado, D. 2003. As Caatingas da América do Sul. Pp. 3–73 in Ecologia e Conservação da
621 Caatinga (Leal, I. R., J. M. C. Silva and M. Tabarelli, eds.). EDUFPE, Brazil
622 Rodrigues, M.T. 2003. Herpetofauna da Caatinga. Pp. 181–236 in Ecologia e Conservação da
623 Caatinga (Leal, I. R., J. M. C. Silva and M. Tabarelli, eds.). EDUFPE, Brazil.
624 Rodrigues, M.T., J. Cassimiro, M.A. Freitas and T.F.S. Silva. 2009. A new microteiid lizard of
625 the genus *Acratosaura* (Squamata: Gymnophthalmidae) from Serra do Sincorá, State
626 of Bahia, Brazil. Zootaxa 2013:17–29.
627 Sabaj, M.H. (ed.).2016. Standard Symbolic Codes for Institutional Resource Collections in
628 Herpetology and Ichthyology: An Online Reference, version 6.5. American Society of
629 Ichthyologists and Herpetologists, USA. Available at
630 http://www.asih.org/sites/default/files/documents/symbolic_codes_for_collections_v6.

5_2016.pdf. Archived by WebCite at http://www.webcitation.org/74ilEB3Nr on 25 October 2019.

Silva, A.C., and A.F. Souza. 2018. Aridity drives plant biogeographical sub regions in the Caatinga, the largest tropical dry forest and woodland block in South America. Plos One 13:e.0196130. DOI: https://doi.org/10.1371/journal.pone.0196130

Silva, J.M.C., L.C.F. Barbosa, I.R. Leal and M. Tabarelli. 2017. The Caatinga: Understanding the Challenges. Pp. 3–22 in Caatinga: The Largest Tropical Dry Forest Region in South America (Silva, J.M.C., I.R. Leal and M. Tabarelli, M., eds.). Springer, USA.

Silva, L.A., M.C. Hoffmann and D.J. Santana. 2014. New record of *Corythomantis greeningi* Boulenger, 1896 (Amphibia, Hylidae) in the Cerrado domain, state of Tocantins, Central Brazil. Herpetology Notes 7: 717-720.

Tabarelli, M., and J.M.C. Silva. 2003. Áreas e Ações Prioritárias Para a Conservação da Biodiversidade da Caatinga. Pp. 777–796 in Ecologia e Conservação da Caatinga (Leal, I. R., J. M. C. Silva and M. Tabarelli, eds.). EDUFPE, Brazil

Talavera, G. and J. Castresana. 2007. Improvement of phylogenies after removing divergent and ambiguously aligned blocks from protein sequence alignments. Systematic Biology 56: 564–577. DOI: https://doi.org/10.1080/10635150701472164

Thomé, M.T.C., F. Sequeira, F. Brusquetti, B. Carstens, C.F.B. Haddad, M.T. Rodrigues, and J. Alexandrino. 2016. Recurrent connections between Amazon and Atlantic forests shaped diversity in Caatinga four-eyed frogs. Journal of Biogeography, 43: 1045–1056.

Werneck, F.P. 2011. The diversification of eastern South American open vegetation biomes: Historical biogeography and perspectives. Quaternary Science Reviews 30:1630–1648.

Werner, E.E. 1986. Amphibian metamorphosis: growth rate, predation risk, and the optimal size at transformation. The American Naturalist 128**:** 319–341.

APPENDIX I

Specimens Examined

Corythomantis "espinhaço" (*n = 21*). BAHIA: *Contendas do Sincorá* (CFBH 30089), *Palmeiras* (CHUFPB 28228–28236, 30489, 30491, 30494, 30496, CFBH 30147); MINAS GERAIS: *Buritizeiro* (MZUFV 11705–06), *Grão Mogol* (CFBH 10211–13), *Três Marias* (ZUEC-AMP 20083).

Corythomantis greeningi (*n = 49*). ALAGOAS: *Murici* (CHUFPB 28280, 28307), *Taipu* (ZUEC-AMP 23426); BAHIA: *Morro do Chapéu* (CHUFPB 30488, 30490, 30499, 30497), *Umburanas* (CHUFPB 28290–91, 28300, 28302, 28304, 28308–09); CEARÁ: *Crato* (CHUFPB 28293), *Ubajara* (CHUFPB 28281–82, 28287–88, 28292, 28295–96, 28305); MARANHÃO: *Chapadinha* (ZUEC-AMP 3907); PERNAMBUCO: *Buíque* (CHUFPB 28283, 28289); PIAUÍ: *Caracol* (CHUFPB 28286, 28301, 28303, 28306), *Piracuruca* (ZUEC-AMP 10864), *Redenção do Gurguéia* (FSCHUFPB 12449–52, 12475, 13126-28, 13162–63, 13228, 13525), *Taipas* (UFG 9066–67); RIO GRANDE DO NORTE: *Angicos* (CHUFPB 28277, 28284), *Martins* (CHUFPB 28278), *Mossoró* (CHSA 211, 260), *Umarizal* (CHUFPB 28279, 28294); TOCANTINS: *Taipas do Tocantins* (UFG 9067).

TABLE 1.—List of specimens, respective localities, voucher numbers, and Genbank accession number for 16S and COI used in gene tree estimation. Dashes are unavailable sequences. Dashes are not sequenced molecular markers. To be submitted upon acceptance (TBS).

Species	Locality	Voucher	Genbank accession number		Reference
			16S	COI	
Corythomantis greeningi	Brazil: Alagoas: Murici	CHUFPB 28280	TBS	TBS	This study
Corythomantis greeningi	Brazil: Alagoas: Murici	CHUFPB 28307	TBS	TBS	This study
Corythomantis greeningi	Brazil: Alagoas: Piranhas	CFBHT 13	TBS	TBS	This study
Corythomantis greeningi	Brazil: Alagoas: Piranhas	CFBHT 43	TBS	TBS	This study
Corythomantis "espinhaço"	Brazil: Bahia: Contendas do Sincorá	MHNJCH 1079	TBS	TBS	This study
Corythomantis "espinhaço"	Brazil: Bahia: Contendas do Sincorá	CFBHT 20992	TBS	TBS	This study
Corythomantis "espinhaço"	Brazil: Bahia: Gameleira do Assuruá	MTR 11281	TBS	TBS	This study
Corythomantis greeningi	Brazil: Bahia: Morro do Chapéu	UFBA-T 2785	TBS	TBS	This study
Corythomantis greeningi	Brazil: Bahia: Morro do Chapéu	UFBA-T 2781	TBS	TBS	This study
Corythomantis greeningi	Brazil: Bahia: Morro do Chapéu	Tad1CHUFPB 30500	TBS	TBS	This study
Corythomantis "espinhaço"	Brazil: Bahia: Palmeiras	CFBHT 20993	TBS	TBS	This study
Corythomantis "espinhaço"	Brazil: Bahia: Palmeiras	CHUFPB 28228	TBS	TBS	This study

Corythomantis "espinhaço"	Brazil: Bahia: Palmeiras	CHUFPB 28229	TBS	TBS	This study
Corythomantis "espinhaço"	Brazil: Bahia: Palmeiras	CHUFPB 28230	TBS	TBS	This study
Corythomantis "espinhaço"	Brazil: Bahia: Palmeiras	CHUFPB 28231	TBS	TBS	This study
Corythomantis "espinhaço"	Brazil: Bahia: Palmeiras	CHUFPB 28232	TBS	TBS	This study
Corythomantis "espinhaço"	Brazil: Bahia: Palmeiras	CHUFPB 28233	TBS	TBS	This study
Corythomantis "espinhaço"	Brazil: Bahia: Palmeiras	CHUFPB 28234	TBS	TBS	This study
Corythomantis "espinhaço"	Brazil: Bahia: Palmeiras	CHUFPB 28235	TBS	TBS	This study
Corythomantis "espinhaço"	Brazil: Bahia: Palmeiras	CHUFPB 28236	TBS	TBS	This study
Corythomantis "espinhaço"	Brazil: Bahia: Palmeiras	Tad1CHUFPB 30501	TBS	TBS	This study
Corythomantis "espinhaço"	Brazil: Bahia: Palmeiras	Tad2CHUFPB 30501	TBS	TBS	This study
Corythomantis greeningi	Brazil: Bahia: Santo Inácio	MTR 11265	TBS	TBS	This study
Corythomantis greeningi	Brazil: Bahia: Umburanas	CHUFPB 28302	TBS	TBS	This study
Corythomantis greeningi	Brazil: Bahia: Umburanas	CHUFPB 28291	TBS	TBS	This study
Corythomantis greeningi	Brazil: Ceará: Crato	CHUFPB 28293	TBS	TBS	This study
Corythomantis greeningi	Brazil: Ceará: Ubajara	CHUFPB 28288	TBS	TBS	This study
Corythomantis greeningi	Brazil: Ceará: Ubajara	CHUFPB 28305	TBS	TBS	This study
Corythomantis "espinhaço"	Brazil: Minas Gerais: Buenópolis	ZUFG 8059	TBS	TBS	This study
Corythomantis "espinhaço"	Brazil: Minas Gerais: Grão Mogol	CFBHT 2383	TBS	TBS	This study
Corythomantis "espinhaço"	Brazil: Minas Gerais: Grão Mogol	CFBHT 2392	TBS	TBS	This study

Corythomantis greeningi	Brazil: Pernambuco: Buíque	CHUFPB 28289	TBS	TBS	This study
Corythomantis greeningi	Brazil: Pernambuco: Buíque	CHUFPB 28283	TBS	TBS	This study
Corythomantis greeningi	Brazil: Piauí: Piracuruca	CHUFPB 28303	TBS	TBS	This study
Corythomantis greeningi	Brazil: Piauí: Piracuruca	CHUFPB 28306	TBS	TBS	This study
Corythomantis greeningi	Brazil: Piauí: Redenção do Gurguéia	FSCHUFPB 12475	TBS	TBS	This study
Corythomantis greeningi	Brazil: Piauí: Redenção do Gurguéia	FSCHUFPB 13228	TBS	TBS	This study
Corythomantis greeningi	Brazil: Rio Grande do Norte: Angicos	CHUFPB 28277	TBS	TBS	This study
Corythomantis greeningi	Brazil: Rio Grande do Norte: Angicos	CHUFPB 28284	TBS	TBS	This study
Corythomantis greeningi	Brazil: Rio Grande do Norte: Martins	CHUFPB 28278	TBS	TBS	This study
Corythomantis greeningi	Brazil: Rio Grande do Norte: Umarizal	CHUFPB 28294	TBS	TBS	This study
Corythomantis greeningi	Brazil: Rio Grande do Norte: Umarizal	CHUFPB 28279	TBS	TBS	This study
Dryaderces pearsoni	Brazil: Amazonas: Areal	MTR 13205	KF002012	KF001884	Jungfer et al. 2013
Itapotihyla langsdorffii	Argentina: Missiones	MACN 38643	AY843706	KF001942	Faivovich et al. 2005
Nyctimantis arapapa	Brazil: Bahia: Uruci-Una	CFBHT 12327	KU495129	KU494336	Lyra et al. 2017
Nyctimantis brunoi	Brazil: Espirito Santo: Linhares	CFBHT 09216	KU495133	KU494340	Lyra et al. 2017
Nyctimantis galeata	Brazil: Bahia: Morro do Chapéu	CHUFPB 30493	TBS	TBS	This study
Nyctimantis galeata	Brazil: Bahia: Morro do Chapéu	CHUFPB 30495	TBS	TBS	This study
Nyctimantis galeata	Brazil: Bahia: Morro do Chapéu	CHUFPB 30498	TBS	TBS	This study

					Faivovich et al.
Nyctimantis siemersi	Argentina: Corrientes	MACN 38644	AY843570	-	2005
Osteocephalus taurinus	Brazil: Amazonas: Campo Tupana	SMS 088	KF002106	KF001909	Jungfer et al. 2013
Osteopilus septentrionalis	Cuba: Guantanamo: Guantanamo Bay	USNM317830	AY843712	KF001943	Jungfer et al. 2013
					Faivovich et al.
Phyllodytes praeceptor	Brazil: Bahia: Uruci-Una	MRT 6144	AY843722	-	2005
Trachycephalus mesophaeus	Brazil: São Paulo: Caraguatatuba	CFBHT 05858	KU495601	KU494808	Lyra et al. 2017
Trachycephalus resinifictrix	Brazil: Mato Grosso: Vila Rica	MTR_UFCX 22P45	KU495604	KU494811	Lyra et al. 2017
Trachycephalus typhonius	Guyana: Dubulay Ranch on Berbice River	AMNH-A 141142	AY549362	KF001946	Jungfer et al. 2013
Boana raniceps	Brazil: Maranhão: Porto Franco	TG 158	KU495288	KU494495	Lyra et al. 2017

678

TABLE 2.—Morphometric measurements (mm) of the type series of *Corythomantis "espinhaço"* sp. nov. and *C. greeningi*. Values are presented as mean ± standard deviation (range). Snout-vent length (SVL), head width (HW), comissure of the mouth to the tip of the snout (CMS), tympanum diameter (TD), eye diameter (ED), eye-nostril distance (END), eye-snout distance (ESD), nostril-snout distance (ESD), nostril-snout distance (NSD), interorbital distance (IOD), internasal distance (IND), elbow to finger III length (EFIII), hand length (HaL), tibia length (TL), foot length (FL), and thigh length (ThL).

	Corythomantis "espinhaço" sp. nov.		*Corythomantis greeningi*	
	Females (n = 10)	Males (n = 11)	Females (n = 18)	Males (n = 31)
SVL	77.7 ± 11.3 (58.2–89.5)	69.0 ± 4.5 (59.8–74.4)	70.9 ± 10.9 (50.1–86.2)	66.1 ± 5.2 (53.6–81.1)
HL	25.4 ± 3.6 (19.0–29.6)	22.7 ± 1.4 (20.3–24.2)	22.8 ± 3.5 (16.7–27.9)	20.9 ± 1.6 (17.7–25.4)
HW	23.1 ± 3.4 (16.6–27.2)	20.8 ± 1.4 (18.5–22.6)	21.3 ± 3.3 (16.1–26.2)	20.2 ± 1.6 (16.8–24.3)
CMS	21.5 ± 3.5 (15.6–25.8)	18.9 ± 1.6 (16.4–20.9)	20.0 ± 3.1 (14.5–24.5)	18.1 ± 1.5 (14.6–21.9)
END	7.3 ± 1.0 (5.6–8.4)	6.6 ± 0.6 (5.6–7.5)	7.4 ± 1.4 (4.5–9.8)	6.81 ± 0.7 (5.7–8.7)
ESD	12.4 ± 2.2 (8.6–14.7)	11.1 ± 1.1 (9.0–12.2)	11.4 ± 2.2 (7.3–14.3)	10.2 ± 0.92 (8.7–12.7)
NSD	5.0 ± 1.3 (2.8–6.7)	4.5 ± 0.6 (3.4–5.5)	3.9 ± 0.9 (2.2–5.7)	3.4 ± 0.4 (2.4–4.6)
IOD	10.2 ± 1.89 (6.9–12.2)	9.2 ± 0.8 (8.0–10.2)	9.2 ± 1.7 (6.5–11.6)	8.6 ± 1.0 (6.5–10.8)

IND	5.1 ± 0.9 (3.7–6.3)	4.6 ± 0.5 (3.6–5.2)	4.4 ± 0.7 (3.0–5.6)	4.2 ± 0.5 (3.3–5.2)
TD	4.1 ± 0.6 (2.8–4.9)	3.7 ± 0.3 (3.3–4.3)	3.8 ± 0.6 (2.6–4.9)	3.7 ± 0.3 (3.2–4.4)
ED	5.9 ± 0.7 (4.5–7.1)	5.5 ± 0.3 (5.0–6.0)	5.4 ± 0.5 (4.5–6.5)	5.3 ± 0.4 (4.4–5.9)
EFIII	30.7 ± 4.8 (22.2–35.7)	28.7 ± 2.4 (23.9–31.1)	28.7 ± 4.4 (19.4–34.7)	28.3 ± 2.1 (23.7–32.7)
HaL	19.4 ± 2.6 (15.3–22.7)	17.8 ± 1.6 (14.7–20.0)	17.6 ± 2.7 (12.9–21.4)	17.1 ± 1.1 (15.0–19.8)
ThL	30.5 ± 4.1 (23.6–34.8)	27.9 ± 1.6 (24.7–30.5)	27.3 ± 4.1 (19.9–32.9)	27.4 ± 2.5 (21.4–33.2)
TL	30.7 ± 4.2 (23.0–34.6)	28.4 ± 1.8 (25.1–30.6)	28.5 ± 3.9 (20.2–33.7)	27.6 ± 1.9 (22.5–32.4)
FL	26.8 ± 3.8 (20.5–31.9)	25.4 ± 1.8 (21.8–27.9)	25.2 ± 3.8 (17.8–30.1)	24.6 ± 2.0 (20.0–30.5)

684

TABLE 3.—Parameters of the advertisement call of the holotype of *Corythomantis "espinhaço"* sp. nov. and advertisement calls of *Corythomantis greeningi* from different localities within Caatinga domain. Mean ± SD (min–max). (*) sequenced specimens.

	Corythomantis "espinhaço" sp. nov.	*Corythomantis greeningi*			
Voucher	CHUFPB 28228*	-	UFBA 15929*	FSCHUFPB 12475*	FSCHUFPB 13228*
(Sound voucher)	(ASUFRN659+660)	(FNJV 31953)	(SUFBA 263+264)	(ASUFRN 680)	(ASUFRN 679)
N calls	278	62	52	60	25
Call duration (s)	0.186 ± 0.0119	0.3076 ± 0.014	0.324 ± 0.019	0.35 ± 0.02	0.32 ± 0.01
	(0.11–0.21)	(0.273–0.346)	(0.284–0.368)	(0.289–0.384)	(0.286–0.359)
Dominant frequency (Hz)	1093.504 ± 104.691	762.097 ± 95.25	757.211 ± 52.003	1400 ± 257.1	1500 ± 0
	(750–1125)	(750–1500)	(750–1125)	(750–1500)	-
Pulses per call	18.127 ± 1.644	17.016 ± 1.1087	18.42 ± 1.016	22.63 ± 1.15	18.96 ± 0.98
	(11–22)	(15–19)	(16–20)	(20–25)	(17–20)
Pulse duration (s)	0.008 ± 0.001	0.008 ± 0.002	0.01 ± 0.001	0.006 ± 0.001	0.007 ± 0.001

	(0.004–0.013)	(0.002–0.01)	(0.004–0.012)	(0.003–0.01)	(0.003–0.01)
Pulse rate/s	97.428 ± 5.635	55.388 ± 3.704	56.8 ± 2.56	65.22 ± 3.02	59.26 ± 2.28
	(66.431–117.271)	(47.689–64.676)	(51.63–62.3)	(59.14–72.95)	(55.05–63.49)
Inter-pulse interval (s)	0.0065 ± 0.003	0.015 ± 0.006	0.009 ± 0.002	0.02 ± 0.006	0.01 ± 0.004
	(0–0.012)	(0–0.032)	(0.001–0.018)	(0.002–0.02)	(0.006–0.026)
Pulses in group 1	7.954 ± 0.375	11.113 ± 0.907	0.002 ± 0.881	15.23 ± 0.68	12.92 ± 0.64
	(7–9)	(9–13)	(13–16)	(14–16)	(11–14)
Part 1 duration (s)	0.115 ± 0.0042	0.257 ± 0.014	0.275 ± 0.019	0.31 ± 0.02	0.27 ± 0.01
	(0.107–0.129)	(0.224–0.296)	(0.233–0.324)	(0.273–0.339)	(0.23–0.31)
Dominant frequency group 1 (Hz)	750 ± 0	822.581 ± 223.548	750 ± 0	925 ± 322.64	1380 ± 280.62
	-	(750–1500)	-	(750–1500)	(750–1500)
Pulses in group 2	9.934 ± 1.35	5.919 ± 0.795	3.843 ± 0.85	7.7 ± 0.60	6 ± 0.76
	(7–12)	(4–7)	(2–6)	(6–9)	(5–7)
Part 2 duration (s)	0.067 ± 0.007	0.049 ± 0.006	0.04 ± 0.009	0.05 ± 0.004	0.04 ± 0.005
	(0.048–0.083)	(0.37–0.69)	(0.022–0.062)	(0.04–0.056)	(0.035–0.053)

Dominant frequency group 2 (Hz)	1097.7275 ± 97.6865	846.774 ± 253.479	757.211 ± 52.003	1450 ± 190.28	1500 ± 0
	(750–1125)	(750–1500)	(750–1125)	(750–1500)	-
Municipality	Palmeiras, Bahia state	Carnaíba, Bahia state	Morro do Chapéu, Bahia state	Redenção do Gurguéia, Piauí state	Redenção do Gurguéia, Piauí state
Air temperature (ºC)	22.2	27	23.7	27.2	26.5

687

TABLE 4.—Measurements of tadpoles (mm) of *Corythomantis "espinhaço"* sp. nov. Values are presented as mean ± standard deviation (range). Total length (TTL), body length (BL), body width (BW), body height (BH), tail length (TAL), tail muscle height (TMH), tail muscle width (TMW), maximum tail height (MTH), upper fin height (UFH), lower fin height (LFH), internostril distance (IND), interorbital distance (IOD), eye diameter (ED), nostril diameter (ND), eye-nostril distance (EN), nostril-snout distance (NS), eye-snout distance (ES), snout-spiracle distance (SS), body end to center of spiracle (BS), and oral disc width (ODW).

Stages	40	37	36	35	34	33	32	31	30	29	28	27
	n = 2	n = 2	n = 5	n = 3	n = 2	n = 2	n = 1	n = 1	n = 2	n = 1	n = 6	n = 11
TTL	40.5 ± 1.1 (39.7–41.3)	37.6 ± 4.6 (34.4–40.9)	39.2 ± 1.6 (37.0–41.5)	37.5 ± 1.9 (35.6–39.3)	38.2 ± 0.4 (37.9–38.4)	33.9 ± 2.5 (32.1–35.6)	34.4 -	29.7 -	11.1 ± 6.7 (6.4–15.9)	24.1 -	25.8 ± 4.5 (20.9–31.8)	19.7 ± 4.0 (14.5–29.5)
BL	15.2 ± 0.4 (14.9–15.5)	14.6 ± 3.1 (12.4–16.8)	15.6 ± 0.3 (15.1–15.9)	14.1 ± 1.3 (12.3–15.3)	14.4 ± 0.5 (14.0–14.8)	13.4 ± 0.6 (13.0–13.9)	14.25 -	10.6 -	5.7 ± 2.7 (3.8–7.6)	8.6 -	9.9 ± 1.9 (8.0–12.4)	7.3 ± 1.6 (5.6–11.6)
BW	9.1 ± 0.2 (9.0–9.3)	8.4 ± 2.0 (7.0–9.9)	7.7 ± 0.1 (7.6–7.9)	7.3 ± 0.4 (6.8–7.5)	7.3 ± 0.5 (7.0–7.6)	7.7 ± 0.3 (7.5–7.9)	7.0 -	6.6 -	4.0 ± 2.1 (2.5–5.5)	4.6 -	5.5 ± 1.1 (4.4–6.8)	4.0 ± 1.1 (3.0–6.9)
BH	6.8 ± 0.4	6.6 ± 1.5	5.7 ± 0.2	5.2 ± 0.7	5.4 ± 0.4	5.9 ± 0.1	5.6	4.5	24.2 ±	2.9	3.7 ± 1.2	2.8 ± 0.9

									16.7 (12.4–36.0)			
	(6.5–7.0)	(5.5–7.6)	(5.5–5.9)	(4.3–6.0)	(5.1–5.6)	(5.9–6.0)	-	-		-	(2.5–5.0)	(2.0–5.4)
TAL	35.4 ± 1.9	32.5 ± 2.7	33.5 ± 2.0	30.4 ± 5.8	33.4 ± 0.1	28.9 ± 2.5	28.8	26.5	2.4 ± 1.6	15.5	19.6 ± 6.6	13.1 ± 4.4
	(34.1–36.7)	(30.6–34.4)	(30.5–36.0)	(21.8–33.9)	(33.3–33.4)	(27.2–30.7)	-	-	(1.3–3.5)	-	(12.8–27.4)	(8.6–25.2)
TMH	3.8 ± 0.4	3.7 ± 0.8	3.3 ± 0.3	2.8 ± 0.6	2.9 ± 0.1	3.2 ± 0.1	3.0	2.8	2.1 ± 1.4	1.8	2.1 ± 0.7	1.4 ± 0.5
	(3.5–4)	(3.1–4.3)	(2.8–3.5)	(1.9–3.1)	(2.9–3)	(3.1–3.3)	-	-	(1.1–3.1)	-	(1.4–3.0)	(1.0–2.9)
TMW	3.7 ± 0.3	3.4 ± 0.4	3.0 ± 0.1	2.5 ± 0.6	2.8 ± 0.1	2.9 ± 0.1	2.9	2.6	4.4 ± 1.8	1.5	1.9 ± 0.6	1.2 ± 0.4
	(3.5–3.9)	(3.1–3.8)	(2.8–3.1)	(1.6–3.0)	(2.8–2.9)	(2.9–3)	-	-	(3.1–5.6)	-	(1.3–2.5)	(0.9–2.4)
MTH	5.9 ± 0	6.7 ± 0.3	5.7 ± 0.6	5.3 ± 0.1	5.2 ± 0.3	6.5 ± 0.2	5.3	5	1.3 ± 0.5	3.8	4.3 ± 0.9	3.1 ± 1.0
	-	(6.5–6.9)	(4.6–6.3)	(5.1–5.4)	(5.0–5.4)	(6.4–6.6)	-	-	(0.9–1.6)	-	(3.3–5.4)	(2.4–5.9)
UFH	1.8 ± 0.5	2.1 ± 0.2	1.5 ± 0.4	1.4 ± 0.2	1.4 ± 0	2.0 ± 0.2	1.4	1.6	0.8 ± 0.1	1.0	1.3 ± 0.3	1.0 ± 0.3
	(1.5–2.1)	(2.0–2.3)	(0.9–1.8)	(1.1–1.6)	-	(1.9–2.1)	-	-	(0.8–0.9)	-	(1.0–1.8)	(0.8–1.9)
LFH	1.4 ± 0.4	1.8 ± 0.3	1.3 ± 0.4	1.3 ± 0.3	1.3 ± 0.1	1.6 ± 0.2	1.4	1.3	3.1 ± 1.6	0.8	1.1 ± 0.2	0.9 ± 0.3

	(1.1–1.8)	(1.6–2.0)	(0.8–1.8)	(0.9–1.5)	(1.3–1.4)	(1.5–1.8)	-	-	(2.0–4.3)	-	(0.8–1.3)	(0.6–1.6)
IND	4.3 ± 0.2	4.2 ± 0.4	4.1 ± 0.1	3.8 ± 0.3	3.8 ± 0.2	3.9 ± 0.3	3.9	3.3	4.1 ± 2.4	2.6	2.9 ± 0.6	2.0 ± 0.5
	(4.1–4.4)	(3.9–4.5)	(3.9–4.3)	(3.4–4.0)	(3.6–3.9)	(3.8–4.1)	-	-	(2.4–5.8)	-	(2.1–3.8)	(1.4–3.4)
IOD	5.6 ± 0	5.6 ± 0.4	5.7 ± 0.1	5.2 ± 0.5	5.1 ± 0.4	4.9 ± 0.3	5.4	4.6	1.1 ± 0.7	3.0	3.6 ± 0.9	2.5 ± 0.7
	-	(5.4–5.9)	(5.5–5.8)	(4.5–5.5)	(4.9–5.4)	(4.8–5.1)	-	-	(0.6–1.6)	-	(2.6–4.6)	(1.9–4.5)
ED	1.6 ± 0	1.7 ± 0.1	1.7 ± 0.1	1.5 ± 0.3	1.5 ± 0	1.4 ± 0.1	1.5	1.4	0.3 ± 0.2	0.8	1.0 ± 0.3	0.7 ± 0.2
	-	(1.6–1.8)	(1.6–1.9)	(1.1–1.6)	-	(1.4–1.5)	-	-	(0.1–0.4)	-	(0.8–1.3)	(0.5–1.1)
ND	0.4 ± 0	0.32 ± 0.09	0.4 ± 0.1	0.4 ± 0.1	0.4 ± 0	0.4 ± 0	0.4	0.4	1.6 ± 1.2	0.2	0.2 ± 0.1	0.2 ± 0
	-	(0.25–0.38)	(0.4–0.5)	(0.4–0.5)	-	-	-	-	(0.8–2.4)	-	(0.2–0.4)	(0.1–0.3)
END	2.7 ± 0.3	2.32 ± 0.26	2.3 ± 0.1	2.2 ± 0.2	2.1 ± 0	2.1 ± 0.2	2.1	1.9	3.6 ± 2.7	1.0	1.4 ± 0.5	0.8 ± 0.3
	(2.5–2.9)	(2.13–2.5)	(2.3–2.4)	(2–2.4)	-	(2.0–2.3)	-	-	(1.6–5.5)	-	(0.8–1.9)	(0.5–1.8)
NSD	4.4 ± 0.7	4.13 ± 0.35	4.9 ± 0.4	4.1 ± 0.4	4.0 ± 0.5	4.3 ± 0.2	3.5	3.5	5.1 ± 3.9	2.2	2.8 ± 1.2	1.9 ± 0.7
	(3.9–4.9)	(3.88–4.38)	(4.4–5.5)	(3.5–4.4)	(3.6–4.4)	(4.1–4.4)	-	-	(2.4–7.9)	-	(1.3–4.3)	(1.3–4.0)
ESD	7.1 ± 0.5	6.44 ± 0.62	7.2 ± 0.5	6.3 ± 0.5	6.1 ± 0.5	6.4 ± 0.4	5.6	5.4	7.9 ± 4.2	3.2	4.1 ± 1.7	2.7 ± 1.1
	(6.8–7.4)	(6–6.88)	(6.8–7.9)	(5.5–6.8)	(5.8–6.5)	(6.1–6.6)	-	-	(4.9–10.9)	-	(2.0–6.1)	(1.9–5.8)

		10.01 ±										
SSD	10.9 ± 0.6	1.94	10.5 ± 0.3	9.6 ± 0.9	9.9 ± 0.4	9.4 ± 0.7	10.0	8.1	3.3 ± 2.5	6.4	7.2 ± 1.4	5.2 ± 1.1
	(10.5–11.4)	(8.63–11.38)	(10.1–10.9)	(8.5–10.6)	(9.6–10.3)	(8.9–9.9)	-	-	(1.5–5.0)	-	(5.6–9.0)	(4.1–8.1)
BS	4.3 ± 0.2	4.57 ± 1.15	5.1 ± 0.2	4.5 ± 0.5	4.4 ± 0.1	4.1 ± 0.1	4.3	2.5	4.5 ± 2.5	2.3	2.7 ± 0.5	2.1 ± 0.6
	(4.1–4.4)	(3.75–5.38)	(4.9–5.4)	(3.8–5.0)	(4.4–4.5)	(4.0–4.1)	-	-	(2.7–6.3)	-	(1.9–3.4)	(1.5–3.5)
ODW	6.3 ± 0.1	5.88 ± 0.88	6.1 ± 0.3	5.8 ± 0.5	5.9 ± 0.2	5.9 ± 0.4	6.0	4.5	6.0 ± 0	4.0	4.1 ± 0.9	3.1 ± 0.8
	(6.3–6.4)	(5.25–6.5)	(5.5–6.3)	(5.3–6.5)	(5.8–6.0)	(5.6–6.1)	-	-	-	-	(3.2–5.6)	(2.6–5.4)

FIGURE CAPTIONS

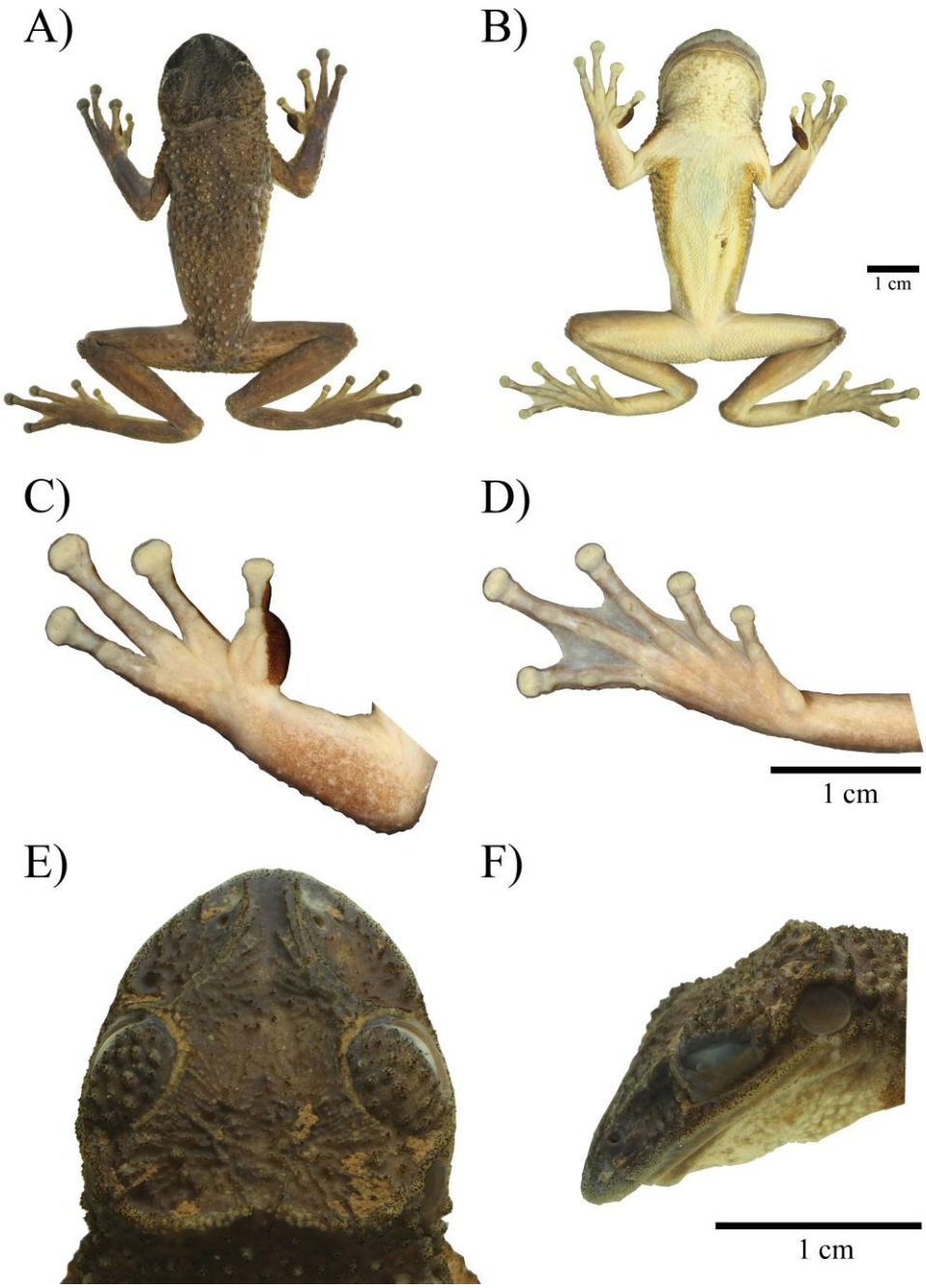

FIG. 1.—Holotype of *Corythomantis "espinhaço"* sp. nov. (adult male, CHUFPB 28228, snout-vent length = 63.4 mm): Dorsal (A) and ventral (B) views of whole specimen; ventral views of left hand (C) and foot (D); dorsal (E) and lateral (F) views of the head.

FIG. 2.—Live paratopotypes of *Corythomantis "espinhaço"* sp. nov. from Palmeiras municipality, state of Bahia, Brazil: (A) adult female (CHUFPB 30496), (B) adult male (CHUFPB 30489), (C) male and female (CHUFPB 28232 and 28236) in axillary amplexus, and (D) live tadpole on a rocky stream. Photo C by Willianilson Pessoa.

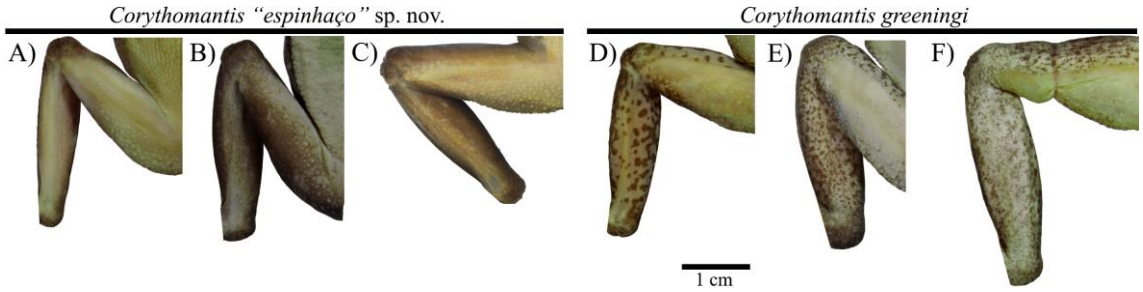

FIG. 3.—Comparison of thigh coloration on males of *Corythomantis "espinhaço"* sp. nov. and *C. greeningi* with different SVL size. Unblotched pattern in specimens of *C. "espinhaço"* sp. nov.: (A) 59.8 mm SVL (UFV 11705 from Buritizeiro, Minas Gerais state), (B) 65.9 mm SVL (CFBH 10213 from Grão Mogol, Minas Gerais state), and (C) 63.4 mm SVL (holotype CHUFPB 28228 from Palmeiras, Bahia state). Blotched pattern in specimens of *C. greeningi*: (D) 56.7 mm SVL (UFG 9067 from Taipas, Tocantins

state), (E) 72.4 mm SVL (CHUFPB 28309 from Umburanas, Bahia state), and (F) 81.1 mm SVL (CHUFPB 28283 from Buíque, Pernambuco state). Females have the same pattern.

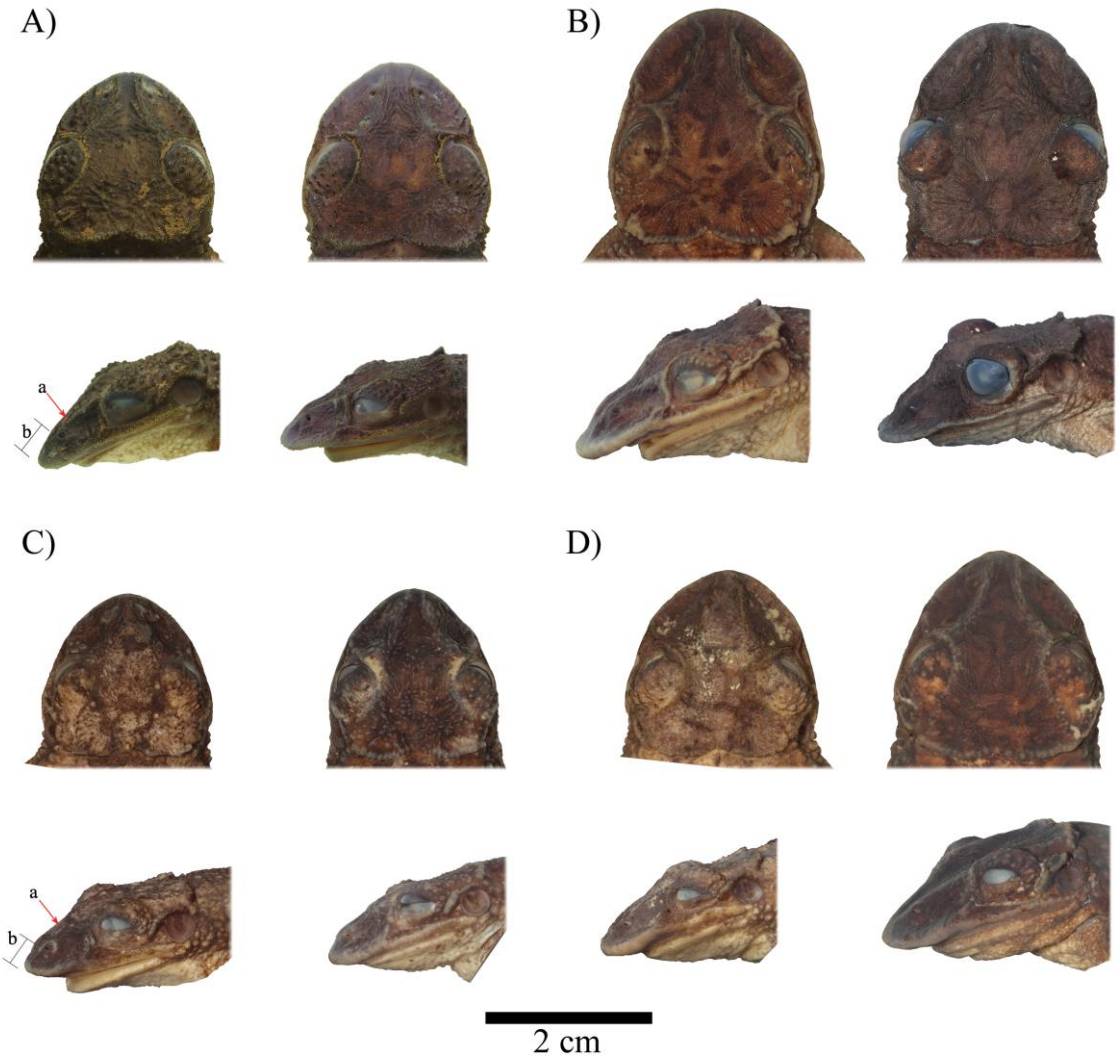

FIG. 4.—Morphological differences between the heads of *Corythomantis* species. Dorsal (top) and profile (bottom) views of the head of *C. "espinhaço"* males (A; holotype CHUFPB 28228 and 28229) and females (B; CHUFPB 28235 and CFBH 30089) and *C. greeningi* males (C; CHUFPB 28284 and 28291) and females (D; CHUFPB 28277 and 28295). We highlight the *canthus rostralis* ridge (a) and nostril-snout distance (b) on both species.

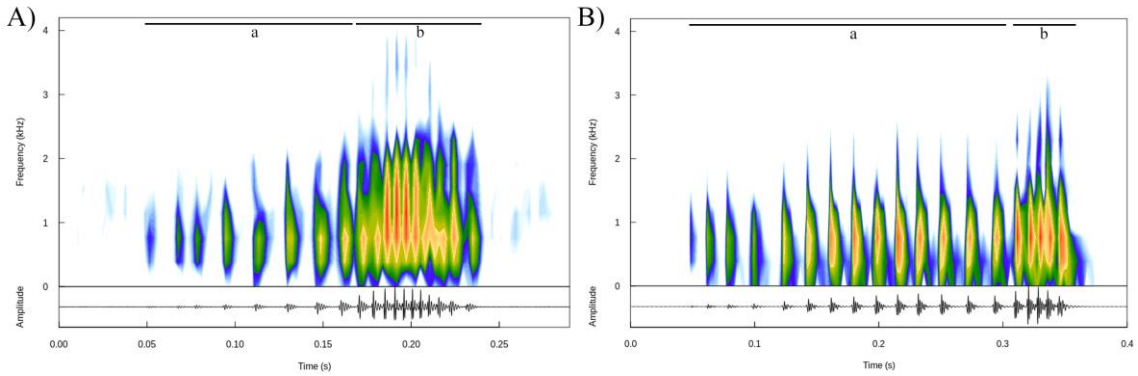

720 FIG. 5.—Comparative oscillogram (top) and audiospectrogram (bottom) from the
721 advertisement calls of the holotype CHUFPB 28228 of *Corythomantis "espinhaço"* sp.
722 nov. (A; ASUFRN660) and *C. greeningi* (B; SUFBA263) with notes divided into group
723 one (a) and group two (b).

724

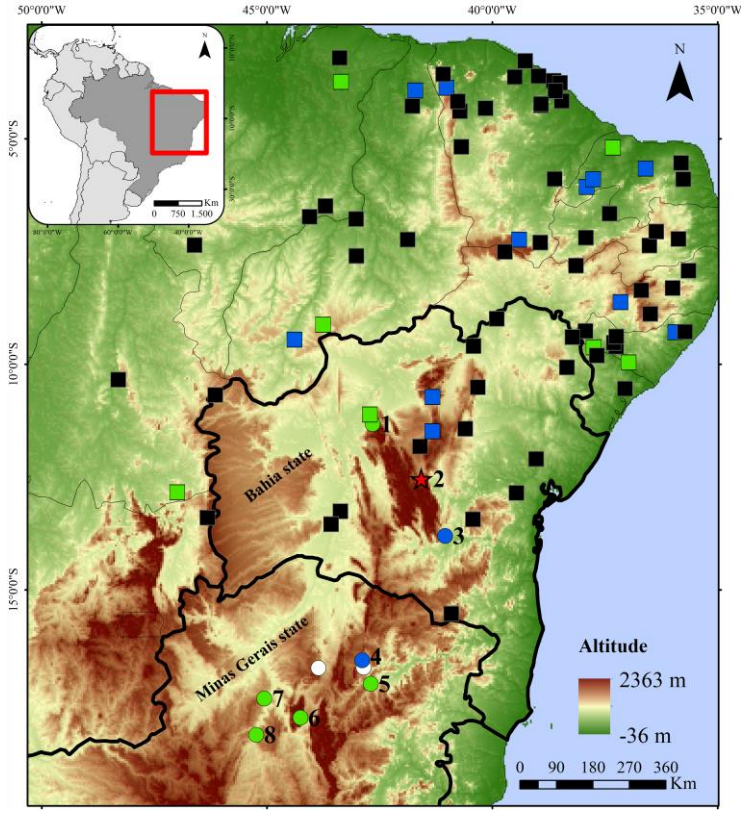

725 FIG. 6.—Distribution map of *Corythomantis "espinhaço"* sp. nov. (circles, red star is the
726 type locality) and *C. greeningi* (squares). Localities with green coloration show we used
727 morphological data on post-metamorphic and tadpoles, or molecular data, blue
728 coloration show we used morphological data on post-metamorphic and molecular data,

white are potential localities for *C. "espinhaço"* based on literature records (see discussion), and black are literature records. Gameleira do Assuruá (1), Palmeiras (2), Contendas do Sincorá (3), Grão Mogol (4), Leme do Prado (5), Buenópolis (6), Buritizeiro (7), and Três Marias (8).

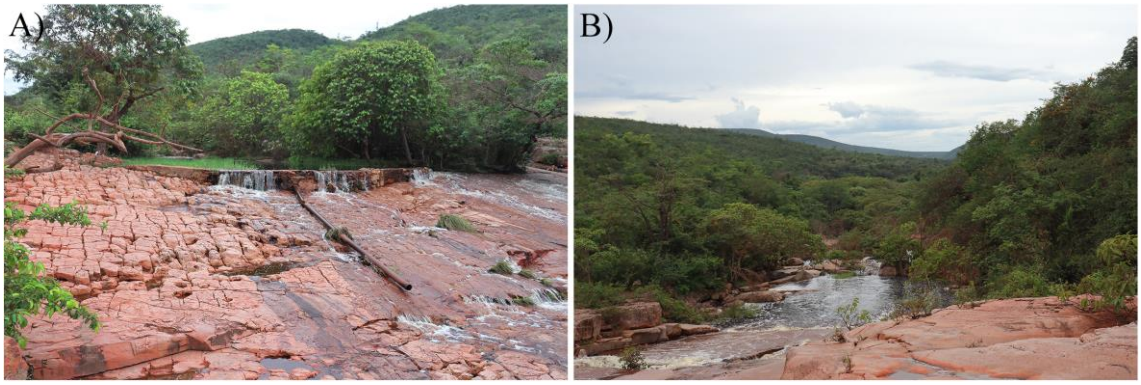

FIG. 7.—Habitat of *Corythomantis "espinhaço"* sp. nov. in the type locality of Palmeiras, Bahia state.

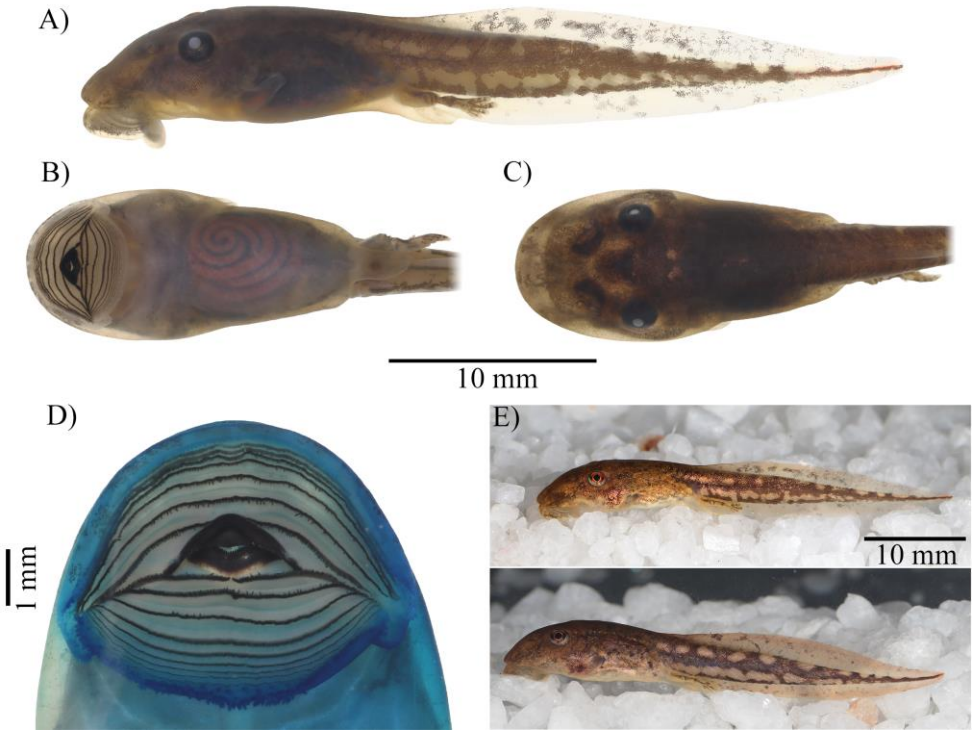

FIG. 8.—Profile (A), dorsal view (B), ventral view (C), and (D) external oral morphology of the tadpole of *Corythomantis "espinhaço"* sp. nov. in stage 36 in Gosner

classification (CHUFPB 30501). (E) show the same tadpole of *C. "espinhaço"* sp. nov. (top) at stage 36 from the type locality (CHUFPB 30501) and *C. greeningi* (bottom) at stage 37 from Morro do Chapéu, Bahia state (CHUFPB 30500). Both tadpoles were sequenced for this study.

FIG. 9.—Resulting Bayesian mitochondrial gene tree placing *Corythomantis "espinhaço"* sp. nov. among other species of Lophyohylini. Numbers near tree nodes show the posterior probability. Terminals of *C. greeningi* and *Nyctimantis galeata* were collapsed for better understanding.

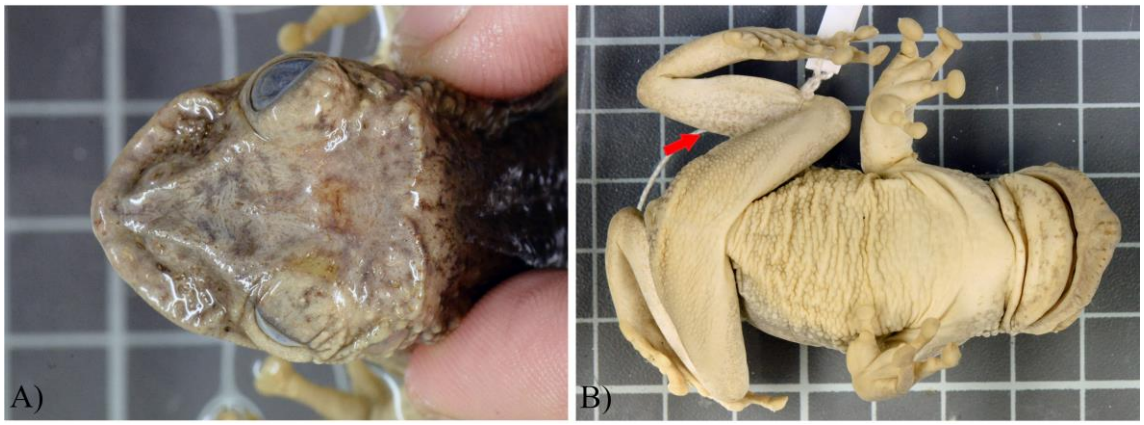

749 FIG. 10.—Holotype of *Corythomantis greeningi* (BMNH 1947.2.25.97) deposited in the
750 British Museum of London. (A) Dorsal view of the head, and (B) ventral view with
751 blotched pattern in tibia highlighted by the red arrow. Photos by Gabriela Bittencourt-
752 Silva.